
Robustifying Algorithms of Learning Latent Trees with Vector Variables

Fengzhuo Zhang

Department of Electrical and Computer Engineering
National University of Singapore
fzzhang@u.nus.edu

Vincent Y. F. Tan

Department of Electrical and Computer Engineering
Department of Mathematics
National University of Singapore
vtan@nus.edu.sg

Abstract

We consider learning the structures of Gaussian latent tree models with vector observations when a subset of them are arbitrarily corrupted. First, we present the sample complexities of Recursive Grouping (RG) and Chow-Liu Recursive Grouping (CLRG) without the assumption that the effective depth is bounded in the number of observed nodes, significantly generalizing the results in Choi et al. (2011). We show that Chow-Liu initialization in CLRG greatly reduces the sample complexity of RG from being exponential in the diameter of the tree to only logarithmic in the diameter for the hidden Markov model (HMM). Second, we robustify RG, CLRG, Neighbor Joining (NJ) and Spectral NJ (SNJ) by using the truncated inner product. These robustified algorithms can tolerate a number of corruptions up to the square root of the number of clean samples. Finally, we derive the first known instance-dependent impossibility result for structure learning of latent trees. The optimalities of the robust version of CLRG and NJ are verified by comparing their sample complexities and the impossibility result.

1 Introduction

Latent graphical models provide a succinct representation of the dependencies among observed and latent variables. Each node in the graphical model represents a random variable or a random vector, and the dependencies among these variables are captured by the edges among nodes. Graphical models are widely used in domains from biology [1], computer vision [2] and social networks [3].

This paper focuses on the structure learning problem of latent tree-structured Gaussian graphical models (GGM) in which the node observations are random *vectors* and a subset of the observations can be *arbitrarily corrupted*. This classical problem, in which the variables are *clean scalar* random variables, has been studied extensively in the past decades. The first information distance-based method, NJ, was proposed in [1] to learn the structure of phylogenetic trees. This method makes use of additive information distances to deduce the existence of hidden nodes and introduce edges between hidden and observed nodes. RG, proposed in [4], generalizes the information distance-based methods to make it applicable for the latent graphical models with general structures. Different from these information distance-based methods, quartet-based methods [5] utilize the relative geometry of every four nodes to estimate the structure of the whole graph. Although experimental comparisons of these algorithms were conducted in some works [4, 6, 7], since there is no instance-dependent

impossibility result of the sample complexity of structure learning problem of latent tree graphical models, no thorough theoretical comparisons have been made, and the optimal dependencies on the diameter of graphs and the maximal distance between nodes ρ_{\max} have not been found.

The success of the previously-mentioned algorithms relies on the assumption that the observations are i.i.d. samples from the generating distribution. The structure learning of latent graphical models in presence of (random or adversarial) noise remains a relatively unexplored problem. The presence of the noise in the samples violates the i.i.d. assumption. Consequently, classical algorithms may suffer from severe performance degradation in the noisy setting. There are some works studying the problem of structure learning of graphical models with noisy samples, where all the nodes in the graphical models are observed and not hidden. Several assumptions on the additive noise are made in these works, which limit the use of these proposed algorithms. For example, the covariance matrix of the noise is specified in [8], and the independence and/or distribution of the noise is assumed in [9–11, 7]. In contrast, we consider the structure learning of latent tree graphical models with *arbitrary* corruptions, where assumptions on the distribution and independence of the noise across nodes are not required [12]. Furthermore, the corruptions are allowed to be presented at *any position* in the data matrix; they do not appear solely as outliers. In this work, we derive bounds on the maximum number of corruptions that can be tolerated for a variety of algorithms, and yet structure learning can succeed with high probability.

Firstly, we derive the sample complexities of RG and CLRG where each node represents a random *vector*; this differs from previous works where each node is *scalar* random variable (e.g., [4, 13]). We explore the dependence of the sample complexities on the parameters of the graph. Compared with [4, Theorem 12], the derived sample complexities are applicable to a wider class of latent trees and capture the dependencies on more parameters of the underlying graphical models, such as ρ_{\max} , the maximum distance between any two nodes, and δ_{\min} , the minimum over all determinants of the covariance matrices of the vector variables. Our sample complexity analysis clearly demonstrates and precisely quantifies the effectiveness of the Chow-Liu [14] initialization step in CLRG; this has been only verified experimentally [4]. For the particular case of the HMM, we show that the Chow-Liu initialization step reduces the sample complexity of RG which is $O\left(\left(\frac{9}{2}\right)^{\text{Diam}(\mathbb{T})}\right)$ to $O(\log \text{Diam}(\mathbb{T}))$, where $\text{Diam}(\mathbb{T})$ is the tree diameter.

Secondly, we robustify RG, CLRG, NJ and SNJ by using the truncated inner product [15] to estimate the information distances in the presence of arbitrary corruptions. We derive their sample complexities and show that they can tolerate $n_1 = O\left(\frac{\sqrt{n_2}}{\log n_2}\right)$ corruptions, where n_2 is the number of clean samples.

Finally, we derive the first known instance-dependent impossibility result for learning latent trees. The dependencies on the number of observed nodes $|\mathcal{V}_{\text{obs}}|$ and the maximum distance ρ_{\max} are delineated. The comparison of the sample complexities of the structure learning algorithms and the impossibility result demonstrates the optimality of Robust Chow-Liu Recursive Grouping (RCLRG) and Robust Neighbor Joining (RNJ) in $\text{Diam}(\mathbb{T})$ for some archetypal latent tree structures.

Notation We use san-serif letters x , boldface letters \mathbf{x} , and bold uppercase letters \mathbf{X} to denote variables, vectors and matrices, respectively. The notations $[\mathbf{x}]_i$, $[\mathbf{X}]_{ij}$, $[\mathbf{X}]_{:,j}$ and $\text{diag}(\mathbf{X})$ are respectively the i^{th} entry of vector \mathbf{x} , the $(i, j)^{\text{th}}$ entry of \mathbf{X} , the j^{th} column of \mathbf{X} , and the diagonal entries of matrix \mathbf{X} . The notation $x^{(k)}$ represents the k^{th} sample of x . $\|\mathbf{x}\|_0$ is the l_0 norm of the vector \mathbf{x} , i.e., the number of non-zero terms in \mathbf{x} . The set $\{1, \dots, n\}$ is denoted as $[n]$. For a tree $\mathbb{T} = (\mathcal{V}, \mathcal{E})$, the internal (non-leaf) nodes, the maximal degree and the diameter of \mathbb{T} are denoted as $\text{Int}(\mathbb{T})$, $\text{Deg}(\mathbb{T})$, and $\text{Diam}(\mathbb{T})$, respectively. We denote the closed neighborhood and the degree of x_i as $\text{nbfd}[x_i; \mathbb{T}]$ and $\text{deg}(i)$, respectively. The length of the (unique) path connecting x_i and x_j is denoted as $d_{\mathbb{T}}(x_i, x_j)$.

2 Preliminaries and problem statement

A GGM [16, 17] is a multivariate Gaussian distribution that factorizes according to an undirected graph $\mathbb{G} = (\mathcal{V}, \mathcal{E})$. More precisely, a l_{sum} -dimensional random vector $\mathbf{x} = [\mathbf{x}_1^{\top}, \dots, \mathbf{x}_p^{\top}]^{\top}$, where $\mathbf{x}_i \in \mathbb{R}^{l_i}$ and $l_{\text{sum}} = \sum_{i=1}^p l_i$, follows a Gaussian distribution $\mathcal{N}(\mathbf{0}, \Sigma)$, and it is said to be *Markov* on a graph $\mathbb{G} = (\mathcal{V}, \mathcal{E})$ with vertex set $\mathcal{V} = \{x_1, \dots, x_p\}$ and edge set $\mathcal{E} \subseteq \binom{\mathcal{V}}{2}$ and $(x_i, x_j) \in \mathcal{E}$ if

and only if the $(i, j)^{\text{th}}$ block Θ_{ij} of the precision $\Theta = \Sigma^{-1}$ is not the zero matrix $\mathbf{0}$. We focus on tree-structured graphical models, which factorize according to acyclic and connected (tree) graphs.

A special class of graphical models is the set of *latent* graphical models $\mathbb{G} = (\mathcal{V}, \mathcal{E})$. The vertex set \mathcal{V} is decomposed as $\mathcal{V} = \mathcal{V}_{\text{hid}} \cup \mathcal{V}_{\text{obs}}$. We only have access to n i.i.d. samples drawn from the observed set of nodes \mathcal{V}_{obs} . The two goals of any structure learning algorithm are to learn the identities of the hidden nodes \mathcal{V}_{hid} and how they are connected to the observed nodes.

2.1 System model for arbitrary corruptions

We consider tree-structured GGMs $\mathbb{T} = (\mathcal{V}, \mathcal{E})$ with observed nodes $\mathcal{V}_{\text{obs}} = \{x_1, \dots, x_o\}$ and hidden nodes $\mathcal{V}_{\text{hid}} = \{x_{o+1}, \dots, x_{o+h}\}$, where $\mathcal{V} = \mathcal{V}_{\text{hid}} \cup \mathcal{V}_{\text{obs}}$ and $\mathcal{E} \subseteq \binom{\mathcal{V}}{2}$. Each node x_i represents a random *vector* $\mathbf{x}_i \in \mathbb{R}^{l_i}$. The concatenation of these random vectors is a multivariate Gaussian random vector with zero mean and covariance matrix Σ with size $l_{\text{sum}} \times l_{\text{sum}}$.

We have n i.i.d. samples $\tilde{\mathbf{X}}_j = [\tilde{\mathbf{x}}_1^{(j)\top}, \dots, \tilde{\mathbf{x}}_o^{(j)\top}]^\top \in \mathbb{R}^{l_{\text{sum}}}$, $j = 1, \dots, n$ drawn from the observed nodes $\mathcal{V}_{\text{obs}} = \{x_1, \dots, x_o\}$. However, the *observed* data matrix $\tilde{\mathbf{X}}_1^n = [\tilde{\mathbf{X}}_1, \dots, \tilde{\mathbf{X}}_n]^\top \in \mathbb{R}^{n \times l_{\text{sum}}}$ may contain some corrupted elements. We allow an level- $(n_1/2)$ arbitrary corruption in the data matrix. This is made precise in the following definition.

Definition 1 (Level- m arbitrary corruption). *For the data matrix $\tilde{\mathbf{X}}_1^n \in \mathbb{R}^{n \times k}$ formed by n clean samples of k random variables (or a random vector of dimension k), an level- m arbitrary corruption transforms $\tilde{\mathbf{X}}_1^n$ into $\mathbf{X}_1^n \in \mathbb{R}^{n \times k}$ such that*

$$\|[\tilde{\mathbf{X}}_1^n]_{:,i} - [\mathbf{X}_1^n]_{:,i}\|_0 \leq m \quad \text{for all } i = 1, \dots, k. \quad (1)$$

Definition 1 implies that there are at most $n_1/2$ corrupted terms in each column of \mathbf{X}_1^n ; the remaining $n - n_1/2$ samples in this column are clean. In particular, the corrupted samples in different columns need not to be in the same rows. If the corruptions in different columns lie in the same rows, as shown in (the left of) Fig. 3, all the samples in the corresponding rows are corrupted; these are called *outliers*. Obviously, outliers form a special case of our corruption model. Since each variable has at most $n_1/2$ corrupted samples, the sample-wise inner product between two variables has at least $n_2 = n - n_1$ clean samples. There is no constraint on the statistical dependence or patterns of the corruptions. Unlike fixing the covariance matrix of the noise [8] or keeping the noise independent [9], we allow *arbitrary* corruptions on the samples, which means that the noise can have unbounded amplitude, can be dependent, and even can be generated from another graphical model (as we will see in the experimental results in Section 3.6).

2.2 Structural and distributional assumptions

To construct the correct latent tree from samples of observed nodes, it is imperative to constrain the class of latent trees to guarantee that the information from the distribution of observed nodes $p(\mathbf{x}_1, \dots, \mathbf{x}_o)$ is sufficient to construct the tree. The distribution $p(\mathbf{x}_1, \dots, \mathbf{x}_{o+h})$ of the observed and hidden nodes is said to have a *redundant* hidden node x_j if the distribution of the observed nodes $p(\mathbf{x}_1, \dots, \mathbf{x}_o)$ remains the same after we marginalize over x_j . To ensure that a latent tree can be constructed with no ambiguity, we need to guarantee that the true distribution does not have any redundant hidden node(s), which is achieved by following two conditions [18]: (C1) Each hidden node has at least three neighbors; the set of such latent trees is denoted as $\mathcal{T}_{\geq 3}$; (C2) Any two variables connected by an edge are neither perfectly dependent nor independent.

Assumption 1. *The dimensions of all the random vectors are all equal to l_{max} .*

In fact, we only require the random vectors of the internal (non-leaf) nodes to have the same length. However, for ease of notation, we assume that the dimensions of all the random vectors are l_{max} .

Assumption 2. *For every $x_i, x_j \in \mathcal{V}$, the covariance matrix $\Sigma_{ij} = \mathbb{E}[\mathbf{x}_i \mathbf{x}_j^\top]$ has full rank, and the smallest singular value of Σ_{ij} is lower bounded by γ_{min} , i.e.,*

$$\sigma_{l_{\text{max}}}(\Sigma_{ij}) \geq \gamma_{\text{min}} \quad \text{for all } x_i, x_j \in \mathcal{V}, \quad (2)$$

where $\sigma_i(\Sigma)$ is the i^{th} largest singular value of Σ .

This assumption is a strengthening of Condition (C2) when each node represents a random vector.

Assumption 3. The determinant of the covariance matrix of any node $\Sigma_{ii} = \mathbb{E}[\mathbf{x}_i \mathbf{x}_i^\top]$ is lower bounded by δ_{\min} , and the diagonal terms of the covariance matrix are upper bounded by σ_{\max}^2 , i.e.,

$$\min_{x_i \in \mathcal{V}} \det(\Sigma_{ii}) \geq \delta_{\min} \quad \text{and} \quad \max_{x_i \in \mathcal{V}} \text{diag}(\Sigma_{ii}) \leq \sigma_{\max}^2. \quad (3)$$

Assumption 3 is natural; otherwise, Σ_{ii} may be arbitrarily close to a singular matrix.

Assumption 4. The degree of each node is upper bounded by d_{\max} , i.e., $\text{Deg}(\mathbb{T}) \leq d_{\max}$.

2.3 Information distance

We define the *information distance* for Gaussian random vectors and prove that it is additive for trees.

Definition 2. The information distance between nodes x_i and x_j is

$$d(x_i, x_j) = -\log \frac{\prod_{k=1}^{l_{\max}} \sigma_k(\Sigma_{ij})}{\sqrt{\det(\Sigma_{ii}) \det(\Sigma_{jj})}}. \quad (4)$$

Condition (C2) can be equivalently restated as constraints on the information distance.

Assumption 5. There exist two constants $0 < \rho_{\min} \leq \rho_{\max} < \infty$ such that.

$$\rho_{\min} \leq d(x_i, x_j) \leq \rho_{\max} \quad \text{for all} \quad x_i, x_j \in \mathcal{V}. \quad (5)$$

Assumptions 2 and 5 both describe the properties of the correlation between random vectors from different perspectives. In fact, we can relate the constraints in these two assumptions as follows:

$$\gamma_{\min} e^{\rho_{\max}/l_{\max}} \geq \delta_{\min}^{1/l_{\max}}. \quad (6)$$

Proposition 1. If Assumptions 1 and 2 hold, $d(\cdot, \cdot)$ defined in Definition 2 is additive on the tree-structured GGM $\mathbb{T} = (\mathcal{V}, \mathcal{E})$. In other words, $d(x_i, x_k) = d(x_i, x_j) + d(x_j, x_k)$ holds for any two nodes $x_i, x_k \in \mathcal{V}$ and any node x_j on the path connecting x_i and x_k in \mathbb{T} .

This additivity property is used extensively in the following algorithms. It was first stated and proved in Huang et al. [19]. We provide an alternative proof in Appendix G.

3 Robustifying latent tree structure learning algorithms

3.1 Robust estimation of information distances

Before delving into the details of robustifying latent tree structure learning algorithms, we first introduce the truncated inner product [15], which estimates the correlation against arbitrary corruption effectively and serves as a basis for the robust latent tree structure learning algorithms. Given $\mathbf{a}, \mathbf{b} \in \mathbb{R}^n$ and an integer n_1 , we compute $q_i = a_i b_i$ for $i = 1, 2, \dots, n$ and sort $\{|q_i|\}$. Let Υ be the index set of the $n - n_1$ smallest $|q_i|$'s. The truncated inner product is $\langle \mathbf{a}, \mathbf{b} \rangle_{n_1} = \sum_{i \in \Upsilon} q_i$. Note that the implementation of the truncated inner product requires the knowledge of corruption level n_1 .

To estimate the information distance defined in Definition 2, we implement the truncated inner product to estimate each term of Σ_{ij} , i.e., $[\hat{\Sigma}_{ij}]_{st} = \frac{1}{n - n_1} \langle [\mathbf{X}_1^n]_{:, (i-1)l_{\max}+s}, [\mathbf{X}_1^n]_{:, (j-1)l_{\max}+t} \rangle_{n_1}$. Then the information distance is computed based on this estimate of Σ_{ij} as

$$\hat{d}(x_i, x_j) = -\log \prod_{k=1}^{l_{\max}} \sigma_k(\hat{\Sigma}_{ij}) + \frac{1}{2} \log \det(\hat{\Sigma}_{ii}) + \frac{1}{2} \log \det(\hat{\Sigma}_{jj}). \quad (7)$$

The truncated inner product guarantees that $\hat{\Sigma}_{ij}$ converges in probability to Σ_{ij} , which further ensures the convergence of the singular values and the determinant of Σ_{ij} to their nominal values.

Proposition 2. If Assumptions 1 and 2 hold, the estimate of the information distance between x_i and x_j based on the truncated inner product $\hat{d}(x_i, x_j)$ satisfies

$$\mathbb{P}\left(|\hat{d}(x_i, x_j) - d(x_i, x_j)| > \frac{2l_{\max}^2}{\gamma_{\min}}(t_1 + t_2)\right) \leq 2l_{\max}^2 e^{-\frac{3n_2}{16\kappa n_1} t_1} + l_{\max}^2 e^{-c \frac{n_2}{\kappa^2} t_2}, \quad (8)$$

where $t_2 < \kappa = \max\{\sigma_{\max}^2, \rho_{\min}\}$, and c is an absolute constant.

The first and second parts of (8) originate from the corrupted and clean samples respectively.

3.2 Robust Recursive Grouping algorithm

The RG algorithm was proposed in [4] to learn latent tree models with additive information distances. We extend the RG to be applicable to GGMs with vector observations and robustify it to learn the tree structure against arbitrary corruptions. We call this robustified algorithm Robust Recursive Grouping (RRG). RRG makes use of the additivity of information distance to identify the relationship between nodes. For any three nodes x_i, x_j and x_k , the difference between the information distances $d(x_i, x_k)$ and $d(x_j, x_k)$ is denoted as $\Phi_{ijk} = d(x_i, x_k) - d(x_j, x_k)$.

Lemma 3. [4] *For information distances $d(x_i, x_j)$ for all nodes $x_i, x_j \in \mathcal{V}$ in a tree $\mathbb{T} \in \mathcal{T}_{\geq 3}$, Φ_{ijk} has following two properties: (1) $\Phi_{ijk} = d(x_i, x_j)$ for all $x_k \in \mathcal{V} \setminus \{x_i, x_j\}$ if and only if x_i is a leaf node and x_j is the parent of x_j and (2) $-d(x_i, x_j) < \Phi_{ijk'} = \Phi_{ijk} < d(x_i, x_j)$ for all $x_k, x_{k'} \in \mathcal{V} \setminus \{x_i, x_j\}$ if and only if x_i and x_j are leaves and share the same parent.*

RRG initializes the active set Γ^1 to be the set of all observed nodes. In the i^{th} iteration, as shown in Algorithm 1, RRG adopts Lemma 3 to identify relationships among nodes in active set Γ^i , and it removes the nodes identified as siblings and children from Γ^i and adds newly introduced hidden nodes to form the active set Γ^{i+1} in the $(i+1)^{\text{st}}$ iteration. The procedure of estimating the distances between the newly-introduced hidden node x_{new} and other nodes is as follows. For the node x_i which is the child of x_{new} , i.e., $x_i \in \mathcal{C}(x_{\text{new}})$, the information distance is estimated as

$$\hat{d}(x_i, x_{\text{new}}) = \frac{1}{2(|\mathcal{C}(x_{\text{new}})| - 1)} \left(\sum_{j \in \mathcal{C}(x_{\text{new}})} \hat{d}(x_i, x_j) + \frac{1}{|\mathcal{K}_{ij}|} \sum_{k \in \mathcal{K}_{ij}} \hat{\Phi}_{ijk} \right), \quad (9)$$

where $\mathcal{K}_{ij} = \{x_k \in \mathcal{V} \setminus \{x_i, x_j\} : \max\{\hat{d}(x_i, x_k), \hat{d}(x_j, x_k)\} < \tau\}$ for some threshold $\tau > 0$. For $x_i \notin \mathcal{C}(x_{\text{new}})$, the distance is estimated as

$$\hat{d}(x_i, x_{\text{new}}) = \begin{cases} \sum_{x_k \in \mathcal{C}(x_{\text{new}})} \frac{\hat{d}(x_k, x_i) - \hat{d}(x_k, x_{\text{new}})}{|\mathcal{C}(x_{\text{new}})|} & \text{if } x_i \in \mathcal{V}_{\text{obs}} \\ \sum_{(x_k, x_j) \in \mathcal{C}(x_{\text{new}}) \times \mathcal{C}(i)} \frac{\hat{d}(x_k, x_j) - \hat{d}(x_k, x_{\text{new}}) - \hat{d}(x_j, x_i)}{|\mathcal{C}(x_{\text{new}})||\mathcal{C}(i)|} & \text{otherwise} \end{cases} \quad (10)$$

The set \mathcal{K}_{ij} is designed to ensure that the nodes involved in the calculation of information distances are not too far, since estimating long distances accurately requires a large number of samples. The maximal cardinality of \mathcal{K}_{ij} over all nodes $x_i, x_j \in \mathcal{V}$ can be found, and we denote this as N_τ , i.e., $|\mathcal{K}_{ij}| \leq N_\tau$.

The observed nodes are placed in the 0^{th} layer. The hidden nodes introduced in i^{th} iteration are placed in i^{th} layer. The nodes in the i^{th} layer are in the active set Γ^{i+1} in the $(i+1)^{\text{st}}$ iteration, but nodes in Γ^{i+1} can be nodes created in the j^{th} iteration, where $j < i$. For example, in Fig. 1, nodes x_{12}, x_{14} and x_{15} are created in the 1^{st} iteration, and they are in Γ^2 . Nodes x_1, x_2 and x_5 are also in Γ^2 , which are observed nodes. Eqns. (9) and (10) imply that the estimation error in the 0^{th} layer will propagate to the nodes in higher layers, and it is necessary to derive concentration results for the information distance related to the nodes in higher layers. To avoid repeating complicated expressions in the various concentration bounds to follow, we define the function

$$f(x) \triangleq 2l_{\max}^2 e^{-\frac{3n_2}{32\lambda\kappa n_1}x} + l_{\max}^2 e^{-c\frac{n_2}{4\lambda^2\kappa^2}x^2} =: ae^{-wx} + be^{-ux^2},$$

where $\lambda = 2l_{\max}^2 e^{\rho_{\max}} / l_{\min}^1$, $w = \frac{3n_2}{32\lambda\kappa n_1}$, $u = c\frac{n_2}{4\lambda^2\kappa^2}$, $a = 2l_{\max}^2$ and $b = l_{\max}^2$. To assess the proximity of the estimates $\hat{d}(x_i, x_{\text{new}})$ in (9) and (10) to their nominal versions, we define

$$h^{(l)}(x) \triangleq s^l f(m^l x) = s^l (ae^{-wm^l x} + be^{-um^{2l} x^2}) \quad \text{for all } l \in \mathbb{N} \cup \{0\}. \quad (11)$$

where $s = d_{\max}^2 + 2d_{\max}^3(1 + 2N_\tau)$ and $m = 2/9$. The following proposition yields *recursive estimates* for the errors of the distances at various layers of the learned latent tree.

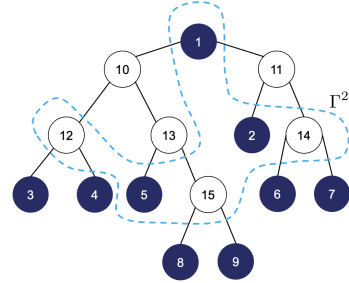


Figure 1: An illustration of the active set. The shaded nodes are the observed nodes and the rest are hidden nodes.

Proposition 4. *With Assumptions 1–5, if we implement the truncated inner product to estimate the information distance among observed nodes and adopt (9) and (10) to estimate the information distances related to newly introduced hidden nodes, then the information distance related to the hidden nodes x_{new} created in the l^{th} layer $\hat{d}(x_i, x_{\text{new}})$ satisfies*

$$\mathbb{P}\left(|\hat{d}(x_i, x_{\text{new}}) - d(x_i, x_{\text{new}})| > \varepsilon\right) < h^{(l)}(\varepsilon) \quad \text{for all } x_i \in \Gamma^{l+1} \quad \text{and } l \in \mathbb{N} \cup \{0\}. \quad (12)$$

We note that Proposition 4 demonstrates that the coefficient of exponential terms in (12) grow exponentially with increasing layers (i.e., m^l and m^{2l} in (11)), which requires a commensurately large number of samples to control the tail probabilities.

Theorem 1. *Under Assumptions 1–5, RRG learns the correct latent tree with probability $1 - \eta$ if*

$$n_2 = \tilde{\Omega}\left(\frac{l_{\max}^4 e^{2\rho_{\max}/l_{\max}} \kappa^2}{\delta_{\min}^{2/l_{\max}} \rho_{\min}^2} \left(\frac{9}{2}\right)^{2L_R} \log \frac{|\mathcal{V}_{\text{obs}}|^3}{\eta}\right) \quad \text{and} \quad n_1 = O\left(\frac{\sqrt{n_2}}{\log n_2}\right), \quad (13)$$

where L_R is the number of iterations of RRG needed to construct the tree.

Theorem 1 indicates that the number of clean samples n_2 required by RRG to learn the correct structure grows exponentially with the number of iterations L_R . Specifically, for the full m -tree illustrated in Fig. 5, n_2 is exponential in the depth of the tree with high probability for structure learning to succeed. The sample complexity of RRG depends on $e^{2\rho_{\max}/l_{\max}}$, and the exponential relationship with ρ_{\max} will be shown to be unavoidable in view of our impossibility result in Theorem 5. Huang et al. [19, Lemma 7.2] also derived a sample complexity result for learning latent trees but the algorithm is based on [5] instead of RG. RRG is able to tolerate $n_1 = O(\sqrt{n_2}/\log n_2)$ corruptions. This tolerance level originates from the properties of the truncated inner product; similar tolerances will also be seen for the sample complexities of subsequent algorithms. We expect this is also the case for [19], which is based on [5], though we have not shown this formally. In addition, the sample complexity is applicable to a wide class of graphical models that satisfies the Assumptions 1 to 5, while the sample complexity result [4, Theorem 11], which hides the dependencies on the parameters, only holds for a limited class of graphical models whose effective depths (the maximal length of paths between hidden nodes and their closest observed nodes) are bounded in $|\mathcal{V}_{\text{obs}}|$.

3.3 Robust Neighbor Joining and Spectral Neighbor Joining algorithms

The NJ algorithm [1] also makes use of additive distances to identify the existence of hidden nodes. To robustify the NJ algorithm, we adopt robust estimates of information distances as the additive distances in the so-called RNJ algorithm. We first recap a result by Atteson [20].

Proposition 5. *If all the nodes have exactly two children, NJ will output the correct latent tree if*

$$\max_{x_i, x_j \in \mathcal{V}_{\text{obs}}} |\hat{d}(x_i, x_j) - d(x_i, x_j)| \leq \rho_{\min}/2. \quad (14)$$

Unlike RG, NJ does not identify the parent relationship among nodes, so it is only applicable to binary trees in which each node has at most two children.

Theorem 2. *If Assumptions 1–5 hold and all the nodes have exactly two children, RNJ constructs the correct latent tree with probability at least $1 - \eta$ if*

$$n_2 = \Omega\left(\frac{l_{\max}^4 e^{2\rho_{\max}/l_{\max}} \kappa^2}{\delta_{\min}^{2/l_{\max}} \rho_{\min}^2} \log \frac{|\mathcal{V}_{\text{obs}}|^2}{\eta}\right) \quad \text{and} \quad n_1 = O\left(\frac{\sqrt{n_2}}{\log n_2}\right). \quad (15)$$

Theorem 2 indicates that the sample complexity of RNJ grows as $\log |\mathcal{V}_{\text{obs}}|$, which is much better than RRG. Similarly to RRG, the sample complexity has an exponential dependence on ρ_{\max} .

In recent years, several variants of NJ algorithm have been proposed. The additivity of information distances results in certain properties of the rank of the matrix $\mathbf{R} \in \mathbb{R}^{|\mathcal{V}_{\text{obs}}| \times |\mathcal{V}_{\text{obs}}|}$, where $\mathbf{R}(i, j) = \exp(-d(x_i, x_j))$ for all $x_i, x_j \in \mathcal{V}_{\text{obs}}$. Jaffe et al. [6] proposed SNJ which utilizes the rank of \mathbf{R} to deduce the sibling relationships among nodes. We robustify the SNJ algorithm by implementing the robust estimation of information distances, as shown in Algorithm 2.

Although SNJ was designed for discrete random variables, the additivity of the information distance proved in Proposition 1 guarantees the consistency of Robust Spectral NJ (RSNJ) for GGMs with vector variables. A sufficient condition for RSNJ to learn the correct tree can be generalized from [6].

Proposition 6. *If Assumptions 1–5 hold and all the nodes have exactly two children, a sufficient condition for RSNJ to recover the correct tree from $\hat{\mathbf{R}}$ is*

$$\|\hat{\mathbf{R}} - \mathbf{R}\|_2 \leq g(|\mathcal{V}_{\text{obs}}|, \rho_{\min}, \rho_{\max}), \quad (16)$$

where

$$g(x, \rho_{\min}, \rho_{\max}) = \begin{cases} \frac{1}{2}(2e^{-\rho_{\max}})^{\log_2(x/2)} e^{-\rho_{\max}} (1 - e^{-2\rho_{\min}}), & e^{-2\rho_{\max}} \leq 0.5 \\ e^{-3\rho_{\max}} (1 - e^{-2\rho_{\min}}), & e^{-2\rho_{\max}} > 0.5 \end{cases}.$$

Similar with RNJ, RSNJ also does not identify the parent relationship between nodes, so it only applies to binary trees. To state the next result succinctly, we assume that $\rho_{\max} \geq \frac{1}{2} \log 2$; this is the regime of interest because we consider large trees which implies that ρ_{\max} is typically large.

Theorem 3. *If Assumptions 1–5 hold, $\rho_{\max} \geq \frac{1}{2} \log 2$, and all the nodes have exactly two children, RSNJ reconstructs the correct latent tree with probability at least $1 - \eta$ if*

$$n_2 = \Omega\left(\frac{l_{\max}^4 e^{2\rho_{\max}(1/l_{\max} + \log_2(|\mathcal{V}_{\text{obs}}|/2) + 1)} \kappa^2 \log \frac{|\mathcal{V}_{\text{obs}}|^2}{\eta}}{\delta_{\min}^{2/l_{\max}} e^{2\rho_{\min}}}\right) \quad \text{and} \quad n_1 = O\left(\frac{\sqrt{n_2}}{\log n_2}\right). \quad (17)$$

Theorem 3 indicates that the sample complexity of RSNJ grows as $\text{poly}(|\mathcal{V}_{\text{obs}}|)$. Specifically, in the binary tree case, the sample complexity grows exponentially with the depth of the tree. Also, the dependence of sample complexity on ρ_{\max} is exponential, i.e., $O(e^{2(1/l_{\max} + \log_2(|\mathcal{V}_{\text{obs}}|/2) + 1)\rho_{\max}})$, but the coefficient of ρ_{\max} is larger than those of RRG and RNJ, which are $O(e^{2\rho_{\max}/l_{\max}})$. Compared to the sample complexity of SNJ in [6], the sample complexity of RSNJ has the same dependence on the number of observed nodes $|\mathcal{V}_{\text{obs}}|$, which means that the robustification of SNJ using the truncated inner product is able to tolerate $O(\frac{\sqrt{n_2}}{\log n_2})$ corruptions.

3.4 Robust Chow-Liu Recursive Grouping

In this section, we show that the exponential dependence on $L_{\mathbf{R}}$ in Theorem 1 can be provably mitigated with an accurate initialization of the structure. Different from RRG, RCLRG takes Chow-Liu algorithm as the initialization stage, as shown in Algorithm 3. The Chow-Liu algorithm [14] learns the maximum likelihood estimate of the tree structure by finding the maximum weight spanning tree of the graph whose edge weights are the mutual information quantities between these variables. In the estimation of the hidden tree structure, instead of taking the mutual information as the weights, we find the minimum spanning tree (MST) of the graph whose weights are information distances, i.e.,

$$\text{MST}(\mathcal{V}_{\text{obs}}; \mathbf{D}) := \arg \min_{\mathbb{T} \in \mathcal{T}_{\mathcal{V}_{\text{obs}}}} \sum_{(x_i, x_j) \in \mathbb{T}} d(x_i, x_j), \quad (18)$$

where $\mathcal{T}_{\mathcal{V}_{\text{obs}}}$ is the set of all the trees with node set \mathcal{V}_{obs} . To describe the process of finding the MST, we recall the definition of the *surrogate node* from [4].

Definition 3. *Given the latent tree $\mathbb{T} = (\mathcal{V}, \mathcal{E})$ and any node $x_i \in \mathcal{V}$, the surrogate node [4] of x_i is $\text{Sg}(x_i; \mathbb{T}, \mathcal{V}_{\text{obs}}) = \arg \min_{x_j \in \mathcal{V}_{\text{obs}}} d(x_i, x_j)$.*

We introduce a new notion of distance that quantifies the sample complexity of RCLRG.

Definition 4. *Given the latent tree $\mathbb{T} = (\mathcal{V}, \mathcal{E})$ and any node $x_i \in \mathcal{V}$, the contrastive distance of x_i with respect to \mathcal{V}_{obs} is defined as*

$$d_{\text{ct}}(x_i; \mathbb{T}, \mathcal{V}_{\text{obs}}) = \min_{x_j \in \mathcal{V}_{\text{obs}} \setminus \{\text{Sg}(x_i; \mathbb{T}, \mathcal{V}_{\text{obs}})\}} d(x_i, x_j) - \min_{x_j \in \mathcal{V}_{\text{obs}}} d(x_i, x_j). \quad (19)$$

Definitions 3 and 4 imply that the surrogate node $\text{Sg}(x_i; \mathbb{T}, \mathcal{V}_{\text{obs}})$ of any observed node x_i is itself x_i , and its contrastive distance is the information distance between the closest observed node and

itself. It is shown that the Chow-Liu tree $\text{MST}(\mathcal{V}_{\text{obs}}; \mathbf{D})$ is equal to the tree where all the hidden nodes are contracted to their surrogate nodes [4], so it will be difficult to identify the surrogate node of some node if its contrastive distance is small. Under this scenario, more accurate estimates of the information distances are required to construct the correct Chow-Liu tree $\text{MST}(\mathcal{V}_{\text{obs}}; \mathbf{D})$.

Proposition 7. *The Chow-Liu tree $\text{MST}(\mathcal{V}_{\text{obs}}; \hat{\mathbf{D}})$ is constructed correctly if*

$$|\hat{d}(x_i, x_j) - d(x_i, x_j)| < \Delta_{\text{MST}}/2 \quad \text{for all } x_i, x_j \in \mathcal{V}_{\text{obs}}, \quad (20)$$

where $\Delta_{\text{MST}} := \min_{x_j \in \text{Int}(\mathbb{T})} d_{\text{ct}}(x_j; \mathbb{T}, \mathcal{V}_{\text{obs}})$.

Hence, the contrastive distance describes the difficulty of learning the correct Chow-Liu tree.

Theorem 4. *With Assumptions 1–5, RCLRG constructs the correct latent tree with probability at least $1 - \eta$ if*

$$n_2 = \tilde{\Omega} \left(\max \left\{ \frac{1}{\rho_{\min}^2} \left(\frac{9}{2}\right)^{2L_C}, \frac{1}{\Delta_{\text{MST}}^2} \right\} \frac{l_{\max}^4 e^{2\rho_{\max}/l_{\max}} \kappa^2 \log \frac{|\mathcal{V}_{\text{obs}}|^3}{\eta}}{\delta_{\min}^{2/l_{\max}}} \right) \quad \text{and} \quad n_1 = O\left(\frac{\sqrt{n_2}}{\log n_2}\right), \quad (21)$$

where L_C is the maximum number of iterations of RRG (over each internal node of the constructed Chow-Liu tree) in RCLRG needed to construct the tree.

If we implement RCLRG with *true* information distances, $L_C \leq \lceil \frac{1}{2} \text{Deg}(\text{MST}(\mathcal{V}_{\text{obs}}; \hat{\mathbf{D}})) - 1 \rceil$. Theorem 4 indicates that the sample complexity of RCLRG grows exponentially in $L_C \ll L_R$. Compared with [4, Theorem 12], the sample complexity of RCLRG in Theorem 4 is applicable to a wide class of graphical models that satisfy Assumptions 1 to 5, while the [4, Theorem 12] requires the assumption that the effective depths of latent trees are *bounded* in $|\mathcal{V}_{\text{obs}}|$, which is rather restrictive.

3.5 Comparison of robust latent tree learning algorithms

Since the sample complexities of RRG, RCLRG, RSNJ and RNJ depend on different parameters and different structures of the underlying graphs, it is instructive to compare the sample complexities of these algorithms on some representative tree structures. These trees are illustrated in Fig. 5. RSNJ and RNJ are not able to identify the parent relationship among nodes, so they are only applicable to trees whose maximal degrees are no larger than 3, including the double-binary tree and the HMM. In particular, RNJ and RSNJ are not applicable to the full m -tree (for $m \geq 3$) and the double star. Derivations and more detailed discussions of the sample complexities are deferred to Appendix K.

n_2 \ Tree \ Algorithm	RRG	RCLRG	RSNJ	RNJ
Double-binary tree	$O(\psi(\frac{9}{2})^{\text{Diam}(\mathbb{T})})$	$O(\psi(\frac{9}{2})^{\frac{1}{2}\text{Diam}(\mathbb{T})})$	$O(e^{2t\rho_{\max}} \text{Diam}(\mathbb{T}))$	$O(\psi \text{Diam}(\mathbb{T}))$
HMM	$O(\psi(\frac{9}{2})^{\text{Diam}(\mathbb{T})})$	$O(\psi \log \text{Diam}(\mathbb{T}))$	$O(e^{2t\rho_{\max}} \log \text{Diam}(\mathbb{T}))$	$O(\psi \log \text{Diam}(\mathbb{T}))$
Full m -tree	$O(\psi(\frac{9}{2})^{\text{Diam}(\mathbb{T})})$	$O(\psi \text{Diam}(\mathbb{T}))$	N.A.	N.A.
Double star	$O(\psi \log d_{\max})$	$O(\psi \log d_{\max})$	N.A.	N.A.

Table 1: The sample complexities of RRG, RCLRG, RSNJ and RNJ on the double-binary tree, the HMM, the full m -tree and the double star. We set $\psi := e^{2\rho_{\max}/l_{\max}}$ and $t = O(l_{\max}^{-1} + \log |\mathcal{V}_{\text{obs}}|)$.

3.6 Experimental results

We present simulation results to demonstrate the efficacy of the robustified algorithms. Samples are generated from a HMM with $l_{\max} = 3$ and $\text{Diam}(\mathbb{T}) = 80$. The Robinson-Foulds distance [21] between the true and estimated trees is adopted to measure the performances of the algorithms. For the implementations of CLRG and RG, we use the code from [4]. Other settings and more extensive experiments are given in Appendix L.

We consider three corruption patterns here. (i) *Uniform corruptions* are independent additive noises in $[-2A, 2A]$; (ii) *Constant magnitude corruptions* are also independent additive noises but taking values in $\{-A, +A\}$ with probability 0.5. These two types of noises are distributed randomly in \mathbf{X}_1^n ; (iii) *HMM corruptions* are generated by a HMM which has the same structure as the original

HMM but has different parameters. They replace the entries in \mathbf{X}_1^n with samples generated by the variables in the same positions. In our simulations, A is set to 60, and the number of corruptions n_1 is 100.

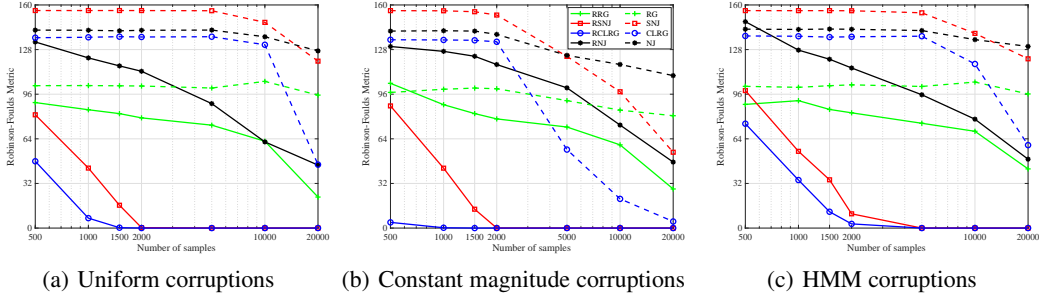


Figure 2: Robinson-Foulds distances of robustified and original algorithms averaged over 100 trials

Fig. 2 (error bars are in Appendix L.1) demonstrates the superiority of RCLRG in learning HMMs compared to other algorithms. The robustified algorithms also result in smaller estimation errors (Robinson-Foulds distances) compared to their unrobustified counterparts in presence of corruptions.

4 Impossibility result

Definition 5. Given a triple $(|\mathcal{V}_{\text{obs}}|, \rho_{\text{max}}, l_{\text{max}})$, the set $\mathcal{T}(|\mathcal{V}_{\text{obs}}|, \rho_{\text{max}}, l_{\text{max}})$ consists of all multi-variate Gaussian distributions $\mathcal{N}(\mathbf{0}, \Sigma)$ such that: (1) The underlying graph $\mathbb{T} = (\mathcal{V}, \mathcal{E})$ is a tree $\mathbb{T} \in \mathcal{T}_{\geq 3}$, and the size of the set of observed nodes is $|\mathcal{V}_{\text{obs}}|$. (2) The distribution $\mathcal{N}(\mathbf{0}, \Sigma)$ satisfies Assumptions 1 and 5 with parameters l_{max} and ρ_{max} .

For the given class of graphical models $\mathcal{T}(|\mathcal{V}_{\text{obs}}|, \rho_{\text{max}}, l_{\text{max}})$, nature chooses some parameter $\theta = \Sigma$ and generates n i.i.d. samples \mathbf{X}_1^n from \mathbb{P}_{θ} . The goal of the statistician is to use the observations \mathbf{X}_1^n to learn the underlying graph \mathbb{T} , which entails the design of a decoder $\phi : \mathbb{R}^{n \times |\mathcal{V}_{\text{obs}}| l_{\text{max}}} \rightarrow \mathcal{T}_{|\mathcal{V}_{\text{obs}}|}$, where $\mathcal{T}_{|\mathcal{V}_{\text{obs}}|}$ is the set of latent trees whose size of the observed node set is $|\mathcal{V}_{\text{obs}}|$.

Theorem 5. Consider the class of graphical models $\mathcal{T}(|\mathcal{V}_{\text{obs}}|, \rho_{\text{max}}, l_{\text{max}})$, where $|\mathcal{V}_{\text{obs}}| \geq 3$. If there exists a graph decoder learns from n i.i.d. samples such that

$$\max_{\theta(\mathbb{T}) \in \mathcal{T}(|\mathcal{V}_{\text{obs}}|, \rho_{\text{max}}, l_{\text{max}})} \mathbb{P}_{\theta(\mathbb{T})}(\phi(\mathbf{X}_1^n) \neq \mathbb{T}) < \delta, \quad (22)$$

then (as $\rho_{\text{max}} \rightarrow \infty$ and $|\mathcal{V}_{\text{obs}}| \rightarrow \infty$),

$$n = \max \left\{ \Omega \left((1 - \delta) e^{\frac{\rho_{\text{max}}}{\lceil \log_3 |\mathcal{V}_{\text{obs}} \rceil l_{\text{max}}} \log |\mathcal{V}_{\text{obs}}|} \right), \Omega \left((1 - \delta) e^{\frac{2\rho_{\text{max}}}{3l_{\text{max}}}} \right) \right\}. \quad (23)$$

Theorem 5 implies that the optimal sample complexity grows as $\Omega(\log |\mathcal{V}_{\text{obs}}|)$ as $|\mathcal{V}_{\text{obs}}|$ grows. To prove this theorem, we construct several classes of Gaussian latent trees parametrized as linear dynamical systems (see Appendix M) and apply the ubiquitous Fano technique to derive the desired impossibility result. Table 1 indicates that the sample complexity of RCLRG when the underlying latent tree is a full m -tree (for $m \geq 3$) or a HMM is optimal in the dependence on $|\mathcal{V}_{\text{obs}}|$. The sample complexity of RNJ is also optimal in $|\mathcal{V}_{\text{obs}}|$ for double binary trees and HMMs. In contrast, the derived sample complexities of RRG and RSNJ are suboptimal in relation to Theorem 5. However, one caveat of our analyses of the latent tree learning algorithms in Section 3 is that we are not claiming that they are the best possible for the given algorithm; there may be room for improvement.

When the maximum information distance ρ_{max} grows, Theorem 5 indicates that the optimal sample complexity grows as $\Omega(e^{\frac{2\rho_{\text{max}}}{3l_{\text{max}}}})$. Table 1 shows the sample complexities of RRG, RCLRG and RNJ grow as $O(e^{2\frac{\rho_{\text{max}}}{l_{\text{max}}}})$, which has the alike dependence as the impossibility result. However, the sample complexity of RSNJ grows as $O(e^{2t\rho_{\text{max}}})$, which is larger (looser) than that prescribed by Theorem 5.

5 Conclusions and future works

In this paper, we first derived the more refined sample complexities of RG and CLRG. The effectiveness of CLRG was observed to be due to the reduction in the effective length that the error propagates, i.e., from L_R to $L_C \ll L_R$. Second, to combat potential adversarial corruptions in the data matrix, we robustified RG, CLRG, NJ and SNJ by adopting the truncated inner product technique. The derived sample complexity results showed that all the common latent tree learning algorithms can tolerate level- $O\left(\frac{\sqrt{n_2}}{\log n_2}\right)$ arbitrary corruptions. The varying efficacies of these robustified algorithms were then corroborated through extensive simulations with different types of corruptions and on different graphs. Finally, we derived the first known instance-dependent impossibility result for learning latent trees. The optimalities of RCLRG and RNJ in their dependencies on $|\mathcal{V}_{\text{obs}}|$ were also discussed in the context of various latent tree structures.

There are several promising avenues for future research. First, the design and analysis of the initialization process of CLRG can be further improved. The correctness of CLRG relies only on the fact that if a hidden node is contracted to an observed node, then *all* the hidden nodes on the path between the hidden node and the observed nodes are contracted to the *same* observed node. One can conceive of a more general initialization algorithm other than that using the MST of the weighted graph with weights being the information distances. Second, the analysis of RG can be tightened with more sophisticated concentration bounds. In particular, the exponential behavior of the sample complexity of RG can also be refined by performing a more careful analysis of the error propagation through the learned tree.

Acknowledgements We would like to thank the NeurIPS reviewers for their valuable and detailed reviews. This work is supported by a National University of Singapore (NUS) President’s Graduate Fellowship, Singapore National Research Foundation (NRF) Fellowship (R-263-000-D02-281), a Singapore Ministry of Education (MoE) AcRF Tier 1 Grant (R-263-000-E80-114), and a Singapore MoE AcRF Tier 2 Grant (R-263-000-C83-112).

References

- [1] N. Saitou and M. Nei. The neighbor-joining method: a new method for reconstructing phylogenetic trees. *Mol. Bio. Evol.*, 4(4):406–425, 1987.
- [2] D. Tang, H. J. Chang, A. Tejani, and T. Kim. Latent regression forest: Structured estimation of 3d articulated hand posture. In *Proc. IEEE Conf. Computer Vision and Pattern Recognition*, pages 3786–3793, 2014.
- [3] J. Eisenstein, B. O’Connor, N. A. Smith, and E. Xing. A latent variable model for geographic lexical variation. In *Proc. Conf. Empirical Methods in Natural Language Processing*, pages 1277–1287, 2010.
- [4] M. J. Choi, V. Y. F. Tan, A. Anandkumar, and A. S. Willsky. Learning latent tree graphical models. *Journal of Machine Learning Research*, 12:1771–1812, 2011.
- [5] A. Anandkumar, K. Chaudhuri, D. Hsu, S. M. Kakade M, L. Song, and T. Zhang. Spectral methods for learning multivariate latent tree structure. *arXiv preprint arXiv:1107.1283*, 2011.
- [6] A. Jaffe, N. Amsel, Y. Aizenbud, B. Nadler, J. T. Chang, and Y. Kluger. Spectral neighbor joining for reconstruction of latent tree models. *SIAM Journal on Mathematics of Data Science*, 3(1):113–141, 2021.
- [7] M. Casanellas, M. Garrote-Lopez, and P. Zwiernik. Robust estimation of tree structured models. *arXiv:2102.05472v1 [stat.ML]*, Feb. 2021.
- [8] A. Katiyar, J. Hoffmann, and C. Caramanis. Robust estimation of tree structured gaussian graphical models. In *International Conference on Machine Learning*, pages 3292–3300. PMLR, 2019.
- [9] K. E. Nikolakakis, D. S. Kalogerias, and A.D. Sarwate. Learning tree structures from noisy data. In *Proc. Artificial Intelligence and Statistics*, pages 1771–1782. PMLR, 2019.

- [10] A. Tandon, V. Y. F. Tan, and S. Zhu. Exact asymptotics for learning tree-structured graphical models: Noiseless and noisy samples. *IEEE Journal on Selected Areas of Information Theory*, 1(3):760–776, 2020.
- [11] A. Tandon, A. H. J. Yuan, and V. Y. F. Tan. SGA: A robust algorithm for partial recovery of tree-structured graphical models with noisy samples. In *International Conference on Machine Learning*. PMLR, 2021.
- [12] L. Wang and Q. Gu. Robust gaussian graphical model estimation with arbitrary corruption. In *International Conference on Machine Learning*, pages 3617–3626. PMLR, 2017.
- [13] A. P. Parikh, L. Song, and E. P. Xing. A spectral algorithm for latent tree graphical models. In *International Conference on Machine Learning*, pages 1065–1072, Jun. 2011.
- [14] C. Chow and C. Liu. Approximating discrete probability distributions with dependence trees. *IEEE Trans. Inform. Theory*, 14(3):462–467, 1968.
- [15] Y. Chen, C. Caramanis, and S. Mannor. Robust high dimensional sparse regression and matching pursuit. *arXiv preprint arXiv:1301.2725*, 2013.
- [16] S. L. Lauritzen. *Graphical models*, volume 17. Clarendon Press, 1996.
- [17] V. Y. F. Tan, A. Anandkumar, and A. S. Willsky. Learning Gaussian tree models: Analysis of error exponents and extremal structures. *IEEE Transactions on Signal Processing*, 58(10):2701–2714, 2010.
- [18] P. Judea. *Probabilistic reasoning in intelligent systems: Networks of plausible inference*. Elsevier, 2014.
- [19] F. Huang, N. U. Naresh, I. Perros, R. Chen, J. Sun, and A. Anandkumar. Guaranteed scalable learning of latent tree models. In *Uncertainty in Artificial Intelligence*, pages 883–893. PMLR, 2020.
- [20] K. Atteson. The performance of neighbor-joining methods of phylogenetic reconstruction. *Algorithmica*, 25(2):251–278, 1999.
- [21] D. F. Robinson and L. R. Foulds. Comparison of phylogenetic trees. *Mathematical Biosciences*, 53(1-2):131–147, 1981.
- [22] R. Vershynin. *Introduction to the non-asymptotic analysis of random matrices*. Cambridge University Press, New York, NY, 2010.
- [23] G. H. Golub and C. F. Van Loan. *Matrix Computations*. The Johns Hopkins University Press, Maryland, US, 2013.
- [24] G. W. Stewart. Perturbation theory for the singular value decomposition. *SVD and Signal Processing, II: Algorithms, Analysis and Applications*, pages 99–109, 1991.
- [25] S. Pettie and V. Ramachandran. An optimal minimum spanning tree algorithm. *J. ACM*, 49(1):16–34, 2002.
- [26] W. Wang, M. J. Wainwright, and K. Ramchandran. Information-theoretic bounds on model selection for Gaussian markov random fields. In *Proc. IEEE Int. Symp. on Inf. Theory*, pages 1373–1377, Austin, Texas, USA, Jun. 2010. IEEE.
- [27] M. Marcus and W. Gordon. An extension of the Minkowski determinant theorem. *Proceedings of the Edinburgh Mathematical Society*, 17(4):321–324, 1971.

Supplementary materials for the NeurIPS 2021 submission “Robustifying Algorithms of Learning Latent Trees with Vector Variables”

A Illustrations of corruption patterns in Section 2.1

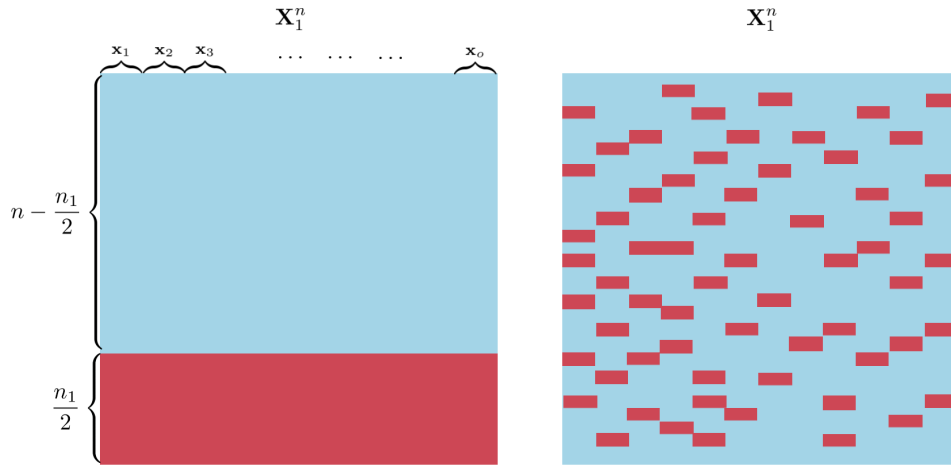


Figure 3: The left figure shows the corruption pattern that corrupted terms lie *in the same rows*. This corruption pattern is known as *outliers*. The right figure shows an *arbitrary corruption pattern* where corrupted entries in each column can be in *any* $n_1/2$ rows.

B Illustrations of active sets defined in Section 3.2

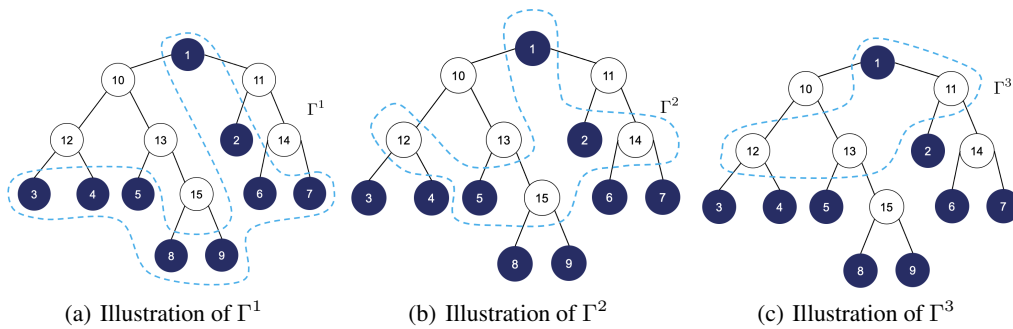


Figure 4: Illustration of active sets.

C Pseudo-code of RRG in Section 3.2

Algorithm 1 RRG

Input: Data matrix \mathbf{X} , corruption level n_1 , threshold ε

Output: Adjacency matrix \mathbf{A}

Procedure:

- 1: Active set $\Gamma^1 \leftarrow$ all the observed nodes
 - 2: Implement truncated inner product to compute $\hat{d}(x_i, x_j)$ for all $x_i, x_j \in \mathcal{V}_{\text{obs}}$.
 - 3: **while** $|\Gamma^i| > 2$ **do**
 - 4: Update $\hat{d}(x_{\text{new}}, x_i)$ for all $x_i \in \Gamma^i$ for all new hidden nodes.
 - 5: Compute $\hat{\Phi}_{ijk} = \hat{d}(x_i, x_k) - \hat{d}(x_j, x_k)$ for all $x_i, x_j, x_k \in \Gamma^i$
 - 6: **for** all nodes x_i and x_j in Γ^i **do**
 - 7: **if** $|\hat{\Phi}_{ijk} - \hat{\Phi}_{ijk'}| < \varepsilon$ for all $x_k, x_{k'} \in \Gamma^i$ **then**
 - 8: **if** $|\hat{\Phi}_{ijk} - \hat{d}(x_i, x_j)| < \varepsilon$ for all $x_k \in \Gamma^i$ **then**
 - 9: x_j is the parent of x_i .
 - 10: Eliminate x_i from Γ^i
 - 11: **else**
 - 12: x_j and x_i are siblings.
 - 13: Create a hidden node x_{new} as the parent of x_j and x_i
 - 14: Add x_{new} and eliminate x_j and x_i from Γ^i
 - 15: **end if**
 - 16: **end if**
 - 17: **end for**
 - 18: **end while**
-

D Pseudo-code of RSNJ in Section 3.3

Algorithm 2 RSNJ

Input: Data matrix \mathbf{X} , corruption level n_1

Output: Adjacent matrix \mathbf{A}

Procedure:

- 1: Implement truncated inner product to compute $\hat{d}(x_i, x_j)$ for all $x_i, x_j \in \mathcal{V}_{\text{obs}}$.
 - 2: Compute the symmetric affinity matrix $\hat{\mathbf{R}}$ as $\hat{\mathbf{R}}(i, j) = \exp(-\hat{d}(x_i, x_j))$ for all $x_i, x_j \in \mathcal{V}_{\text{obs}}$
 - 3: Set $B_i = \{x_i\}$ for all $x_i \in \Omega$
 - 4: Compute the matrix \mathbf{S} as $\hat{\mathbf{S}}(i, j) = \sigma_2(\hat{\mathbf{R}}^{B_i \cup B_j})$
 - 5: **while** The number of B_i 's is larger than 3 **do**
 - 6: Find $(\hat{i}, \hat{j}) = \arg \min_{i, j} \hat{\mathbf{S}}(i, j)$.
 - 7: Merge B_i and B_j as $\hat{B}_i = B_i \cup B_j$ and delete B_j .
 - 8: Update $\hat{\mathbf{S}}(k, \hat{i}) = \sigma_2(\hat{\mathbf{R}}^{B_k \cup \hat{B}_i})$.
 - 9: **end while**
-

E Pseudo-code of RCLRG in Section 3.4

Algorithm 3 RCLRG

Input: Data matrix \mathbf{X} , corruption level n_1 , threshold ε

Output: Adjacency matrix \mathbf{A}

Procedure:

- 1: Construct a Chow-Liu tree with $\hat{d}(x_j, x_k)$ for observed nodes $x_j, x_k \in \mathcal{V}_{\text{obs}}$
 - 2: Identify the set of internal nodes of the Chow-Liu tree
 - 3: **for** all internal nodes x_i of the Chow-Liu tree **do**
 - 4: Implement RRG algorithm on the closed neighborhood of x_i
 - 5: Replace the closed neighborhood of x_i with the output of RRG
 - 6: **end for**
-

F Illustrations of representative trees in Section 3.5

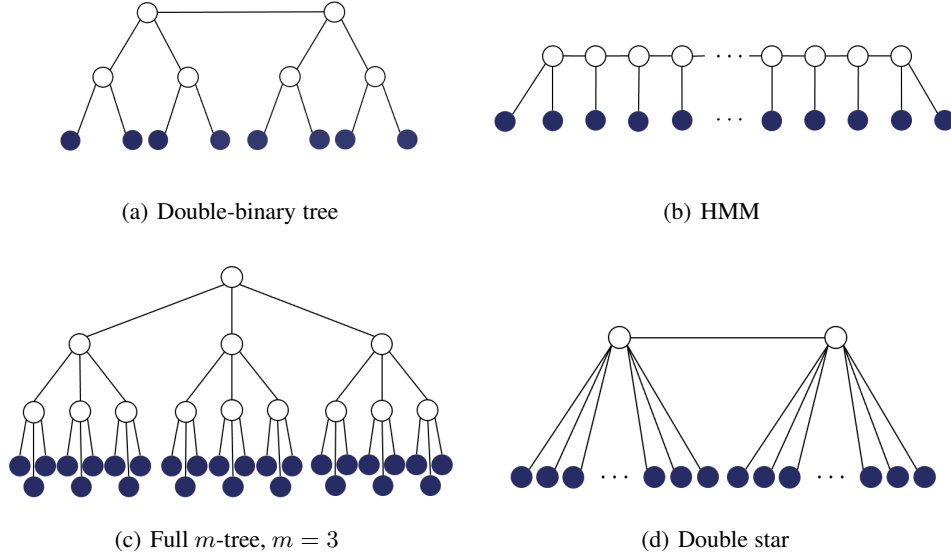


Figure 5: Representative tree structures.

G Proofs of results in Section 3.1

Proof of Proposition 1. For the sake of brevity, we prove the additivity property for paths of length 2. The proof for the general cases can be derived similarly. We consider the case x_j is on the path connected x_i and x_k and $x_i, x_j, x_k \in \mathcal{V}$.

For any square matrix $\mathbf{A} \in \mathbb{R}^{n \times n}$, the determinant of \mathbf{A} is denoted as $|\mathbf{A}| = \det(\mathbf{A})$.

Then we can write information distance as

$$d(x_i, x_k) = -\frac{1}{2} \log |\boldsymbol{\Sigma}_{ik} \boldsymbol{\Sigma}_{ik}^\top| + \frac{1}{4} \log |\boldsymbol{\Sigma}_{ii} \boldsymbol{\Sigma}_{ii}^\top| + \frac{1}{4} \log |\boldsymbol{\Sigma}_{kk} \boldsymbol{\Sigma}_{kk}^\top| \quad (\text{G.1})$$

Note that $\mathbb{E}[\mathbf{x}_i | \mathbf{x}_j] = \boldsymbol{\Sigma}_{ij} \boldsymbol{\Sigma}_{jj}^{-1} \mathbf{x}_j$ and $\boldsymbol{\Sigma}_{ij}$ is of full rank by Assumption 2, and

$$\mathbf{A}_{i|j} = \boldsymbol{\Sigma}_{ij} \boldsymbol{\Sigma}_{jj}^{-1} \quad (\text{G.2})$$

is also of full rank.

Furthermore, we have

$$\boldsymbol{\Sigma}_{ik} = \mathbf{A}_{i|j} \boldsymbol{\Sigma}_{jj} \mathbf{A}_{k|j}^\top \quad \text{and} \quad \boldsymbol{\Sigma}_{ik} \boldsymbol{\Sigma}_{ik}^\top = \mathbf{A}_{i|j} \boldsymbol{\Sigma}_{jj} \mathbf{A}_{k|j}^\top \mathbf{A}_{k|j} \boldsymbol{\Sigma}_{jj} \mathbf{A}_{i|j}^\top. \quad (\text{G.3})$$

Then we have

$$|\boldsymbol{\Sigma}_{ik}\boldsymbol{\Sigma}_{ik}^\top| = |\mathbf{A}_{i|j}\boldsymbol{\Sigma}_{jj}\mathbf{A}_{k|j}^\top\mathbf{A}_{k|j}\boldsymbol{\Sigma}_{jj}\mathbf{A}_{i|j}^\top| \quad (\text{G.4})$$

$$= |\mathbf{A}_{i|j}^\top\mathbf{A}_{i|j}\boldsymbol{\Sigma}_{jj}\mathbf{A}_{k|j}^\top\mathbf{A}_{k|j}\boldsymbol{\Sigma}_{jj}| \quad (\text{G.5})$$

$$= \frac{|\boldsymbol{\Sigma}_{jj}^\top\mathbf{A}_{i|j}^\top\mathbf{A}_{i|j}\boldsymbol{\Sigma}_{jj}| |\boldsymbol{\Sigma}_{jj}^\top\mathbf{A}_{k|j}^\top\mathbf{A}_{k|j}\boldsymbol{\Sigma}_{jj}|}{|\boldsymbol{\Sigma}_{jj}| |\boldsymbol{\Sigma}_{jj}|}. \quad (\text{G.6})$$

Furthermore,

$$|\boldsymbol{\Sigma}_{jj}^\top\mathbf{A}_{i|j}^\top\mathbf{A}_{i|j}\boldsymbol{\Sigma}_{jj}| = |\mathbf{A}_{i|j}\boldsymbol{\Sigma}_{jj}\boldsymbol{\Sigma}_{jj}^\top\mathbf{A}_{i|j}^\top| = |\boldsymbol{\Sigma}_{ij}\boldsymbol{\Sigma}_{ij}^\top|, \quad (\text{G.7})$$

$$|\boldsymbol{\Sigma}_{jj}^\top\mathbf{A}_{k|j}^\top\mathbf{A}_{k|j}\boldsymbol{\Sigma}_{jj}| = |\boldsymbol{\Sigma}_{kj}\boldsymbol{\Sigma}_{kj}^\top|. \quad (\text{G.8})$$

Substituting (G.4) and (G.7) into (G.1), we have

$$\begin{aligned} d(x_i, x_k) &= -\frac{1}{2}\log|\boldsymbol{\Sigma}_{ij}\boldsymbol{\Sigma}_{ij}^\top| + \frac{1}{4}\log|\boldsymbol{\Sigma}_{ii}\boldsymbol{\Sigma}_{ii}^\top| + \frac{1}{4}\log|\boldsymbol{\Sigma}_{jj}\boldsymbol{\Sigma}_{jj}^\top| \\ &\quad -\frac{1}{2}\log|\boldsymbol{\Sigma}_{kj}\boldsymbol{\Sigma}_{kj}^\top| + \frac{1}{4}\log|\boldsymbol{\Sigma}_{kk}\boldsymbol{\Sigma}_{kk}^\top| + \frac{1}{4}\log|\boldsymbol{\Sigma}_{jj}\boldsymbol{\Sigma}_{jj}^\top| \end{aligned} \quad (\text{G.9})$$

$$= d(x_i, x_j) + d(x_j, x_k), \quad (\text{G.10})$$

as desired. \square

Lemma 8. (Bernstein-type inequality [22]) Let X_1, \dots, X_n be n centered sub-exponential random variables, and $K = \max_{1 \leq i \leq n} \|X_i\|_{\psi_1}$, where $\|\cdot\|_{\psi_1}$ is the sub-exponential norm and is defined as

$$\|X\|_{\psi_1} := \sup_{p \geq 1} p^{-1} (\mathbb{E}|X|^p)^{1/p}. \quad (\text{G.11})$$

Then for every $a = (a_1, \dots, a_n) \in \mathbb{R}^n$ and every $t > 0$, we have

$$\mathbb{P}\left(\left|\sum_{i=1}^n a_i X_i\right| \geq t\right) \leq 2 \exp\left[-c \min\left\{\frac{t^2}{K^2\|a\|_2^2}, \frac{t}{K\|a\|_\infty}\right\}\right] \quad (\text{G.12})$$

Lemma 9. Let the estimate of the covariance matrix $\boldsymbol{\Sigma}_{ij}$ based on the truncated inner product be $\hat{\boldsymbol{\Sigma}}_{ij}$. If $t_2 < \kappa = \max\{\sigma_{\max}^2, \rho_{\min}\}$, we have

$$\mathbb{P}(\|\hat{\boldsymbol{\Sigma}}_{ij} - \boldsymbol{\Sigma}_{ij}\|_{\infty, \infty} > t_1 + t_2) \leq 2l_{\max}^2 e^{-\frac{3n_2}{16\kappa n_1} t_1} + l_{\max}^2 e^{-c\frac{t_2^2 n_2}{\kappa^2}} \quad \forall x_i, x_j \in \mathcal{V}_{\text{obs}}. \quad (\text{G.13})$$

Proof of Lemma 9. Let $I_{ij,1}^{st}$ be the set of indexes of the uncorrupted samples of $[\mathbf{x}_i]_s[\mathbf{x}_j]_t$. Without loss of generality, we assume that $|I_{ij,1}^{st}| = n_2$. Let $I_{ij,2}^{st}$ and $I_{ij,3}^{st}$ be the sets of the indexes of truncated uncorrupted samples and the reserved corrupted samples, respectively.

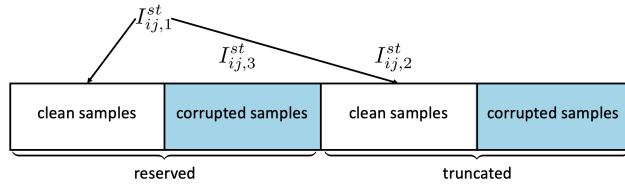


Figure 6: Illustration of the truncated inner product.

Then,

$$[\hat{\boldsymbol{\Sigma}}_{ij}]_{st} = \frac{1}{n_2} \left(\sum_{m \in I_{ij,1}^{st}} [\mathbf{x}_i]_s^{(m)} [\mathbf{x}_j]_t^{(m)} - \sum_{m \in I_{ij,2}^{st}} [\mathbf{x}_i]_s^{(m)} [\mathbf{x}_j]_t^{(m)} + \sum_{m \in I_{ij,3}^{st}} [\mathbf{x}_i]_s^{(m)} [\mathbf{x}_j]_t^{(m)} \right) \quad (\text{G.14})$$

The (s, t) th entry of the error covariance matrix $\tilde{\Sigma}_{ij} = \hat{\Sigma}_{ij} - \Sigma_{ij} \in \mathbb{R}^{d \times d}$ is defined as

$$[\tilde{\Sigma}_{ij}]_{st} = \frac{1}{n_2} \left(- \sum_{m \in I_{ij,2}^{st}} [\mathbf{x}_i]_s^{(m)} [\mathbf{x}_j]_t^{(m)} + \sum_{m \in I_{ij,3}^{st}} [\mathbf{x}_i]_s^{(m)} [\mathbf{x}_j]_t^{(m)} \right). \quad (\text{G.15})$$

From the definition of the truncated inner product, we can bound the right-hand side of (G.15) as

$$|[\tilde{\Sigma}_{ij}]_{st}| \leq \frac{2}{n_2} \sum_{m \in I_{ij,2}^{st}} |[\mathbf{x}_i]_s^{(m)} [\mathbf{x}_j]_t^{(m)}|. \quad (\text{G.16})$$

Equipped with the expression of the moment-generating function of a chi-squared distribution, the moment-generating function of each term in the sum of (G.16) can be upper bounded as

$$\mathbb{E} \left[e^{\lambda |[\mathbf{x}_i]_s^{(m)} [\mathbf{x}_j]_t^{(m)}|} \right] \leq \mathbb{E} \left[e^{\lambda \frac{([\mathbf{x}_i]_s^{(m)})^2 + ([\mathbf{x}_j]_t^{(m)})^2}{2}} \right] \quad (\text{G.17})$$

$$\leq \sqrt{\mathbb{E} [e^{\lambda ([\mathbf{x}_i]_s^{(m)})^2}] \mathbb{E} [e^{\lambda ([\mathbf{x}_j]_t^{(m)})^2}]} \quad (\text{G.18})$$

$$\leq \frac{1}{\sqrt{1 - 2\sigma_{\max}^2 \lambda}}. \quad (\text{G.19})$$

Using the power mean inequality, we have

$$\left(e^{\frac{2\lambda}{n_2} \sum_{m \in I_{ij,2}^{st}} |[\mathbf{x}_i]_s^{(m)} [\mathbf{x}_j]_t^{(m)}|} \right)^{\frac{1}{|I_{ij,2}^{st}|}} \leq \frac{\sum_{m \in I_{ij,2}^{st}} e^{\frac{2\lambda}{n_2} |[\mathbf{x}_i]_s^{(m)} [\mathbf{x}_j]_t^{(m)}|}}{|I_{ij,2}^{st}|} \quad (\text{G.20})$$

$$\leq \left(\frac{\sum_{m \in I_{ij,2}^{st}} e^{\frac{2\lambda n_1}{n_2} |[\mathbf{x}_i]_s^{(m)} [\mathbf{x}_j]_t^{(m)}|}}{|I_{ij,2}^{st}|} \right)^{\frac{1}{n_1}}. \quad (\text{G.21})$$

Thus,

$$\mathbb{E} \left[e^{\lambda |[\tilde{\Sigma}_{ij}]_{st}|} \right] \leq \mathbb{E} \left[e^{\frac{2\lambda}{n_2} \sum_{m \in I_{ij,2}^{st}} |[\mathbf{x}_i]_s^{(m)} [\mathbf{x}_j]_t^{(m)}|} \right] \leq \max_{m \in I_{ij,2}^{st}} \mathbb{E} \left[e^{\frac{2\lambda n_1}{n_2} |[\mathbf{x}_i]_s^{(m)} [\mathbf{x}_j]_t^{(m)}|} \right] \quad (\text{G.22})$$

$$\leq \frac{1}{\sqrt{1 - \frac{4\sigma_{\max}^2 n_1}{n_2} \lambda}} \quad (\text{G.23})$$

and

$$\mathbb{E} \left[e^{\lambda \max_{s,t} |[\tilde{\Sigma}_{ij}]_{st}|} \right] = \mathbb{E} \left[\max_{s,t} e^{\lambda |[\tilde{\Sigma}_{ij}]_{st}|} \right] \leq l_{\max}^2 \mathbb{E} \left[e^{\lambda |[\tilde{\Sigma}_{ij}]_{st}|} \right] \leq \frac{l_{\max}^2}{\sqrt{1 - \frac{4\sigma_{\max}^2 n_1}{n_2} \lambda}}. \quad (\text{G.24})$$

Thus,

$$\mathbb{P}(\|\tilde{\Sigma}_{ij}\|_{\infty, \infty} > t) = \mathbb{P} \left(\max_{s,t} |[\tilde{\Sigma}_{ij}]_{st}| > t \right) = \mathbb{P} \left(e^{\lambda \max_{s,t} |[\tilde{\Sigma}_{ij}]_{st}|} > e^{\lambda t} \right) \quad (\text{G.25})$$

$$\leq e^{-\lambda t} \mathbb{E} \left[e^{\lambda \max_{s,t} |[\tilde{\Sigma}_{ij}]_{st}|} \right] \leq e^{-\lambda t} \frac{l_{\max}^2}{\sqrt{1 - \frac{4\sigma_{\max}^2 n_1}{n_2} \lambda}}. \quad (\text{G.26})$$

Let $\lambda = \frac{3n_2}{16\sigma_{\max}^2 n_1}$, then we have

$$\mathbb{P}(\|\tilde{\Sigma}_{ij}\|_{\infty, \infty} > t) \leq 2l_{\max}^2 e^{-\frac{3n_2}{16\sigma_{\max}^2 n_1} t}. \quad (\text{G.27})$$

According to Lemma 8 (since the involved random variables are sub-exponential), we have

$$\mathbb{P} \left(\left| \frac{1}{n_2} \sum_{m \in I_{ij,1}^{st}} ([\mathbf{x}_i]_s^{(m)} [\mathbf{x}_j]_t^{(m)} - [\Sigma_{ij}]_{st}) \right| > t \right) \leq \exp \left(-c \min \left\{ \frac{t^2 n_2}{K^2}, \frac{tn_2}{K} \right\} \right), \quad (\text{G.28})$$

where $K = \sigma_{\max}^2$.

Thus, if $t < \kappa$, we have

$$\mathbb{P}(\|\hat{\Sigma}_{ij} - \Sigma_{ij}\|_{\infty, \infty} > t_1 + t_2) \leq 2l_{\max}^2 e^{-\frac{3n_2}{16\kappa n_1} t_1} + l_{\max}^2 e^{-c \frac{t_2^2 n_2}{\kappa^2}}, \quad (\text{G.29})$$

as desired. \square

Proof of Proposition 2. From the definition of the information distance, we have

$$d(x_i, x_j) = - \sum_{n=1}^{l_{\max}} \log \sigma_n(\mathbf{\Sigma}_{ij}) + \frac{1}{2} \log \det(\mathbf{\Sigma}_{ii}) + \frac{1}{2} \log \det(\mathbf{\Sigma}_{jj}). \quad (\text{G.30})$$

According to the inequality $\|\mathbf{A}\|_2 \leq \sqrt{\|\mathbf{A}\|_1 \|\mathbf{A}\|_\infty}$ which holds for all $\mathbf{A} \in \mathbb{R}^{n \times m}$ [23], we have

$$|\sigma_k(\hat{\mathbf{\Sigma}}_{ij}) - \sigma_k(\mathbf{\Sigma}_{ij})| \leq \|\hat{\mathbf{\Sigma}}_{ij} - \mathbf{\Sigma}_{ij}\|_2 \quad (\text{G.31})$$

$$\leq \sqrt{\|\hat{\mathbf{\Sigma}}_{ij} - \mathbf{\Sigma}_{ij}\|_\infty \|\hat{\mathbf{\Sigma}}_{ij} - \mathbf{\Sigma}_{ij}\|_1} \leq l_{\max} \|\hat{\mathbf{\Sigma}}_{ij} - \mathbf{\Sigma}_{ij}\|_{\infty, \infty}. \quad (\text{G.32})$$

Using the triangle inequality, we arrive at

$$\begin{aligned} |\hat{d}(x_i, x_j) - d(x_i, x_j)| &\leq \sum_{n=1}^{l_{\max}} |\log \sigma_n(\hat{\mathbf{\Sigma}}_{ij}) - \log \sigma_n(\mathbf{\Sigma}_{ij})| + \frac{1}{2} \sum_{n=1}^{\dim(\mathbf{x}_i)} |\log \sigma_n(\hat{\mathbf{\Sigma}}_{ii}) - \log \sigma_n(\mathbf{\Sigma}_{ii})| \\ &\quad + \frac{1}{2} \sum_{n=1}^{\dim(\mathbf{x}_j)} |\log \sigma_n(\hat{\mathbf{\Sigma}}_{jj}) - \log \sigma_n(\mathbf{\Sigma}_{jj})|. \end{aligned} \quad (\text{G.33})$$

Furthermore, since the singular value is lower bounded by γ_{\min} , using Taylor's theorem and (G.31), we obtain

$$|\log \sigma_n(\hat{\mathbf{\Sigma}}_{ij}) - \log \sigma_n(\mathbf{\Sigma}_{ij})| \leq \frac{1}{\gamma_{\min}} |\sigma_n(\hat{\mathbf{\Sigma}}_{ij}) - \sigma_n(\mathbf{\Sigma}_{ij})| \leq \frac{l_{\max}}{\gamma_{\min}} \|\hat{\mathbf{\Sigma}}_{ij} - \mathbf{\Sigma}_{ij}\|_{\infty, \infty}. \quad (\text{G.34})$$

Finally,

$$\begin{aligned} |\hat{d}(x_i, x_j) - d(x_i, x_j)| &\leq \left(l_{\max} + \frac{\dim(\mathbf{x}_i) + \dim(\mathbf{x}_j)}{2} \right) \frac{l_{\max}}{\gamma_{\min}} \|\hat{\mathbf{\Sigma}}_{ij} - \mathbf{\Sigma}_{ij}\|_{\infty, \infty} \\ &\leq \frac{2l_{\max}^2}{\gamma_{\min}} \|\hat{\mathbf{\Sigma}}_{ij} - \mathbf{\Sigma}_{ij}\|_{\infty, \infty}. \end{aligned} \quad (\text{G.35})$$

From Lemma 9, the proposition is proved. \square

H Proofs of results in Section 3.2

Lemma 10. Consider the optimization problem

$$\begin{aligned} \mathcal{P} : \quad &\max_{\{x_i\}} f(\mathbf{x}) = \sum_{i=1}^n x_i(x_i - 1) \\ &\text{s.t.} \quad \sum_{i=1}^N x_i \leq N \quad 0 \leq x_i \leq k \quad i = 1, \dots, N. \end{aligned} \quad (\text{H.1})$$

Assume $nk \geq N$. An optimal solution is given by $x_i = k$ for all $i = 1, \dots, \lfloor \frac{N}{k} \rfloor$ and $x_{\lfloor \frac{N}{k} \rfloor + 1} = N - k \lfloor \frac{N}{k} \rfloor$, and $x_i = 0$ for $i = \lfloor \frac{N}{k} \rfloor + 2, \dots, n$.

This lemma can be verified by direct calculation, and so we will omit the details.

Proof of Proposition 4. We prove the proposition by induction.

Proposition 2 and Eqn. (6) show that at the 0th layer [24]

$$\mathbb{P}(|\Delta_{ij}| > \varepsilon) < f(\varepsilon) = h^{(0)}(\varepsilon). \quad (\text{H.2})$$

Now suppose that the distances related to the nodes created in the $(l-1)$ st iteration satisfy

$$\mathbb{P}\left(|\hat{d}(x_i, x_h) - d(x_i, x_h)| > \varepsilon\right) < h^{(l-1)}(\varepsilon). \quad (\text{H.3})$$

Since $s > 1$ and $m < 1$, it is obvious that

$$h^{(l)}(\varepsilon) \leq h^{(l+k)}(\varepsilon) \quad \text{for all } l, k \in \mathbb{N} \quad \text{and for all } \varepsilon > 0. \quad (\text{H.4})$$

Then we can deduce that

$$\mathbb{P}(|\hat{d}(x_i, x_j) - d(x_i, x_j)| > \varepsilon) < h^{(l-1)}(\varepsilon) \quad \text{for all } x_i, x_j \in \Gamma^l. \quad (\text{H.5})$$

From the update equation of the distance in (9), we have

$$\hat{d}(x_i, x_h) = \frac{1}{2(|\mathcal{C}(h) - 1|)} \left(\sum_{j \in \mathcal{C}(h)} (d(x_i, x_j) + \Delta_{ij}) + \frac{1}{|\mathcal{K}_{ij}|} \sum_{k \in \mathcal{K}_{ij}} (\Phi_{ijk} + \Delta_{ik} - \Delta_{jk}) \right) \quad (\text{H.6})$$

and

$$\hat{d}(x_i, x_h) = \frac{1}{2(|\mathcal{C}(h) - 1|)} \left(\sum_{j \in \mathcal{C}(h)} \Delta_{ij} + \frac{1}{|\mathcal{K}_{ij}|} \sum_{k \in \mathcal{K}_{ij}} (\Delta_{ik} - \Delta_{jk}) \right) + d(x_i, x_h). \quad (\text{H.7})$$

Using the union bound, we find that

$$\begin{aligned} & \mathbb{P}\left(|\hat{d}(x_i, x_h) - d(x_i, x_h)| > \varepsilon\right) \\ & \leq \mathbb{P}\left(\bigcup_{j \in \mathcal{C}(h)} \left\{ \left| \Delta_{ij} + \frac{1}{|\mathcal{K}_{ij}|} \sum_{k \in \mathcal{K}_{ij}} (\Delta_{ik} - \Delta_{jk}) \right| > 2\varepsilon \right\}\right) \end{aligned} \quad (\text{H.8})$$

$$\leq \sum_{j \in \mathcal{C}(h)} \mathbb{P}\left(\left| \Delta_{ij} + \frac{1}{|\mathcal{K}_{ij}|} \sum_{k \in \mathcal{K}_{ij}} (\Delta_{ik} - \Delta_{jk}) \right| > 2\varepsilon\right) \quad (\text{H.9})$$

$$\leq \sum_{j \in \mathcal{C}(h)} \left[\mathbb{P}\left(|\Delta_{ij}| > \frac{2}{3}\varepsilon\right) + \sum_{k \in \mathcal{K}_{ij}} \mathbb{P}\left(|\Delta_{ik}| > \frac{2}{3}\varepsilon\right) + \mathbb{P}\left(|\Delta_{jk}| > \frac{2}{3}\varepsilon\right) \right]. \quad (\text{H.10})$$

The estimates of the distances related to the nodes in the l^{th} layer satisfy

$$\mathbb{P}\left(|\hat{d}(x_i, x_h) - d(x_i, x_h)| > \varepsilon\right) < |\mathcal{C}(h)|(1 + 2|\mathcal{K}_{ij}|)h^{(l-1)}\left(\frac{2}{3}\varepsilon\right) \quad (\text{H.11})$$

$$\leq d_{\max}(1 + 2N_\tau)h^{(l-1)}\left(\frac{2}{3}\varepsilon\right). \quad (\text{H.12})$$

Similarly, from (10), we have

$$\begin{aligned} & \mathbb{P}\left(|\hat{d}(x_k, x_h) - d(x_k, x_h)| > \varepsilon\right) \\ & \leq \begin{cases} \sum_{i \in \mathcal{C}(h)} \mathbb{P}\left(|\Delta_{ik}| > \frac{1}{2}\varepsilon\right) + \mathbb{P}\left(|\Delta_{ih}| > \frac{1}{2}\varepsilon\right), & \text{if } k \in \mathcal{V}_{\text{obs}} \\ \sum_{(i,j) \in \mathcal{C}(h) \times \mathcal{C}(k)} \mathbb{P}\left(|\Delta_{ij}| > \frac{1}{3}\varepsilon\right) + \mathbb{P}\left(|\Delta_{ih}| > \frac{1}{3}\varepsilon\right) + \mathbb{P}\left(|\Delta_{jk}| > \frac{1}{3}\varepsilon\right), & \text{otherwise.} \end{cases} \end{aligned} \quad (\text{H.13})$$

Using the concentration bound at the $(l-1)^{\text{st}}$ layer in inequality (H.3), we have

$$\begin{aligned} & \mathbb{P}\left(|\hat{d}(x_k, x_h) - d(x_k, x_h)| > \varepsilon\right) \\ & \leq \begin{cases} d_{\max}h^{(l-1)}\left(\frac{1}{2}\varepsilon\right) + d_{\max}^2(1 + 2N_\tau)h^{(l-1)}\left(\frac{1}{3}\varepsilon\right), & \text{if } k \in \mathcal{V}_{\text{obs}} \\ d_{\max}^2h^{(l-1)}\left(\frac{2}{3}\varepsilon\right) + 2d_{\max}^3(1 + 2N_\tau)h^{(l-1)}\left(\frac{2}{9}\varepsilon\right), & \text{otherwise.} \end{cases} \end{aligned} \quad (\text{H.14})$$

Summarizing the above three concentration bounds, we have that for the nodes at the l^{th} layer, estimates of the information distances (based on the truncated inner product) satisfy

$$\mathbb{P}\left(|\hat{d}(x_k, x_h) - d(x_k, x_h)| > \varepsilon\right) < [d_{\max}^2 + 2d_{\max}^3(1 + 2N_\tau)]h^{(l-1)}\left(\frac{2}{9}\varepsilon\right) = h^{(l)}(\varepsilon). \quad (\text{H.15})$$

□

Proposition 11. *The cardinalities of the active sets in l^{th} and $(l+1)^{\text{st}}$ iterations admit following relationship*

$$\frac{|\Gamma^l|}{d_{\max}} \leq |\Gamma^{l+1}| \leq |\Gamma^l| - 2. \quad (\text{H.16})$$

Proof of Proposition 11. Note that at the l^{th} iteration, the number of families is $|\Gamma^{l+1}|$, and thus we have

$$\sum_{i=1}^{|\Gamma^{l+1}|} n_i = |\Gamma^l|, \quad (\text{H.17})$$

where n_i is the number of nodes in Γ^l in each family. Since $1 \leq n_i \leq d_{\max}$, we have $\frac{|\Gamma^l|}{d_{\max}} \leq |\Gamma^{l+1}|$.

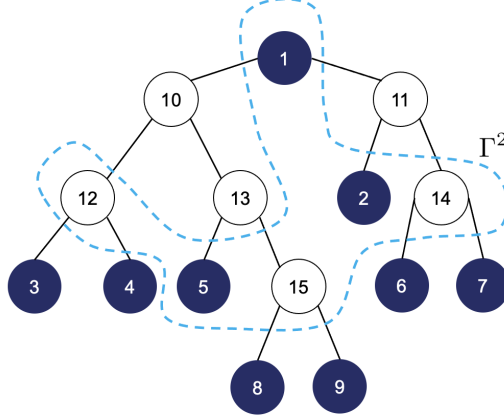


Figure 7: Illustration of RRG. The shaded nodes are the observed nodes and the rest are hidden nodes. $\Gamma^1 = \{x_1, x_2, \dots, x_9\}$, and Γ^2 is the nodes in the dotted lines. If we delete the nodes in Γ^2 , the remained unknown hidden nodes are x_{10} , x_{11} and x_{13} . Nodes x_{10} and x_{13} are at the end of the chain formed by these two nodes, and x_{11} is at the end of the degenerate chain formed by itself.

We next prove that there are at least two of n_i 's not less than 2. If we delete the nodes in active set Γ^l , the remaining hidden nodes form a single tree or a forest. There will at least two nodes at the end of the chain, which means that they only have one neighbor in hidden nodes, as shown in Fig. 7. Since they at least have three neighbors, they have at least two neighbors in Γ^l . Thus, there are at least two of n_i 's not less than 2, and thus $|\Gamma^{l+1}| \leq |\Gamma^l| - 2$. \square

Corollary 1. *The maximum number of iterations of Algorithm 1, L_R , is bounded as*

$$\frac{\log \frac{|\mathcal{V}_{\text{obs}}|}{2}}{\log d_{\max}} \leq L_R \leq |\mathcal{V}_{\text{obs}}| - 2. \quad (\text{H.18})$$

Proof. When Algorithm 1 terminates, $|\Gamma| \leq 2$. Combining Proposition 11 and $|\Gamma| \leq 2$ proves the corollary. \square

Theorem 6. *Under Assumptions 1–5, RRG algorithm constructs the correct latent tree with probability at least $1 - \eta$ if*

$$n_2 \geq \frac{64\lambda^2\kappa^2}{c\varepsilon^2} \left(\frac{9}{2}\right)^{2L_R-2} \log \frac{17l_{\max}^2 s^{L_R-1} |\mathcal{V}_{\text{obs}}|^3}{\eta} \quad (\text{H.19})$$

$$\frac{n_2}{n_1} \geq \frac{128\lambda\kappa}{3\varepsilon} \left(\frac{9}{2}\right)^{L_R-1} \log \frac{34l_{\max}^2 s^{L_R-1} |\mathcal{V}_{\text{obs}}|^3}{\eta}, \quad (\text{H.20})$$

where

$$\lambda = \frac{2l_{\max}^2 e^{\rho_{\max}/l_{\max}}}{\delta_{\min}^{1/l_{\max}}} \quad \kappa = \max\{\sigma_{\max}^2, \rho_{\min}\} \quad s = d_{\max}^2 + 2d_{\max}^3(1 + 2N_\tau) \quad \varepsilon = \frac{\rho_{\min}}{2}, \quad (\text{H.21})$$

c is an absolute constant, and L_R is the number of iterations of RRG needed to construct the tree.

Proof of Theorem 6. It is easy to see by substituting the constants λ , κ , s and ε into (H.19) and (H.20) that Theorem 6 implies Theorem 1, so we provide the proof of Theorem 6 here.

The error events of learning structure in the l^{th} layer of the latent tree (the 0^{th} layer consists of the observed nodes, and the $(l+1)^{\text{st}}$ layer is the active set formed from l^{th} layer). The error events could be enumerated as: misclassification of families \mathcal{E}_f^l , misclassification of non-families $\mathcal{E}_{\text{nf}}^l$, misclassification of parents \mathcal{E}_p^l and misclassification of siblings \mathcal{E}_s^l . We will bound the probabilities of these four error events in the following.

The event representing misclassification of families \mathcal{E}_f^l represents classifying the nodes that are not in the same family as a family. Suppose nodes x_i and x_j are in different families. The event that classifying them to be in the same family $\mathcal{E}_{f,i,j}^l$ at layer l can be expressed as

$$\mathcal{E}_{f,i,j}^l = \{|\hat{\Phi}_{ijk} - \hat{\Phi}_{ijk'}| < \varepsilon \text{ for all } x_k, x_{k'} \in \Gamma^l\}. \quad (\text{H.22})$$

We have

$$\mathbb{P}(\mathcal{E}_{f,i,j}^l) = \mathbb{P}\left(\bigcap_{x_k, x_{k'} \in \Gamma} \{|\hat{\Phi}_{ijk} - \hat{\Phi}_{ijk'}| < \varepsilon\}\right) \leq \min_{x_k, x_{k'} \in \Gamma} \mathbb{P}\left(|\hat{\Phi}_{ijk} - \hat{\Phi}_{ijk'}| < \varepsilon\right), \quad (\text{H.23})$$

$$\mathbb{P}(\mathcal{E}_f^l) = \mathbb{P}\left(\bigcup_{x_i, x_j \text{ not in same family}} \mathcal{E}_{f,i,j}^l\right) = \mathbb{P}\left(\bigcup_{(x_i, x_j) \in \Gamma_f^l} \mathcal{E}_{f,i,j}^l\right). \quad (\text{H.24})$$

We enumerate all possible structural relationships between x_i, x_j, x_k and $x_{k'}$

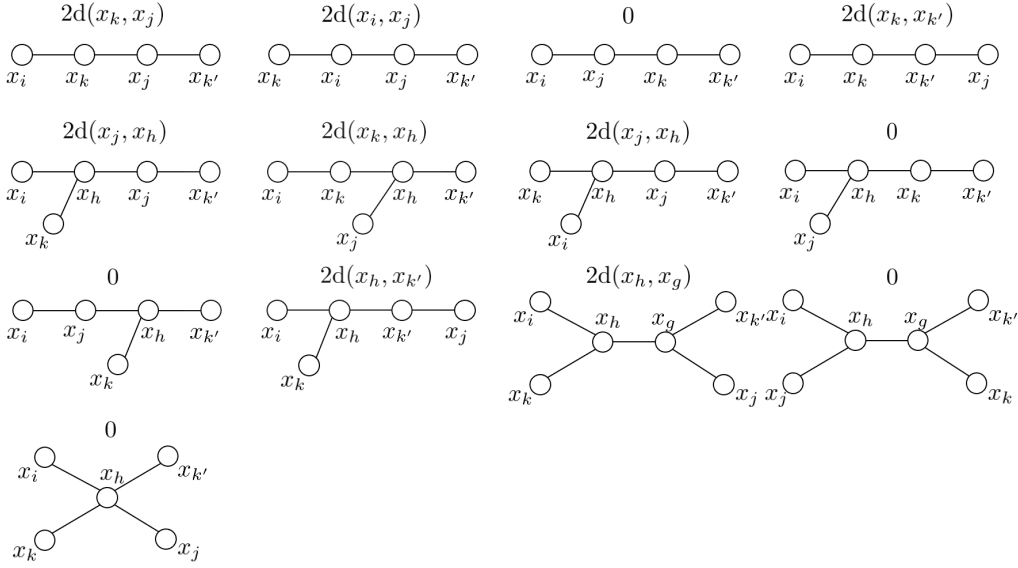


Figure 8: Enumerating of four-node topology and the corresponding $|\Phi_{ijk} - \Phi_{ijk'}|$.

Let $\varepsilon < 2\rho_{\min}$, by decomposing the estimate of the information distance as $\hat{d}(x_i, x_j) = d(x_i, x_j) + \Delta_{ij}$, we have

$$\begin{aligned} \mathbb{P}\left(|\hat{\Phi}_{ijk} - \hat{\Phi}_{ijk'}| < \varepsilon\right) &= \mathbb{P}\left(|\Phi_{ijk} - \Phi_{ijk'} + \Delta_{ik} - \Delta_{jk} - \Delta_{ik'} + \Delta_{jk'}| < \varepsilon\right) \\ &\leq \mathbb{P}\left(\Delta_{ik} - \Delta_{jk} - \Delta_{ik'} + \Delta_{jk'} < \varepsilon - (\Phi_{ijk} - \Phi_{ijk'})\right) \\ &\leq \mathbb{P}\left(\Delta_{ik} - \Delta_{jk} - \Delta_{ik'} + \Delta_{jk'} < \varepsilon - 2\rho_{\min}\right) \\ &\leq \mathbb{P}\left(|\Delta_{ik}| > \frac{2\rho_{\min} - \varepsilon}{4}\right) + \mathbb{P}\left(|\Delta_{jk}| > \frac{2\rho_{\min} - \varepsilon}{4}\right) \\ &\quad + \mathbb{P}\left(\Delta_{jk'} > \frac{2\rho_{\min} - \varepsilon}{4}\right) + \mathbb{P}\left(|\Delta_{ik'}| > \frac{2\rho_{\min} - \varepsilon}{4}\right). \end{aligned} \quad (\text{H.25})$$

The event representing misclassification of the parents \mathcal{E}_p^l represents classifying a sibling relationship as a parent relationship. Following similar procedures, we have

$$\mathbb{P}(\mathcal{E}_p^l) = \mathbb{P}\left(\bigcup_{x_i, x_j \text{ are siblings}} \mathcal{E}_{p,ij}^l\right) = \mathbb{P}\left(\bigcup_{(x_i, x_j) \in \Gamma_p^l} \mathcal{E}_{p,ij}^l\right) \quad (\text{H.26})$$

$$\mathbb{P}(\mathcal{E}_{p,ij}^l) = \mathbb{P}\left(\bigcap_{x_k \in \Gamma^l} \left\{|\hat{\Phi}_{ijk} - \hat{d}(x_i, x_j)| < \varepsilon\right\}\right) \leq \min_{x_k \in \Gamma^l} \mathbb{P}\left(|\hat{\Phi}_{ijk} - \hat{d}(x_i, x_j)| < \varepsilon\right) \quad (\text{H.27})$$

$$\leq \mathbb{P}\left(|\Delta_{ij}| > \frac{2\rho_{\min} - \varepsilon}{3}\right) + \mathbb{P}\left(|\Delta_{ik}| > \frac{2\rho_{\min} - \varepsilon}{3}\right) + \mathbb{P}\left(|\Delta_{jk}| > \frac{2\rho_{\min} - \varepsilon}{3}\right) \quad (\text{H.28})$$

The event representing misclassification of non-families \mathcal{E}_{nf}^l represents classifying family members as non-family members. We have

$$\mathbb{P}(\mathcal{E}_{nf}^l) = \mathbb{P}\left(\bigcup_{x_i, x_j \text{ in the same family}} \mathcal{E}_{nf,ij}^l\right) = \mathbb{P}\left(\bigcup_{(x_i, x_j) \in \Gamma_{nf}^l} \mathcal{E}_{nf,ij}^l\right) \quad (\text{H.29})$$

$$\mathbb{P}(\mathcal{E}_{nf}^l) = \mathbb{P}\left(\bigcup_{x_i, x_j \text{ in the same family}} \bigcup_{x_k, x_{k'} \in \Gamma} \left\{|\hat{\Phi}_{ijk} - \hat{\Phi}_{ijk'}| > \varepsilon\right\}\right) \quad (\text{H.30})$$

and

$$\mathbb{P}\left(|\hat{\Phi}_{ijk} - \hat{\Phi}_{ijk'}| \geq \varepsilon\right) \leq \mathbb{P}\left(|\Delta_{ik}| > \frac{\varepsilon}{4}\right) + \mathbb{P}\left(|\Delta_{jk}| > \frac{\varepsilon}{4}\right) + \mathbb{P}\left(|\Delta_{jk'}| > \frac{\varepsilon}{4}\right) + \mathbb{P}\left(|\Delta_{ik'}| > \frac{\varepsilon}{4}\right) \quad (\text{H.31})$$

The event representing misclassification of siblings \mathcal{E}_s^l represents classifying parent relationship as sibling relationship. Similarly, we have

$$\mathbb{P}(\mathcal{E}_s^l) = \mathbb{P}\left(\bigcup_{x_i \text{ is the parent of } x_j} \mathcal{E}_{s,ij}^l\right) = \mathbb{P}\left(\bigcup_{(x_i, x_j) \in \Gamma_s^l} \mathcal{E}_{s,ij}^l\right) \quad (\text{H.32})$$

$$\mathbb{P}(\mathcal{E}_{s,ij}^l) = \mathbb{P}\left(\bigcup_{x_k \in \Gamma} \left\{|\hat{\Phi}_{jik} - \hat{d}(x_i, x_j)| > \varepsilon\right\}\right) \quad (\text{H.33})$$

and

$$\mathbb{P}\left(|\hat{\Phi}_{jik} - \hat{d}(x_i, x_j)| > \varepsilon\right) \leq \mathbb{P}\left(|\Delta_{ij}| > \frac{\varepsilon}{3}\right) + \mathbb{P}\left(|\Delta_{ik}| > \frac{\varepsilon}{3}\right) + \mathbb{P}\left(|\Delta_{jk}| > \frac{\varepsilon}{3}\right) \quad (\text{H.34})$$

To bound the probability of error event in l^{th} layer, we first analyze the cardinalities of Γ_f^l , Γ_p^l , Γ_{nf}^l and Γ_s^l . Note that the definitions of these four sets are

$$\Gamma_f^l = \{(x_i, x_j) : x_i \text{ and } x_j \text{ are not in the same family } x_i, x_j \in \Gamma^l\} \quad (\text{H.35})$$

$$\Gamma_p^l = \{(x_i, x_j) : x_i \text{ and } x_j \text{ are siblings } x_i, x_j \in \Gamma^l\} \quad (\text{H.36})$$

$$\Gamma_{nf}^l = \{(x_i, x_j) : x_i \text{ and } x_j \text{ are in the same family } x_i, x_j \in \Gamma^l\} \quad (\text{H.37})$$

$$\Gamma_s^l = \{(x_i, x_j) : x_i \text{ and } x_j \text{ is the parent of } x_i, x_j \in \Gamma^l\}. \quad (\text{H.38})$$

Clearly, we have

$$|\Gamma_f^l| \leq \binom{|\Gamma^l|}{2} \quad \text{and} \quad |\Gamma_s^l| \leq |\Gamma^l|. \quad (\text{H.39})$$

The cardinality of Γ_p^l can be bounded as

$$|\Gamma_p^l| \leq \sum_{i=1}^{|\Gamma^{l+1}|} \binom{n_i}{2} \quad (\text{H.40})$$

where n_i is the size of each family in Γ^l .

From Lemma 10, we deduce that

$$|\Gamma_p^l| \leq \frac{1}{2}d_{\max}(d_{\max} - 1)\frac{|\Gamma^l|}{d_{\max}} = \frac{1}{2}|\Gamma^l|(d_{\max} - 1). \quad (\text{H.41})$$

Similarly, we have

$$|\Gamma_{\text{nf}}^l| \leq \frac{1}{2}|\Gamma^l|(d_{\max} - 1). \quad (\text{H.42})$$

The probability of the error event in l^{th} layer can be bounded as

$$\begin{aligned} \mathbb{P}(\mathcal{E}^l) &= \mathbb{P}(\mathcal{E}_f^l \cup \mathcal{E}_p^l \cup \mathcal{E}_{\text{nf}}^l \cup \mathcal{E}_s^l) \\ &\leq \mathbb{P}(\mathcal{E}_f^l) + \mathbb{P}(\mathcal{E}_p^l) + \mathbb{P}(\mathcal{E}_{\text{nf}}^l) + \mathbb{P}(\mathcal{E}_s^l) \\ &\leq 4 \binom{|\Gamma^l|}{2} h^{(l)} \left(\frac{2\rho_{\min} - \varepsilon}{4} \right) + \frac{3}{2} |\Gamma^l| (d_{\max} - 1) h^{(l)} \left(\frac{2\rho_{\min} - \varepsilon}{3} \right) \\ &\quad + 3 |\Gamma^l|^2 h^{(l)} \left(\frac{\varepsilon}{3} \right) + 2 |\Gamma^l|^3 (d_{\max} - 1) h^{(l)} \left(\frac{\varepsilon}{4} \right). \end{aligned} \quad (\text{H.43})$$

The probability of learning the wrong structure is

$$\begin{aligned} \mathbb{P}(\mathcal{E}) &= \mathbb{P} \left(\bigcup_l \mathcal{E}^l \right) \leq \sum_l \mathbb{P}(\mathcal{E}^l) \\ &\leq \sum_l 4 \binom{|\Gamma^l|}{2} h^{(l)} \left(\frac{2\rho_{\min} - \varepsilon}{4} \right) + \frac{3}{2} |\Gamma^l| (d_{\max} - 1) h^{(l)} \left(\frac{2\rho_{\min} - \varepsilon}{3} \right) \\ &\quad + 3 |\Gamma^l|^2 h^{(l)} \left(\frac{\varepsilon}{3} \right) + 2 |\Gamma^l|^3 (d_{\max} - 1) h^{(l)} \left(\frac{\varepsilon}{4} \right) \end{aligned} \quad (\text{H.44})$$

$$\quad (\text{H.45})$$

With Proposition 11, we have

$$\begin{aligned} \mathbb{P}(\mathcal{E}) &\leq \sum_{l=0}^{L-1} 4 \binom{|\mathcal{V}_{\text{obs}}| - 2l}{2} h^{(l)} \left(\frac{2\rho_{\min} - \varepsilon}{4} \right) + \frac{3}{2} (|\mathcal{V}_{\text{obs}}| - 2l) (d_{\max} - 1) h^{(l)} \left(\frac{2\rho_{\min} - \varepsilon}{3} \right) \\ &\quad + 3 (|\mathcal{V}_{\text{obs}}| - 2l)^2 h^{(l)} \left(\frac{\varepsilon}{3} \right) + 2 (|\mathcal{V}_{\text{obs}}| - 2l)^3 (d_{\max} - 1) h^{(l)} \left(\frac{\varepsilon}{4} \right), \end{aligned} \quad (\text{H.46})$$

where L is the number of iterations of RRG.

We can separately bound the two parts of the first term in the summation $\binom{|\mathcal{V}_{\text{obs}}| - 2l}{2} h^{(l)} \left(\frac{2\rho_{\min} - \varepsilon}{4} \right)$ as

$$\frac{4 \binom{|\mathcal{V}_{\text{obs}}| - 2l}{2} s^l a e^{-wm^l x}}{4 \binom{|\mathcal{V}_{\text{obs}}| - 2L}{2} s^{L-1} a e^{-wm^{L-1} x}} \leq \frac{(|\mathcal{V}_{\text{obs}}| - 2l)(|\mathcal{V}_{\text{obs}}| - 2l - 1)}{2s^{L-1-l}} \leq \frac{|\mathcal{V}_{\text{obs}}|^2}{2s^{L-1-l}} \text{ for } x > 0$$

and

$$\frac{4 \binom{|\mathcal{V}_{\text{obs}}| - 2l}{2} s^l b e^{-um^{2l} x^2}}{4 \binom{|\mathcal{V}_{\text{obs}}| - 2L}{2} s^{L-1} b e^{-um^{2L-2} x^2}} \leq \frac{(|\mathcal{V}_{\text{obs}}| - 2l)(|\mathcal{V}_{\text{obs}}| - 2l - 1)}{2s^{L-1-l}} \leq \frac{|\mathcal{V}_{\text{obs}}|^2}{2s^{L-1-l}}. \quad (\text{H.47})$$

These bounds imply that

$$\sum_{l=0}^{L-1} 4 \binom{|\mathcal{V}_{\text{obs}}| - 2l}{2} h^{(l)}(x) \leq \left[1 + \frac{|\mathcal{V}_{\text{obs}}|^2}{2} \sum_{i=1}^{\infty} \frac{1}{s^i} \right] 4h^{(L-1)}(x) = 4 \left(1 + \frac{|\mathcal{V}_{\text{obs}}|^2}{2(s-1)} \right) 4h^{(L-1)}(x) \text{ for } x > 0$$

Similar procedures could be implemented on other terms, and we will obtain

$$\begin{aligned} \mathbb{P}(\mathcal{E}) &\leq \left[4 \left(1 + \frac{|\mathcal{V}_{\text{obs}}|^2}{2(s-1)} \right) + \frac{3}{2} (d_{\max} - 1) \left(1 + \frac{|\mathcal{V}_{\text{obs}}|}{2(s-1)} \right) \right] h^{(L-1)} \left(\frac{2\rho_{\min} - \varepsilon}{4} \right) \\ &\quad + \left[3 \left(1 + \frac{|\mathcal{V}_{\text{obs}}|^2}{4(s-1)} \right) + 2(d_{\max} - 1) \left(1 + \frac{|\mathcal{V}_{\text{obs}}|^3}{8(s-1)} \right) \right] h^{(L-1)} \left(\frac{\varepsilon}{4} \right) \\ &= \left[4 \left(1 + \frac{|\mathcal{V}_{\text{obs}}|^2}{2(s-1)} \right) + \frac{3}{2} (d_{\max} - 1) \left(1 + \frac{|\mathcal{V}_{\text{obs}}|}{2(s-1)} \right) \right] \left(a e^{-wm^{L-1} \frac{2\rho_{\min} - \varepsilon}{4}} + b e^{-um^{2L-2} \left(\frac{2\rho_{\min} - \varepsilon}{4} \right)^2} \right) \\ &\quad + \left[3 \left(1 + \frac{|\mathcal{V}_{\text{obs}}|^2}{4(s-1)} \right) + 2(d_{\max} - 1) \left(1 + \frac{|\mathcal{V}_{\text{obs}}|^3}{8(s-1)} \right) \right] \left(a e^{-wm^{L-1} \frac{\varepsilon}{4}} + b e^{-um^{2L-2} \left(\frac{\varepsilon}{4} \right)^2} \right) \leq \eta. \end{aligned} \quad (\text{H.48})$$

Upper bounding each of the four terms in inequality (H.48) by $\eta/4$, we obtain the following sufficient conditions of n_1 and n_2 to ensure that $\mathbb{P}(\mathcal{E}) \leq \eta$:

$$n_2 \geq \max \left\{ \frac{64\lambda^2\kappa^2}{c(2\rho_{\min} - \varepsilon)^2} \left(\frac{9}{2}\right)^{2L-2} \log \frac{4l_{\max}^2 s^{L-1} \left[4\left(1 + \frac{|\mathcal{V}_{\text{obs}}|^2}{2(s-1)}\right) + \frac{3}{2}(d_{\max} - 1)\left(1 + \frac{|\mathcal{V}_{\text{obs}}|}{2(s-1)}\right)\right]}{\eta}, \right. \\ \left. \frac{64\lambda^2\kappa^2}{c\varepsilon^2} \left(\frac{9}{2}\right)^{2L-2} \log \frac{4l_{\max}^2 s^{L-1} \left[3\left(1 + \frac{|\mathcal{V}_{\text{obs}}|^2}{4(s-1)}\right) + 2(d_{\max} - 1)\left(1 + \frac{|\mathcal{V}_{\text{obs}}|^3}{8(s-1)}\right)\right]}{\eta} \right\},$$

$$\frac{n_2}{n_1} \geq \max \left\{ \frac{128\lambda\kappa}{3(2\rho_{\min} - \varepsilon)} \left(\frac{9}{2}\right)^{L-1} \log \frac{8l_{\max}^2 s^{L-1} \left[4\left(1 + \frac{|\mathcal{V}_{\text{obs}}|^2}{2(s-1)}\right) + \frac{3}{2}(d_{\max} - 1)\left(1 + \frac{|\mathcal{V}_{\text{obs}}|}{2(s-1)}\right)\right]}{\eta}, \right. \\ \left. \frac{128\lambda\kappa}{3\varepsilon} \left(\frac{9}{2}\right)^{L-1} \log \frac{8l_{\max}^2 s^{L-1} \left[3\left(1 + \frac{|\mathcal{V}_{\text{obs}}|^2}{4(s-1)}\right) + 2(d_{\max} - 1)\left(1 + \frac{|\mathcal{V}_{\text{obs}}|^3}{8(s-1)}\right)\right]}{\eta} \right\}.$$

Note that

$$\max \left\{ 4\left(1 + \frac{|\mathcal{V}_{\text{obs}}|^2}{2(s-1)}\right) + \frac{3}{2}(d_{\max} - 1)\left(1 + \frac{|\mathcal{V}_{\text{obs}}|}{2(s-1)}\right), \right. \\ \left. 3\left(1 + \frac{|\mathcal{V}_{\text{obs}}|^2}{(s-1)}\right) + 2(d_{\max} - 1)\left(1 + \frac{|\mathcal{V}_{\text{obs}}|^3}{8(s-1)}\right) \right\} \\ < 4\left(1 + \frac{|\mathcal{V}_{\text{obs}}|^2}{2(s-1)}\right) + 2(d_{\max} - 1)\left(1 + \frac{|\mathcal{V}_{\text{obs}}|^3}{2(s-1)}\right) \quad (\text{H.49})$$

$$\leq 2(d_{\max} - 1)\left(2 + \frac{|\mathcal{V}_{\text{obs}}|^3 + 2|\mathcal{V}_{\text{obs}}|^2}{2(s-1)}\right) \quad (\text{H.50})$$

$$< 2(d_{\max} - 1)\left(2 + \frac{|\mathcal{V}_{\text{obs}}|^3 + 2|\mathcal{V}_{\text{obs}}|^2}{s}\right) \quad (\text{H.51})$$

$$\stackrel{(a)}{<} 2(d_{\max} - 1)\frac{|\mathcal{V}_{\text{obs}}|^3 + 2|\mathcal{V}_{\text{obs}}|^2 + 7N_\tau|\mathcal{V}_{\text{obs}}|^3}{s} \quad (\text{H.52})$$

$$< 17d_{\max}N_\tau\frac{|\mathcal{V}_{\text{obs}}|^3}{s} \quad (\text{H.53})$$

$$\stackrel{(b)}{<} \frac{17}{4}|\mathcal{V}_{\text{obs}}|^3, \quad (\text{H.54})$$

where inequality (a) and (b) result from $s < 7N_\tau|\mathcal{V}_{\text{obs}}|^3$ and $d_{\max}N_\tau < \frac{s}{4}$, respectively. Choosing $\varepsilon < \rho_{\min}$, we then can derive the sufficient conditions to ensure that $\mathbb{P}(\mathcal{E}) \leq \eta$ as

$$n_2 \geq \frac{64\lambda^2\kappa^2}{c\varepsilon^2} \left(\frac{9}{2}\right)^{2L-2} \log \frac{17l_{\max}^2 s^{L-1} |\mathcal{V}_{\text{obs}}|^3}{\eta}, \quad (\text{H.55})$$

$$\frac{n_2}{n_1} \geq \frac{128\lambda\kappa}{3\varepsilon} \left(\frac{9}{2}\right)^{L-1} \log \frac{34l_{\max}^2 s^{L-1} |\mathcal{V}_{\text{obs}}|^3}{\eta}. \quad (\text{H.56})$$

In Theorem 1, we choose $\varepsilon = \frac{\rho_{\min}}{2}$.

Then the following conditions

$$n_2 \geq \frac{64\lambda^2\kappa^2}{c\varepsilon^2} \left(\frac{9}{2}\right)^{2L-2} \log \frac{17l_{\max}^2 s^{L-1} |\mathcal{V}_{\text{obs}}|^3}{\eta}, \quad (\text{H.57})$$

$$n_1 = O\left(\frac{\sqrt{n_2}}{\log n_2}\right). \quad (\text{H.58})$$

are sufficient to guarantee that $\mathbb{P}(\mathcal{E}) \leq \eta$.

We are going to prove that there exists $C' > 0$, such that

$$C' \frac{\sqrt{n_2}}{\log n_2} \leq \frac{n_2}{\frac{128\lambda\kappa}{3\varepsilon} \left(\frac{9}{2}\right)^{L-1} \log \frac{34l_{\max}^2 s^{L-1} |\mathcal{V}_{\text{obs}}|^3}{\eta}}, \quad (\text{H.59})$$

which is equivalent to

$$C' \frac{128\lambda\kappa}{3\varepsilon} \left(\frac{9}{2}\right)^{L-1} \log \frac{34l_{\max}^2 s^{L-1} |\mathcal{V}_{\text{obs}}|^3}{\eta} \leq \sqrt{n_2} \log n_2. \quad (\text{H.60})$$

Since n_2 is lower bounded as in (H.57), it is sufficient to show that there exists $C' > 0$, such that

$$\begin{aligned} & (C')^2 \left(\frac{128\lambda\kappa}{3\varepsilon} \left(\frac{9}{2}\right)^{L-1} \log \frac{34l_{\max}^2 s^{L-1} |\mathcal{V}_{\text{obs}}|^3}{\eta} \right)^2 \\ & \leq \frac{64\lambda^2 \kappa^2}{c\varepsilon^2} \left(\frac{9}{2}\right)^{2L-2} \log \frac{17l_{\max}^2 s^{L-1} |\mathcal{V}_{\text{obs}}|^3}{\eta} \log \left[\frac{64\lambda^2 \kappa^2}{c\varepsilon^2} \left(\frac{9}{2}\right)^{2L-2} \log \frac{17l_{\max}^2 s^{L-1} |\mathcal{V}_{\text{obs}}|^3}{\eta} \right], \end{aligned}$$

which is equivalent to

$$(C')^2 \leq \frac{9 \log \frac{17l_{\max}^2 s^{L-1} |\mathcal{V}_{\text{obs}}|^3}{\eta}}{256c \log \frac{34l_{\max}^2 s^{L-1} |\mathcal{V}_{\text{obs}}|^3}{\eta}} \frac{\left(\log \left(\frac{64\lambda^2 \kappa^2}{c\varepsilon^2} \left(\frac{9}{2}\right)^{2L-2} \right) + \log \log \frac{17l_{\max}^2 s^{L-1} |\mathcal{V}_{\text{obs}}|^3}{\eta} \right)^2}{\log \frac{34l_{\max}^2 s^{L-1} |\mathcal{V}_{\text{obs}}|^3}{\eta}}. \quad (\text{H.61})$$

We have

$$\log \frac{17l_{\max}^2 s^{L-1} |\mathcal{V}_{\text{obs}}|^3}{\eta} / \log \frac{34l_{\max}^2 s^{L-1} |\mathcal{V}_{\text{obs}}|^3}{\eta} > \frac{1}{2} \quad \text{and} \quad (\text{H.62})$$

$$\frac{\left(\log \left(\frac{64\lambda^2 \kappa^2}{c\varepsilon^2} \left(\frac{9}{2}\right)^{2L-2} \right) + \log \log \frac{17l_{\max}^2 s^{L-1} |\mathcal{V}_{\text{obs}}|^3}{\eta} \right)^2}{\log \frac{34l_{\max}^2 s^{L-1} |\mathcal{V}_{\text{obs}}|^3}{\eta}} > \frac{\left(\log \left(\frac{64\lambda^2 \kappa^2}{c\varepsilon^2} \left(\frac{9}{2}\right)^{2L-2} \right) \right)^2}{\log \frac{34l_{\max}^2 s^{L-1} |\mathcal{V}_{\text{obs}}|^3}{\eta}}. \quad (\text{H.63})$$

Since

$$\lim_{L \rightarrow \infty} \frac{\left(\log \left(\frac{64\lambda^2 \kappa^2}{c\varepsilon^2} \left(\frac{9}{2}\right)^{2L-2} \right) \right)^2}{\log \frac{34l_{\max}^2 s^{L-1} |\mathcal{V}_{\text{obs}}|^3}{\eta}} = +\infty, \quad (\text{H.64})$$

we can see that there exists $C' > 0$ that satisfies inequality (H.59). \square

I Proofs of results in Section 3.3

Theorem 7. *If Assumptions 1 to 5 hold and all the nodes have exactly two children, RNJ constructs the correct latent tree with probability at least $1 - \eta$ if*

$$n_2 > \frac{16\lambda^2 \kappa^2}{c\rho_{\min}^2} \log \left(\frac{2|\mathcal{V}_{\text{obs}}|^2 l_{\max}^2}{\eta} \right) \quad (\text{I.1})$$

$$\frac{n_2}{n_1} > \frac{64\lambda\kappa}{3\rho_{\min}} \log \left(\frac{4|\mathcal{V}_{\text{obs}}|^2 l_{\max}^2}{\eta} \right) \quad (\text{I.2})$$

where

$$\lambda = \frac{2l_{\max}^2 e^{\rho_{\max}/l_{\max}}}{\delta_{\min}^{1/l_{\max}}} \quad \text{and} \quad \kappa = \max\{\sigma_{\max}^2, \rho_{\min}\}, \quad (\text{I.3})$$

and c is an absolute constant.

Proof of Theorem 7. It is easy to see by substituting the constants λ and κ into (I.1) and (I.2) that Theorem 7 implies Theorem 2, so we provide the proof of Theorem 7 here.

With the sufficient condition in Proposition 5, we can bound the probability of error event by the union bound as follows

$$\mathbb{P}(\mathcal{E}) \leq \mathbb{P}\left(\max_{x_i, x_j \in \mathcal{V}_{\text{obs}}} |\hat{d}(x_i, x_j) - d(x_i, x_j)| > \frac{\rho_{\min}}{2} \right) \quad (\text{I.4})$$

$$\leq |\mathcal{V}_{\text{obs}}|^2 \mathbb{P}\left(|\hat{d}(x_i, x_j) - d(x_i, x_j)| > \frac{\rho_{\min}}{2} \right). \quad (\text{I.5})$$

We bound two terms in the tail probability separately as

$$2l_{\max}^2 e^{-\frac{3n_2}{64\lambda\kappa n_1}\rho_{\min}} < \frac{\eta}{2|\mathcal{V}_{\text{obs}}|^2} \quad (\text{I.6})$$

$$l_{\max}^2 e^{-c\frac{n_2}{16\lambda^2\kappa^2}\rho_{\min}^2} < \frac{\eta}{2|\mathcal{V}_{\text{obs}}|^2}. \quad (\text{I.7})$$

Then we have

$$n_2 > \frac{16\lambda^2\kappa^2}{c\rho_{\min}^2} \log\left(\frac{2|\mathcal{V}_{\text{obs}}|^2 l_{\max}^2}{\eta}\right), \quad (\text{I.8})$$

$$\frac{n_2}{n_1} > \frac{64\lambda\kappa}{3\rho_{\min}} \log\left(\frac{4|\mathcal{V}_{\text{obs}}|^2 l_{\max}^2}{\eta}\right). \quad (\text{I.9})$$

The proof that $n_1 = O(\sqrt{n_2}/\log n_2)$ can be derived by following the similar procedures in the proof of Theorem 1. \square

Proposition 12. *If Assumption 1 to 5 hold and the truncated inner product is adopted to estimate the information distances,*

$$\mathbb{P}(\|\hat{\mathbf{R}} - \mathbf{R}\|_2 > t) \leq |\mathcal{V}_{\text{obs}}|^2 f\left(e^{\rho_{\min}} \frac{t}{|\mathcal{V}_{\text{obs}}|}\right), \quad (\text{I.10})$$

where the function f is defined as

$$f(x) \triangleq 2l_{\max}^2 e^{-\frac{3n_2}{32\lambda\kappa n_1}x} + l_{\max}^2 e^{-c\frac{n_2}{4\lambda^2\kappa^2}x^2} = ae^{-wx} + be^{-ux^2}, \quad (\text{I.11})$$

with $\lambda = 2l_{\max}^2 e^{\rho_{\max}/l_{\max}}/\delta_{\min}^{1/l_{\max}}$, $w = \frac{3n_2}{32\lambda\kappa n_1}$, $u = c\frac{n_2}{4\lambda^2\kappa^2}$, $a = 2l_{\max}^2$ and $b = l_{\max}^2$.

Proof of Proposition 12. Noting that $\mathbf{R}_{ij} = \exp(-d(x_i, x_j))$, we have

$$\mathbb{P}(|\hat{\mathbf{R}}_{ij} - \mathbf{R}_{ij}| > t) = \mathbb{P}\left(\left|\exp(-\hat{d}(x_i, x_j)) - \exp(-d(x_i, x_j))\right| > t\right) \quad (\text{I.12})$$

$$\stackrel{(a)}{\leq} \mathbb{P}\left(|\hat{d}(x_i, x_j) - d(x_i, x_j)| > e^{\rho_{\min}} t\right) \quad (\text{I.13})$$

$$< f(e^{\rho_{\min}} t), \quad (\text{I.14})$$

where inequality (a) is derived from Taylor's Theorem.

Since

$$\|\hat{\mathbf{R}} - \mathbf{R}\|_2 \leq |\mathcal{V}_{\text{obs}}| \max_{i,j} |\hat{\mathbf{R}}_{ij} - \mathbf{R}_{ij}|, \quad (\text{I.15})$$

we have

$$\mathbb{P}(\|\hat{\mathbf{R}} - \mathbf{R}\|_2 > t) \leq \mathbb{P}\left(\max_{i,j} |\hat{\mathbf{R}}_{ij} - \mathbf{R}_{ij}| > \frac{t}{|\mathcal{V}_{\text{obs}}|}\right) \leq |\mathcal{V}_{\text{obs}}|^2 f\left(e^{\rho_{\min}} \frac{t}{|\mathcal{V}_{\text{obs}}|}\right) \quad (\text{I.16})$$

as desired. \square

Theorem 8. *If Assumptions 1 to 5 hold and all the nodes have exactly two children, RSNJ constructs the correct latent tree with probability at least $1 - \eta$ if*

$$n_2 \geq \frac{16\lambda^2\kappa^2|\mathcal{V}_{\text{obs}}|^2}{ce^{2\rho_{\min}}g(|\mathcal{V}_{\text{obs}}|, \rho_{\min}, \rho_{\max})^2} \log \frac{2|\mathcal{V}_{\text{obs}}|^2 l_{\max}^2}{\eta} \quad (\text{I.17})$$

$$\frac{n_2}{n_1} \geq \frac{64\lambda\kappa|\mathcal{V}_{\text{obs}}|}{3e^{\rho_{\min}}g(|\mathcal{V}_{\text{obs}}|, \rho_{\min}, \rho_{\max})} \log \frac{4|\mathcal{V}_{\text{obs}}|^2 l_{\max}^2}{\eta} \quad (\text{I.18})$$

where

$$g(x, \rho_{\min}, \rho_{\max}) = \begin{cases} \frac{1}{2}(2e^{-\rho_{\max}})^{\log_2(x/2)} e^{-\rho_{\max}}(1 - e^{-2\rho_{\min}}), & e^{-2\rho_{\max}} \leq 0.5 \\ e^{-3\rho_{\max}}(1 - e^{-2\rho_{\min}}), & e^{-2\rho_{\max}} > 0.5 \end{cases} \quad (\text{I.19})$$

$$\lambda = \frac{2l_{\max}^2 e^{\rho_{\max}/l_{\max}}}{\delta_{\min}^{1/l_{\max}}} \quad \kappa = \max\{\sigma_{\max}^2, \rho_{\min}\}, \quad (\text{I.20})$$

and c is an absolute constant.

Proof of Theorem 8. It is easy to see by substituting the constants λ and κ into (I.17) and (I.18) that Theorem 8 implies Theorem 3, so we provide the proof of Theorem 8 here.

Proposition 6 shows that the probability of learning the wrong tree $\mathbb{P}(\mathcal{E})$ could be bounded as

$$\mathbb{P}(\mathcal{E}) \leq \mathbb{P}(\|\hat{\mathbf{R}} - \mathbf{R}\|_2 > g(|\mathcal{V}_{\text{obs}}|, \rho_{\min}, \rho_{\max})) \leq |\mathcal{V}_{\text{obs}}|^2 f\left(e^{\rho_{\min}} \frac{g(|\mathcal{V}_{\text{obs}}|, \rho_{\min}, \rho_{\max})}{|\mathcal{V}_{\text{obs}}|}\right). \quad (\text{I.21})$$

Substituting the expression of f and bounding the right-hand-side of inequality (I.21) by η , we have

$$n_2 \geq \frac{16\lambda^2\kappa^2|\mathcal{V}_{\text{obs}}|^2}{ce^{2\rho_{\min}}g(|\mathcal{V}_{\text{obs}}|, \rho_{\min}, \rho_{\max})^2} \log \frac{2|\mathcal{V}_{\text{obs}}|^2 t_{\max}^2}{\eta} \quad \text{and} \quad (\text{I.22})$$

$$\frac{n_2}{n_1} \geq \frac{64\lambda\kappa|\mathcal{V}_{\text{obs}}|}{3e^{\rho_{\min}}g(|\mathcal{V}_{\text{obs}}|, \rho_{\min}, \rho_{\max})} \log \frac{4|\mathcal{V}_{\text{obs}}|^2 t_{\max}^2}{\eta}. \quad (\text{I.23})$$

The proof that $n_1 = O(\sqrt{n_2}/\log n_2)$ can be derived by following the similar procedures in the proof of Theorem 1. \square

J Proofs of results in Section 3.4

Lemma 13. *The MST of a weighted graph \mathbb{T} has the following properties:*

- (1) *For any cut C of the graph, if the weight of an edge e in the cut-set of C is strictly smaller than the weights of all other edges of the cut-set of C , then this edge belongs to all MSTs of the graph.*
- (2) *If \mathbb{T}' is a tree of MST edges, then we can contract \mathbb{T}' into a single vertex while maintaining the invariant that the MST of the contracted graph plus \mathbb{T}' gives the MST for the graph before contraction [25].*

Proof of Proposition 7. We prove this argument by induction. Choosing any node as the root node, we first prove that the edges which are related to the observed nodes with the largest depth are identified or contracted correctly.

Since we consider the edges which involve at least one observed node, we only need to discuss the edges formed by two observed nodes and one observed node and one hidden node. We first consider the identification of the edges between two observed nodes.

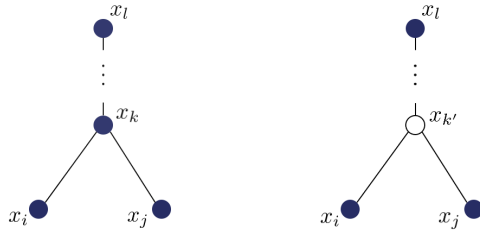


Figure 9: Two kinds of edges related at least one observed node.

To correctly identify the edge (x_k, x_j) in Fig. 9, we consider the cut of the graph which splits the nodes into $\{x_j\}$ and all the other nodes. Lemma 13 says that the condition that

$$\hat{d}(x_k, x_j) < \hat{d}(x_l, x_j) \quad \forall x_l \in \mathcal{V}_{\text{obs}}, x_l \neq x_k, x_j \quad (\text{J.1})$$

is sufficient to guarantee that this edge is identified correctly. This condition is equivalent to

$$\Delta_{kj} < \Delta_{lj} + d(x_l, x_k) \quad \forall x_l \in \mathcal{V}_{\text{obs}}, x_l \neq x_k, x_j, \quad (\text{J.2})$$

which is guaranteed by choosing $\Delta_{\text{MST}} = d_{\text{ct}}(x_k; \mathbb{T}, \mathcal{V}_{\text{obs}})$.

Furthermore, we need to guarantee that x_j is not connected to other nodes except x_k . We consider the cut of the graph which split the nodes into $\{x_j, x_k\}$ and all the other nodes. Lemma 13 says that the condition that

$$\hat{d}(x_l, x_k) < \hat{d}(x_l, x_j) \quad \forall x_l \in \mathcal{V}_{\text{obs}}, x_l \neq x_k, x_j \quad (\text{J.3})$$

is sufficient to guarantee x_j is not connected to other nodes. This condition is equivalent to

$$\Delta_{lk} < \Delta_{lj} + d(x_k, x_j) \quad \forall x_l \in \mathcal{V}_{\text{obs}}, x_l \neq x_k, x_j, \quad (\text{J.4})$$

which is guaranteed by choosing $\Delta_{\text{MST}} = d_{\text{ct}}(x_k; \mathbb{T}, \mathcal{V}_{\text{obs}})$.

A similar proof can be used to guarantee (x_i, x_k) can be identified correctly. Then we can contract x_i, x_j to x_k to form a super node in the subsequent edges identification for Lemma 13.

Now we discuss the edges involving one observed node and one hidden node. There are two cases: (i) The hidden node $x_{k'}$ should be contracted to either x_i or x_j . (ii) The hidden node $x_{k'}$ should be contracted to $x_l \in \mathcal{V}_{\text{obs}}, x_l \neq x_i, x_j$.

We first consider the case (i). Without loss of generality, we assume that $x_{k'}$ should be contracted to x_j . Contracting $x_{k'}$ to x_j is equivalent to that x_i is not connected to other nodes except x_j . Lemma 13 shows that

$$\hat{d}(x_i, x_j) < \hat{d}(x_i, x_l) \quad \hat{d}(x_j, x_l) < \hat{d}(x_i, x_l) \quad \forall x_l \in \mathcal{V}_{\text{obs}}, x_l \neq x_i, x_j \quad (\text{J.5})$$

is sufficient to achieve that x_i is not connected to other nodes except x_j . This condition is equivalent to

$$\begin{aligned} \Delta_{ij} + d(x_{k'}, x_j) < \Delta_{lj} + d(x_{k'}, x_l) \quad \text{and} \quad \Delta_{jl} + d(x_{k'}, x_j) < \Delta_{il} + d(x_{k'}, x_i) \\ \forall x_l \in \mathcal{V}_{\text{obs}}, x_l \neq x_k, x_j, \end{aligned} \quad (\text{J.6})$$

which is guaranteed by choosing $\Delta_{\text{MST}} = d_{\text{ct}}(x_{k'}; \mathbb{T}, \mathcal{V}_{\text{obs}})$. Then we can contract x_i to x_j to form a super node in the subsequent edges identification for Lemma 13.

Then we consider the case (ii). Here we need to prove that $x_{k'}$ will not be contracted to x_i or x_j . Without loss of generality, we assume that $x_{k'}$ is contracted to x_l , which guaranteed by that there is no edge between x_i and x_j . Lemma 13 shows that

$$\hat{d}(x_i, x_l) < \hat{d}(x_i, x_j) \quad \hat{d}(x_j, x_l) < \hat{d}(x_i, x_j) \quad (\text{J.7})$$

is sufficient to guarantee that there is no edge between x_i and x_j . This condition is equivalent to

$$\Delta_{il} + d(x_{k'}, x_l) < \Delta_{ij} + d(x_{k'}, x_j) \quad \Delta_{jl} + d(x_{k'}, x_l) < \Delta_{ij} + d(x_{k'}, x_i), \quad (\text{J.8})$$

which is guaranteed by choosing $\Delta_{\text{MST}} = d_{\text{ct}}(x_{k'}; \mathbb{T}, \mathcal{V}_{\text{obs}})$.

Assume that all the edges related to the nodes with depths larger than l are identified or contracted correctly. We now consider the edges related to the nodes with depths l . For the edges between two observed nodes and edges of case (i) and (ii), similar procedures can be adopted to prove the statements. Here we discuss the case where x_l should contract the hidden nodes which are its descendants. Contracting $x_{k'}$ to x_l is equivalent to that there are edges between (x_l, x_i) and (x_l, x_j) , and there is no other edges related to x_i and x_j . Recall that condition (J.7) is satisfied by the induction hypothesis. Lemma 13 shows that

$$\hat{d}(x_i, x_l) < \hat{d}(x_i, x_k) \quad \hat{d}(x_k, x_l) < \hat{d}(x_k, x_i) \quad \forall x_k \in \mathcal{V}_{\text{obs}}, x_k \neq x_i, x_j, x_l \quad (\text{J.9})$$

$$\hat{d}(x_j, x_l) < \hat{d}(x_j, x_k) \quad \hat{d}(x_k, x_l) < \hat{d}(x_k, x_j) \quad \forall x_k \in \mathcal{V}_{\text{obs}}, x_k \neq x_i, x_j, x_l \quad (\text{J.10})$$

is sufficient to guarantee that $x_{k'}$ is contracted to x_l . This condition is equivalent to

$$\Delta_{il} < \Delta_{ik} + d(x_k, x_l) \quad \Delta_{kl} < \Delta_{ki} + d(x_i, x_l) \quad \forall x_k \in \mathcal{V}_{\text{obs}}, x_k \neq x_i, x_j, x_l \quad (\text{J.11})$$

$$\Delta_{jl} < \Delta_{jk} + d(x_k, x_l) \quad \Delta_{kl} < \Delta_{kj} + d(x_j, x_l) \quad \forall x_k \in \mathcal{V}_{\text{obs}}, x_k \neq x_i, x_j, x_l \quad (\text{J.12})$$

which is guaranteed by choosing $\Delta_{\text{MST}} = d_{\text{ct}}(x_l; \mathbb{T}, \mathcal{V}_{\text{obs}})$. Then we can contract x_i and x_j to x_l to form a super node in the subsequent edges identification for Lemma 13.

Thus, the results are proved by induction. \square

Theorem 9. *If Assumptions 1–4, RCLRG constructs the correct latent tree with probability at least $1 - \eta$ if*

$$n_2 \geq \max \left\{ \frac{4}{\varepsilon^2} \left(\frac{9}{2} \right)^{2L_C-2}, \frac{1}{\Delta_{\text{MST}}^2} \right\} \frac{16\lambda^2\kappa^2}{c} \log \frac{17l_{\text{max}}^2 s^{L_C-1} |\mathcal{V}_{\text{obs}}|^3 + l_{\text{max}}^2 |\mathcal{V}_{\text{obs}}|^2}{\eta}, \quad (\text{J.13})$$

$$\frac{n_2}{n_1} \geq \max \left\{ \frac{2}{\varepsilon} \left(\frac{9}{2} \right)^{L_C-1}, \frac{1}{\Delta_{\text{MST}}} \right\} \frac{64\lambda\kappa}{3} \log \frac{34l_{\text{max}}^2 s^{L_C-1} |\mathcal{V}_{\text{obs}}|^3 + 2l_{\text{max}}^2 |\mathcal{V}_{\text{obs}}|^2}{\eta}, \quad (\text{J.14})$$

where

$$\lambda = \frac{2l_{\text{max}}^2 e^{\rho_{\text{max}}/l_{\text{max}}}}{\delta_{\text{min}}^{1/l_{\text{max}}}} \quad \kappa = \max\{\sigma_{\text{max}}^2, \rho_{\text{min}}\} \quad s = d_{\text{max}}^2 + 2d_{\text{max}}^3(1 + 2N_\tau) \quad \varepsilon = \frac{\rho_{\text{min}}}{2}, \quad (\text{J.15})$$

c is an absolute constant, and L_C is the number of iterations of RCLRG needed to construct the tree.

Proof of Theorem 9. It is easy to see by substituting the constants λ , κ , s and ε into (J.13) and (J.14) that Theorem 9 implies Theorem 4, so we provide the proof of Theorem 9 here.

The RCLRG algorithm consists of two stages: Calculation of MST and implementation of RRG on internal nodes. The probability of error of RCLRG could be decomposed as

$$\mathbb{P}(\mathcal{E}) = \mathbb{P}(\mathcal{E}_{\text{MST}} \cup (\mathcal{E}_{\text{MST}}^c \cap \mathcal{E}_{\text{RRG}})) = \mathbb{P}(\mathcal{E}_{\text{MST}}) + \mathbb{P}(\mathcal{E}_{\text{MST}}^c \cap \mathcal{E}_{\text{RRG}}) \leq \mathbb{P}(\mathcal{E}_{\text{MST}}) + \mathbb{P}(\mathcal{E}_{\text{RRG}})$$

We define the correct event of calculation of the MST as

$$\mathcal{C}_{\text{MST}} = \bigcap_{x_i, x_j \in \mathcal{V}_{\text{obs}}} \left\{ |\hat{d}(x_i, x_j) - d(x_i, x_j)| < \frac{\Delta_{\text{MST}}}{2} \right\} = \bigcap_{x_i, x_j \in \mathcal{V}_{\text{obs}}} \mathcal{C}_{ij} \quad (\text{J.16})$$

Proposition 7 shows that

$$\mathbb{P}(\mathcal{E}_{\text{MST}}) \leq 1 - \mathbb{P}(\mathcal{C}_{\text{MST}}) = \mathbb{P}\left(\bigcap_{x_i, x_j \in \mathcal{V}_{\text{obs}}} \mathcal{C}_{ij}^c\right) \quad (\text{J.17})$$

$$= \mathbb{P}\left(\bigcup_{x_i, x_j \in \mathcal{V}_{\text{obs}}} \mathcal{C}_{ij}^c\right) \leq \sum_{x_i, x_j \in \mathcal{V}_{\text{obs}}} \mathbb{P}(\mathcal{C}_{ij}^c) \leq \binom{|\mathcal{V}_{\text{obs}}|}{2} f\left(\frac{\Delta_{\text{MST}}}{2}\right) \quad (\text{J.18})$$

We define the event that RRG yields the correct subtree based on $\text{nbnd}[x_i, \mathbb{T}]$

$$\mathcal{C}_{\text{RRG}} = \bigcap_{x_i \in \text{Int}(\text{MST}(\mathcal{V}_{\text{obs}}; \hat{\mathbf{D}}))} \{\text{Output of RRG is correct with input } \text{nbnd}[x_i, \mathbb{T}]\} \quad (\text{J.19})$$

$$= \bigcap_{x_i \in \text{Int}(\text{MST}(\mathcal{V}_{\text{obs}}; \hat{\mathbf{D}}))} \mathcal{C}_i \quad (\text{J.20})$$

Then we have

$$\mathbb{P}(\mathcal{E}_{\text{RRG}}) = 1 - \mathbb{P}(\mathcal{C}_{\text{RRG}}) = \mathbb{P}\left(\left(\bigcap_{x_i \in \text{Int}(\text{MST}(\mathcal{V}_{\text{obs}}; \hat{\mathbf{D}}))} \mathcal{C}_i\right)^c\right) = \mathbb{P}\left(\bigcup_{x_i \in \text{Int}(\text{MST}(\mathcal{V}_{\text{obs}}; \hat{\mathbf{D}}))} \mathcal{C}_i^c\right). \quad (\text{J.21})$$

By defining $L_C = \lceil \frac{\text{Deg}(\text{MST}(\mathcal{V}_{\text{obs}}; \hat{\mathbf{D}}))}{2} - 1 \rceil$, we have

$$\mathbb{P}(\mathcal{E}) \leq \mathbb{P}(\mathcal{E}_{\text{MST}}) + \mathbb{P}(\mathcal{E}_{\text{RRG}}) \quad (\text{J.22})$$

$$\begin{aligned} &\leq \binom{|\mathcal{V}_{\text{obs}}|}{2} f\left(\frac{\Delta_{\text{MST}}}{2}\right) + (|\mathcal{V}_{\text{obs}}| - 2) \left\{ \left[4 \left(1 + \frac{|\mathcal{V}_{\text{obs}}|^2}{2(s-1)} \right) + \frac{3}{2} (d_{\text{max}} - 1) \left(1 + \frac{|\mathcal{V}_{\text{obs}}|}{2(s-1)} \right) \right] \right. \\ &\quad \left. \times h^{(L_C-1)} \left(\frac{2\rho_{\text{min}} - \varepsilon}{4} \right) + \left[3 \left(1 + \frac{|\mathcal{V}_{\text{obs}}|^2}{4(s-1)} \right) + 2(d_{\text{max}} - 1) \left(1 + \frac{|\mathcal{V}_{\text{obs}}|^3}{8(s-1)} \right) \right] h^{(L_C-1)} \left(\frac{\varepsilon}{4} \right) \right\} \end{aligned} \quad (\text{J.23})$$

To derive the sufficient conditions of $\mathbb{P}(\mathcal{E}) \leq \eta$, we consider the following conditions

$$\mathbb{P}(\mathcal{E}_{\text{MST}}) \leq (1-r)\eta \quad \text{and} \quad \mathbb{P}(\mathcal{E}_{\text{RRG}}) \leq r\eta \quad \text{for some } r \in (0, 1) \quad (\text{J.24})$$

Following the same calculations with inequalities (13), we have

$$n_2 \geq \max \left\{ \frac{64\lambda^2\kappa^2}{c\varepsilon^2} \left(\frac{9}{2}\right)^{2L_C-2} \log \frac{17l_{\max}^2 s^{L_C-1} |\mathcal{V}_{\text{obs}}|^3}{r\eta}, \frac{16\lambda^2\kappa^2}{c\Delta_{\text{MST}}^2} \log \frac{l_{\max}^2 |\mathcal{V}_{\text{obs}}|^2}{(1-r)\eta} \right\} \quad (\text{J.25})$$

$$\frac{n_2}{n_1} \geq \max \left\{ \frac{128\lambda\kappa}{3\varepsilon} \left(\frac{9}{2}\right)^{L_C-1} \log \frac{34l_{\max}^2 s^{L_C-1} |\mathcal{V}_{\text{obs}}|^3}{r\eta}, \frac{64\lambda\kappa}{3\Delta_{\text{MST}}} \log \frac{2l_{\max}^2 |\mathcal{V}_{\text{obs}}|^2}{(1-r)\eta} \right\} \quad (\text{J.26})$$

By choosing $r = \frac{17s^{L_C-1} |\mathcal{V}_{\text{obs}}|^3}{17s^{L_C-1} |\mathcal{V}_{\text{obs}}|^3 + |\mathcal{V}_{\text{obs}}|^2}$, we have

$$n_2 \geq \max \left\{ \frac{4}{\varepsilon^2} \left(\frac{9}{2}\right)^{2L_C-2}, \frac{1}{\Delta_{\text{MST}}^2} \right\} \frac{16\lambda^2\kappa^2}{c} \log \frac{17l_{\max}^2 s^{L_C-1} |\mathcal{V}_{\text{obs}}|^3 + l_{\max}^2 |\mathcal{V}_{\text{obs}}|^2}{\eta}, \quad (\text{J.27})$$

$$\frac{n_2}{n_1} \geq \max \left\{ \frac{2}{\varepsilon} \left(\frac{9}{2}\right)^{L_C-1}, \frac{1}{\Delta_{\text{MST}}} \right\} \frac{64\lambda\kappa}{3} \log \frac{34l_{\max}^2 s^{L_C-1} |\mathcal{V}_{\text{obs}}|^3 + 2l_{\max}^2 |\mathcal{V}_{\text{obs}}|^2}{\eta} \quad (\text{J.28})$$

Following a similar proof as that for RRG, we claim that

$$n_2 \geq \max \left\{ \frac{4}{\varepsilon^2} \left(\frac{9}{2}\right)^{2L_C-2}, \frac{1}{\Delta_{\text{MST}}^2} \right\} \frac{16\lambda^2\kappa^2}{c} \log \frac{17l_{\max}^2 s^{L_C-1} |\mathcal{V}_{\text{obs}}|^3 + l_{\max}^2 |\mathcal{V}_{\text{obs}}|^2}{\eta}, \quad (\text{J.29})$$

$$n_1 = O\left(\frac{\sqrt{n_2}}{\log n_2}\right) \quad (\text{J.30})$$

are sufficient to guarantee $\mathbb{P}(\mathcal{E}) \leq \eta$. □

K Discussions and Proofs of results in Section 3.5

In this section, we provide more discussions of the results in Table 1. We also provide the proofs of results listed in Table 1.

The sample complexities of RRG and RCLRG are achieved w.h.p., since the number of iterations L_R and L_C depend on the quality of the estimates of the information distances. The parameter t for RSNJ scales as $O(\frac{1}{l_{\max}} + \log |\mathcal{V}_{\text{obs}}|)$. For the dependence on $\text{Diam}(\mathbb{T})$, RRG and RSNJ have the worst performance. This is because RRG constructs new hidden nodes and estimates the information distances related to them in each iteration (or layer), which results in more severe error propagation on larger and deeper graphs. In contrast, our impossibility result in Theorem 5 suggests that RNJ has the optimal dependence on $\text{Diam}(\mathbb{T})$. RCLRG also has the optimal dependence on the diameter of graphs on HMM, which demonstrates that the Chow-Liu initialization procedure greatly reduces the sample complexity from $O((\frac{9}{2})^{\text{Diam}(\mathbb{T})})$ to $O(\log \text{Diam}(\mathbb{T}))$. Since the dependence on ρ_{\max} only relies on the parameters, the dependence of ρ_{\max} of all these algorithms remains the same for graphical models with different underlying structures. RRG, RCLRG and RNJ have the same dependence $O(e^{2\frac{\rho_{\max}}{l_{\max}}})$, while RSNJ has a worse dependence on ρ_{\max} .

K.1 Proofs of entries in Table 1

Double-binary tree For RRG, the number of iterations needed to construct the tree $L_R = \frac{1}{2}(\text{Diam}(\mathbb{T}) - 1)$. Thus, the sample complexity of RRG is $O(e^{2\frac{\rho_{\max}}{l_{\max}}} (\frac{9}{2})^{\text{Diam}(\mathbb{T})})$.

For RCLRG, as mentioned previously, the MST can be obtained by contracting the hidden nodes to its closest observed node. For example, the MST of the double-binary tree with $\text{Diam}(\mathbb{T}) = 5$ could be derived by contracting hidden nodes as Fig. 10. Then $L_C = \lceil \frac{\text{Diam}(\mathbb{T})+1}{4} \rceil - 1$, and the number of observed nodes is $|\mathcal{V}_{\text{obs}}| = 2^{\frac{\text{Diam}(\mathbb{T})+1}{2}}$. Thus, the sample complexity is $O(e^{2\frac{\rho_{\max}}{l_{\max}}} (\frac{9}{2})^{\frac{\text{Diam}(\mathbb{T})}{2}})$.

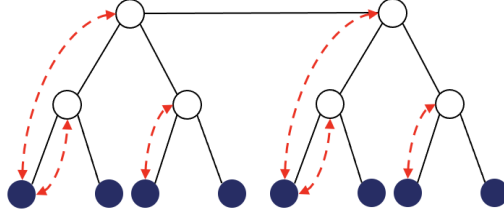


Figure 10: The contraction of hidden nodes in double-binary trees.

For RSNJ, the number of observed nodes is $|\mathcal{V}_{\text{obs}}| = 2^{\frac{\text{Diam}(\mathbb{T})+1}{2}}$, so the sample complexity is $O(e^{2t\rho_{\max}} \text{Diam}(\mathbb{T}))$.

For RNJ, the number of observed nodes is $|\mathcal{V}_{\text{obs}}| = 2^{\frac{\text{Diam}(\mathbb{T})+1}{2}}$, so the sample complexity is $O(e^{2\frac{\rho_{\max}}{t_{\max}}} \text{Diam}(\mathbb{T}))$.

HMM For RRG, the number of iterations needed to construct the tree $L_R = \lceil \frac{\text{Diam}(\mathbb{T})}{2} - 1 \rceil$. Thus, the sample complexity of RRG is $O(e^{2\frac{\rho_{\max}}{t_{\max}}} (\frac{9}{2})^{\text{Diam}(\mathbb{T})})$.

For RCLRG, MST could be derived as contracting hidden nodes as shown in Fig. 11. Then $L_C = 1$ and $|\mathcal{V}_{\text{obs}}| = \text{Diam}(\mathbb{T}) + 1$. The sample complexity is thus $O(e^{2\frac{\rho_{\max}}{t_{\max}}} \log \text{Diam}(\mathbb{T}))$.

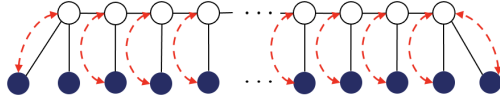


Figure 11: The contraction of hidden nodes in HMMs.

For RSNJ, the number of observed nodes is $|\mathcal{V}_{\text{obs}}| = \text{Diam}(\mathbb{T}) + 1$, so the sample complexity is $O(e^{2t\rho_{\max}} \log \text{Diam}(\mathbb{T}))$.

For RNJ, the number of observed nodes is $|\mathcal{V}_{\text{obs}}| = \text{Diam}(\mathbb{T}) + 1$, so the sample complexity is $O(e^{2\frac{\rho_{\max}}{t_{\max}}} \log \text{Diam}(\mathbb{T}))$.

Full m -tree For RRG, the number of iterations needed to construct the tree $L_R = \frac{1}{2}\text{Diam}(\mathbb{T})$. Thus, the sample complexity of RRG is $O(e^{2\frac{\rho_{\max}}{t_{\max}}} (\frac{9}{2})^{\text{Diam}(\mathbb{T})})$.

For RCLRG, the MST can be derived by contracting hidden nodes as shown in Fig. 12. Then $L_C = 2$ and $|\mathcal{V}_{\text{obs}}| = m^{\text{Diam}(\mathbb{T})/2}$. Thus, its sample complexity is $O(e^{2\frac{\rho_{\max}}{t_{\max}}} \text{Diam}(\mathbb{T}))$.

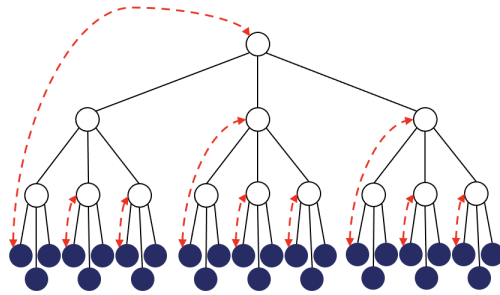


Figure 12: The contraction of hidden nodes in full m -trees.

Double star For RRG, the number of iterations needed to construct the tree $L_R = 1$. Thus, the sample complexity of RRG is $O(e^{2t_{\max}^*})$.

For RCLRG, the maximum number of iterations over each RRG step (over each internal node of the constructed Chow-Liu tree) in RCLRG is. $L_C = 1$ and $|\mathcal{V}_{\text{obs}}| = 2d_{\max}$, so the sample complexity of RCLRG is $O(e^{2t_{\max}^*} \log d_{\max})$.

L Additional numerical details and results

L.1 Standard deviations of results in Fig. 2

We first report the standard deviations of the results presented in Fig. 2 in the main paper. All results are averaged over 100 independent runs.

Constant magnitude corruptions (Fig. 2(a))

$\sigma/(\sigma/\text{AVG}) \times 100$ / # Samples	500	1000	1500	2000	5000	10000	20000
Algorithm							
RRG	9.7/9.3	4.4/5.0	3.7/4.5	4.0/5.0	5.0/6.8	14.4/24.1	21.0/75.0
RSNJ	3.3/3.8	3.0/7.0	3.9/28.8	0.3/703.5	0.0/0.0	0.0/0.0	0.0/0.0
RCLRG	2.1/52.0	0.5/229.1	0.0/0.0	0.0/0.0	0.0/0.0	0.0/0.0	0.0/0.0
RNJ	5.6/4.3	9.0/7.1	12.3/10.0	17.1/15.1	28.4/28.3	35.4/47.9	32.2/68.1
RG	9.2/9.5	8.8/8.8	8.3/8.3	7.8/7.8	5.7/6.2	4.1/4.9	1.9/2.3
SNJ	0.4/0.3	0.6/0.4	1.4/0.9	2.7/1.8	3.2/2.6	3.6/3.7	3.2/5.9
CLRG	3.0/2.2	3.5/2.6	3.4/2.5	4.0/3.0	11.2/19.9	4.7/22.4	2.1/43.5
NJ	1.8/1.3	2.2/1.6	2.2/1.5	3.1/2.3	6.0/4.8	11.5/9.8	17.9/16.35

Table 2: The standard deviations and standard deviations divided by the means of the Robinson-Foulds distances for different algorithms

Uniform corruptions (Fig. 2(b))

$\sigma/(\sigma/\text{AVG}) \times 100$ / # Samples	500	1000	1500	2000	5000	10000	20000
Algorithm							
RRG	4.5/5.0	3.3/4.0	3.8/4.6	3.1/4.0	4.3/5.9	10.9/17.4	23.0/103.2
RSNJ	3.3/4.0	2.9/6.7	5.0/30.1	0.7/230.3	0.0/0.0	0.0/0.0	0.0/0.0
RCLRG	4.6/9.7	2.5/35.8	0.6/197.1	0.1/1971.0	0.0/0.0	0.0/0.0	0.0/0.0
RNJ	9.2/6.9	11.5/9.4	16.4/14.1	18.7/16.6	31.1/35.0	31.4/50.9	33.7/74.5
RG	9.2/9.0	9.8/9.6	8.0/7.8	8.1/8.0	9.0/9.0	7.8/7.4	5.9/6.1
SNJ	0.0/0.0	0.0/0.0	0.0/0.0	0.2/0.1	0.5/0.3	4.4/3.0	3.5/3.0
CLRG	3.3/2.4	3.4/2.5	3.3/2.4	3.5/2.5	3.0/2.2	6.0/4.5	8.0/17.5
NJ	1.7/1.2	1.9/1.3	2.0/1.4	2.0/1.4	2.1/1.5	3.9/2.8	6.1/4.8

Table 3: The standard deviations and standard deviations divided by the means of the Robinson-Foulds distances for different algorithms

HMM corruptions (Fig. 2(c))

$\sigma/(\sigma/\text{AVG}) \times 100$ / # Samples	500	1000	1500	2000	5000	10000	20000
Algorithm							
RRG	4.0/4.5	5.3/5.8	3.8/4.5	3.3/4.0	3.4/4.6	7.5/10.9	21.1/49.6
RSNJ	5.9/6.0	3.5/6.4	3.4/9.7	3.6/35.2	0.0/0.0	0.0/0.0	0.0/0.0
RCLRG	13.1/17.4	4.9/14.1	3.4/29.1	1.6/54.6	0.0/0.0	0.0/0.0	0.0/0.0
RNJ	6.7/4.5	11.3/8.9	12.7/10.5	19.2/16.7	29.3/30.7	38.0/48.7	32.3/65.4
RG	9.3/9.1	8.4/8.3	8.7/8.5	8.6/8.3	9.0/8.8	8.6/8.2	5.5/5.7
SNJ	0.3/0.2	0.4/0.3	0.4/0.3	0.5/0.3	2.0/1.2	4.8/3.4	3.9/3.2
CLRG	3.4/2.5	3.3/2.4	3.2/2.3	3.1/2.3	3.5/2.6	15.0/12.7	8.2/13.7
NJ	1.8/1.3	1.6/1.2	2.0/1.4	1.9/1.3	2.8/2.0	4.5/3.3	5.7/4.4

Table 4: The standard deviations and standard deviations divided by the means of the Robinson-Foulds distances for different algorithms

We note that most of the standard deviations (relative to the means) are reasonably small. However, some entries in Tables 2–4 appear to be rather large, for example 0.5/229.1. The reason is that

the mean value of the errors are already quite small in these cases, so any deviation from the small means result in large standard deviations. This, however, seems unavoidable.

L.2 More simulation results complementing those in Section 3.6

In the following more extensive simulations, we consider eight corruption patterns:

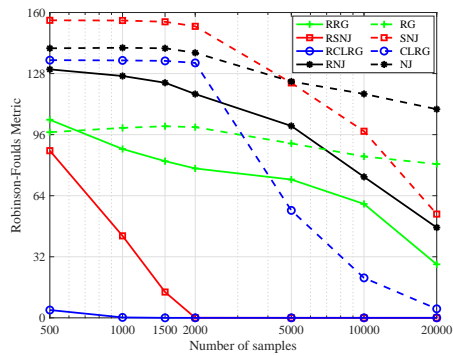
- **Uniform corruptions:** Uniform corruptions are independent additive noises in $[-2A, 2A]$ and distributed randomly in the data matrix \mathbf{X}_1^n .
- **Constant magnitude corruptions:** Constant magnitude corruptions are independent additive noises but taking values in $\{-A, +A\}$ with probability 0.5 and distributed randomly in \mathbf{X}_1^n .
- **Gaussian corruptions:** Gaussian corruptions are independent additive Gaussian noises $\mathcal{N}(0, A^2)$ and distributed randomly in \mathbf{X}_1^n .
- **HMM corruptions:** HMM corruptions are generated by a HMM which shares the same structure as the original HMM but has different parameters. They replace the entries in \mathbf{X}_1^n with the samples generated by the variables in the same positions.
- **Double binary corruptions:** Double binary corruptions are generated by a double binary tree-structured graphical model which shares the same structure as the original double binary graphical model but has different parameters. They replace the entries in \mathbf{X}_1^n with the samples generated by the variables in the same positions.
- **Gaussian outliers:** Gaussian outliers are outliers that are generated by independent Gaussian random variables distributed as $\mathcal{N}(0, A^2)$.
- **HMM outliers:** HMM outliers are outliers that are generated by a HMM that shares the same structure as the original HMM but has different parameters.
- **Double binary outliers:** Double binary outliers are outliers that are generated by a double binary tree-structured graphical model which shares the same structure as the original HMM but has different parameters.

In all our experiments, the parameter A is set to 60 and the number of corruptions n_1 is set to 100.

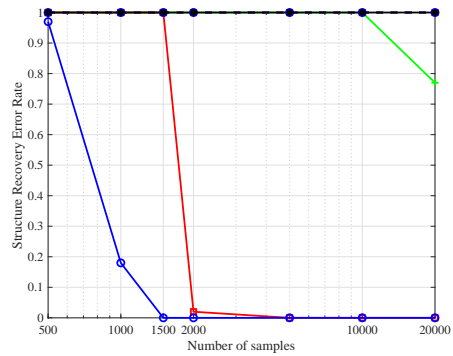
Samples are generated from two graphical models: HMM (Fig. 5(b)) and double binary tree (Fig. 5(a)). The dimensions of the random vectors at each node are $l_{\max} = 3$. The Robinson-Foulds distance [21] between the nominal tree and the estimate and the error rate (zero-one loss) are adopted to measure the performance of learning algorithms. These are computed based on 100 independent trials. We use the code for RG and CLRG provided by Choi et al. [4]. All our experiments are run on an Intel(R) Xeon(R) CPU E5-2697 v4 @ 2.30 GHz.

L.2.1 HMM

Just as in the experiments in Choi et al. [4], the diameter of the HMM (Fig. 5(b)) is chosen to be $\text{Diam}(\mathbb{T}) = 80$. The matrices $(\mathbf{A}, \Sigma_r, \Sigma_n)$ are chosen so that the condition in Proposition 14 are satisfied with $\alpha = 1$, and we set \mathbf{A} commutable with Σ_r . The information distances between neighboring nodes are chosen to be the same value 0.24, which implies that $\rho_{\min} = 0.24$ and $\rho_{\max} = 0.24 \cdot \text{Diam}(\mathbb{T}) = 19.2$.

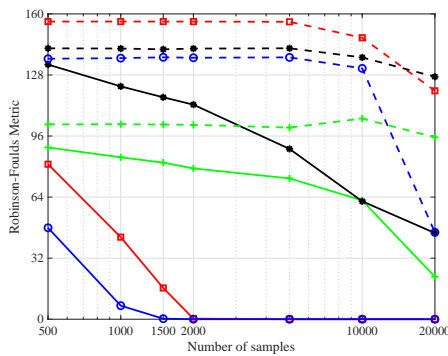


(a) Robinson-Foulds distances

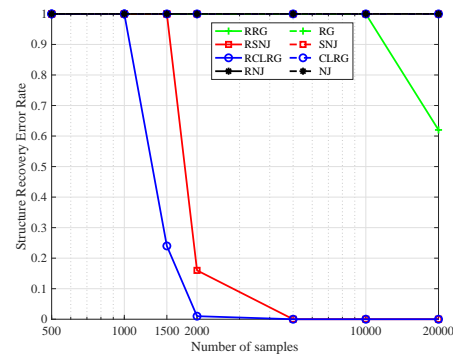


(b) Structure recovery error rate

Figure 13: Performances of robustified and original learning algorithms with constant magnitude corruptions

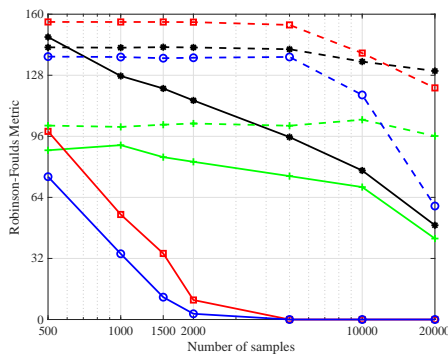


(a) Robinson-Foulds distances

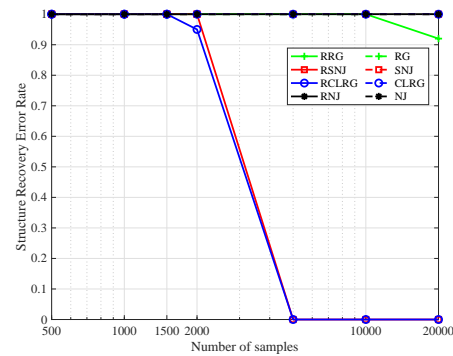


(b) Structure recovery error rate

Figure 14: Performances of robustified and original learning algorithms with uniform corruptions

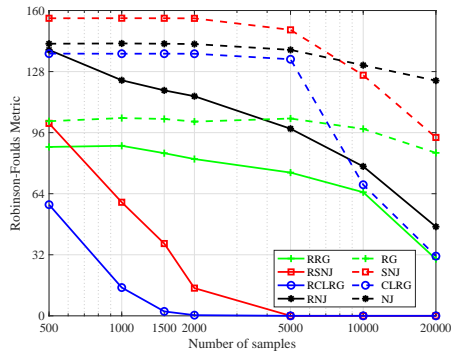


(a) Robinson-Foulds distances

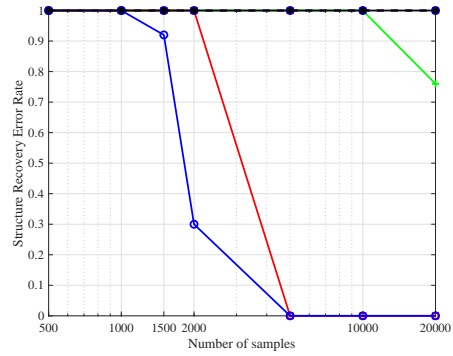


(b) Structure recovery error rate

Figure 15: Performances of robustified and original learning algorithms with HMM corruptions

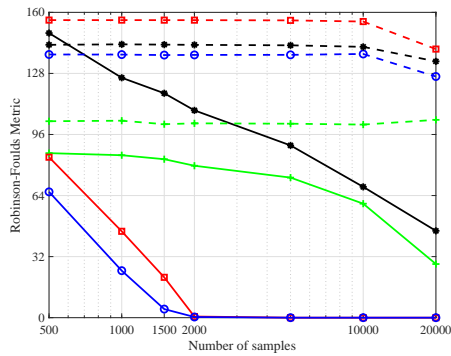


(a) Robinson-Foulds distances

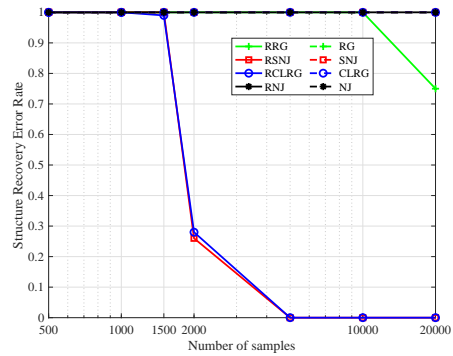


(b) Structure recovery error rate

Figure 16: Performances of robustified and original learning algorithms with Gaussian corruptions

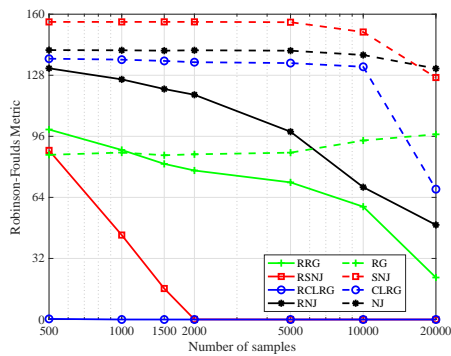


(a) Robinson-Foulds distances

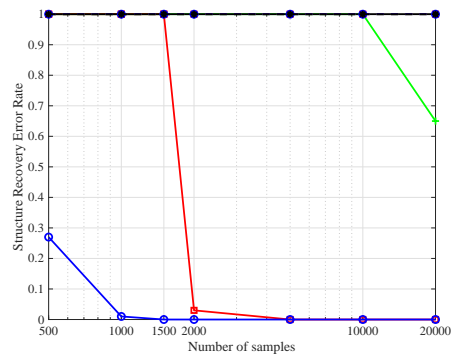


(b) Structure recovery error rate

Figure 17: Performances of robustified and original learning algorithms with double binary corruptions



(a) Robinson-Foulds distances



(b) Structure recovery error rate

Figure 18: Performances of robustified and original learning algorithms with Gaussian outliers

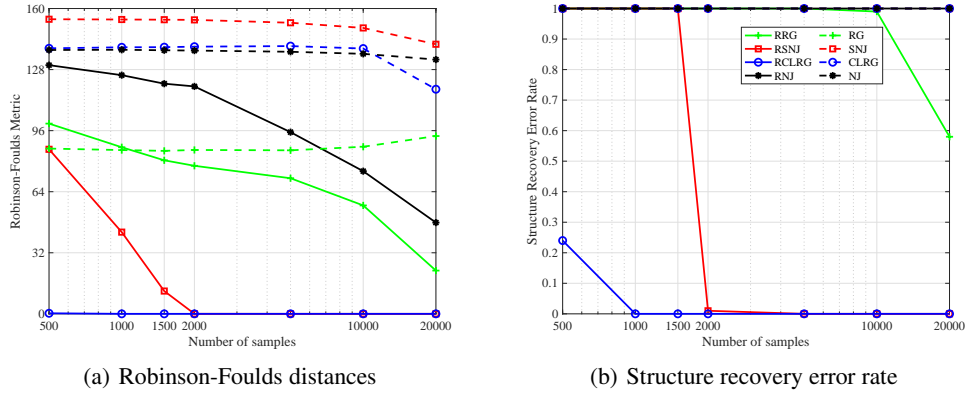


Figure 19: Performances of robustified and original learning algorithms with HMM outliers

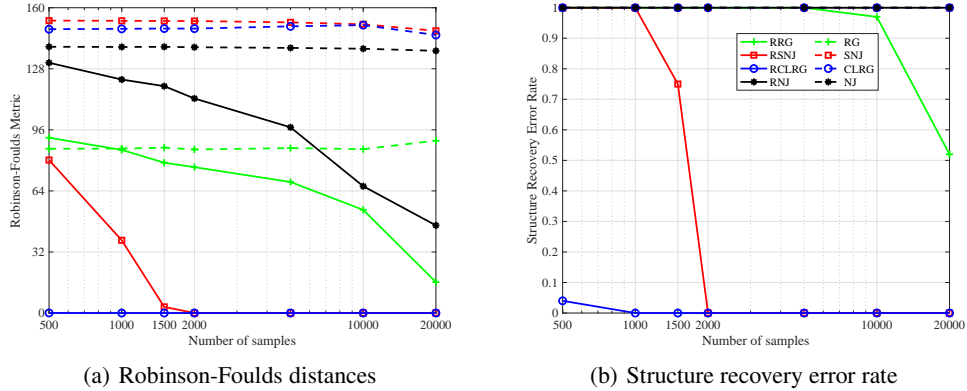


Figure 20: Performances of robustified and original learning algorithms with double binary outliers

These figures show that for the HMM, RCLRG performs best among all these algorithms. The reason is that the Chow-Liu initialization greatly reduces the effective depth of the original tree, which mitigates the error propagation. These simulation results also corroborate the effectiveness of the truncated inner product in combating any form of corruptions. We observe that the errors of robustified algorithms are significantly less than those of original algorithms.

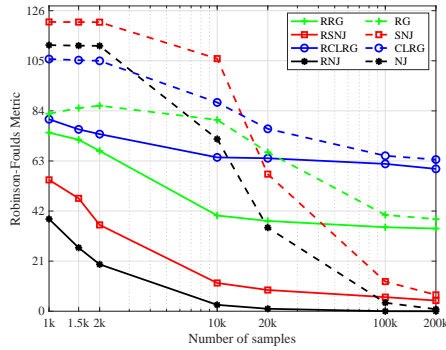
Table 1 shows that for the HMM, RCLRG and RNJ both have optimal dependence on the diameter of the tree. In fact, by changing the parameters ρ_{\min} and ρ_{\max} , we find that RNJ can sometimes perform better than RCLRG when ρ_{\min} and ρ_{\max} are both very small. In the experiments shown above, the parameters favor RCLRG.

Finally, it is also instructive to observe the effect of the different corruption patterns. By comparing the simulation results of HMM (resp. Gaussian and double binary) corruptions and HMM (resp. Gaussian and double binary) outliers, we can see that the algorithms perform worse in the presence of HMM (resp. Gaussian and double binary) corruptions. Since the truncated inner product truncates the samples with large absolute values, if corruptions appear in the *same* positions for all the samples, i.e., they appear as outliers, it is easier for the truncated inner product to identify these outliers and truncate them, resulting in higher quality estimates.

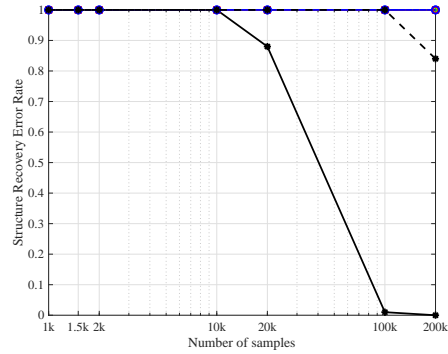
L.2.2 Double binary tree

The diameter of the double binary tree (Fig. 5(a)) is $\text{Diam}(\mathbb{T}) = 11$. The matrices $(\mathbf{A}, \Sigma_r, \Sigma_n)$ are chosen so that the condition in Proposition 14 are satisfied with $\alpha = 1$, and we set \mathbf{A} commutable

with Σ_r . The information distance between neighboring nodes is 1, which implies that $\rho_{\min} = 1$ and $\rho_{\max} = \text{Diam}(\mathbb{T}) = 11$.

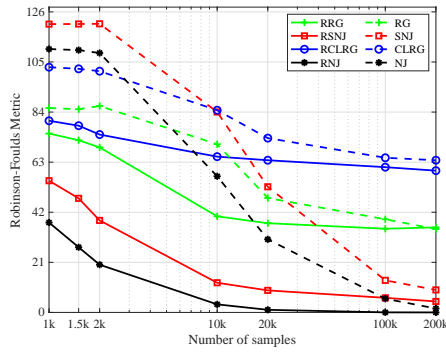


(a) Robinson-Foulds distances

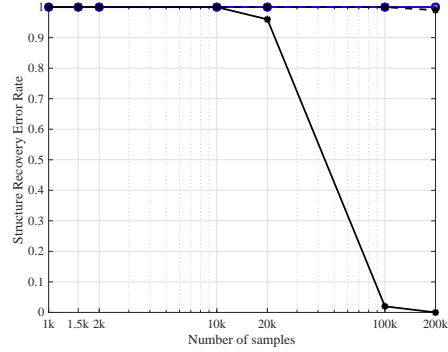


(b) Structure recovery error rate

Figure 21: Performances of robustified and original learning algorithms with constant magnitude corruptions

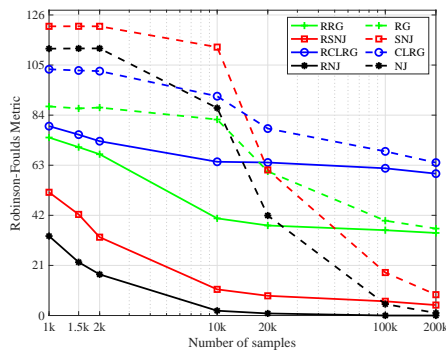


(a) Robinson-Foulds distances

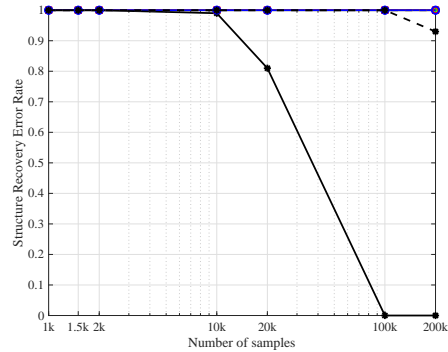


(b) Structure recovery error rate

Figure 22: Performances of robustified and original learning algorithms with uniform corruptions

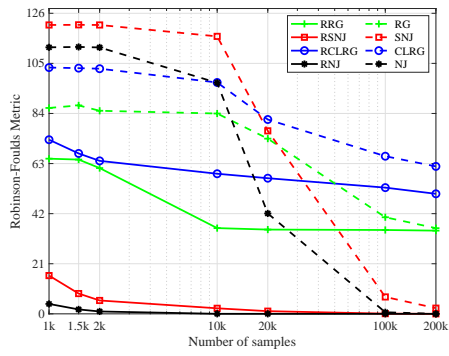


(a) Robinson-Foulds distances

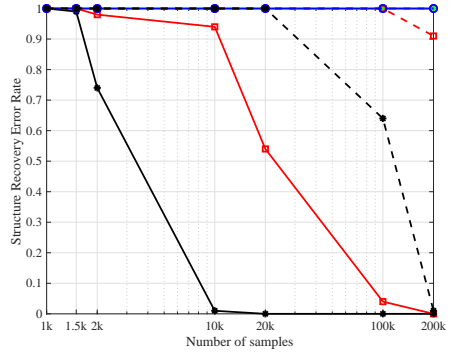


(b) Structure recovery error rate

Figure 23: Performances of robustified and original learning algorithms with Gaussian corruptions

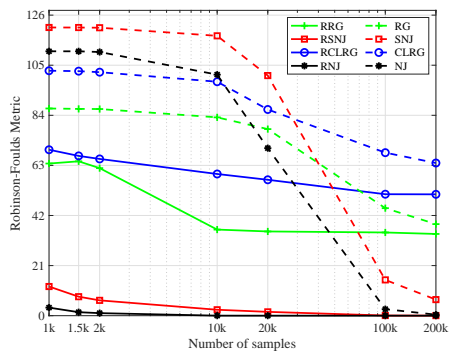


(a) Robinson-Foulds distances

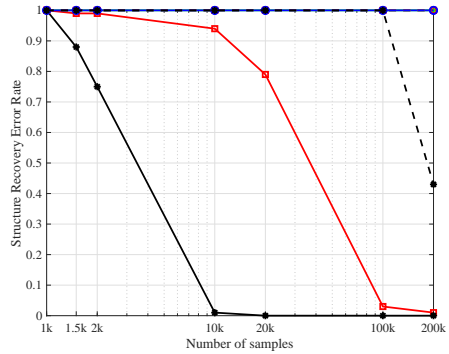


(b) Structure recovery error rate

Figure 24: Performances of robustified and original learning algorithms with HMM corruptions

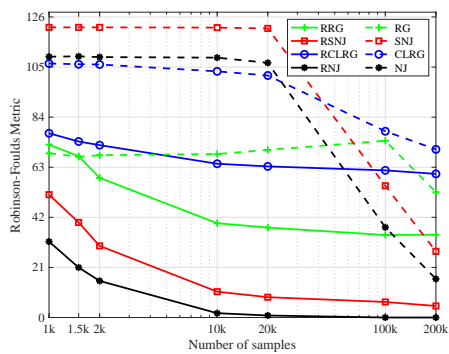


(a) Robinson-Foulds distances

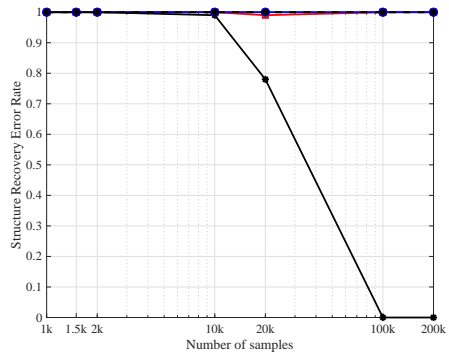


(b) Structure recovery error rate

Figure 25: Performances of robustified and original learning algorithms with double binary corruptions



(a) Robinson-Foulds distances



(b) Structure recovery error rate

Figure 26: Performances of robustified and original learning algorithms with Gaussian outliers

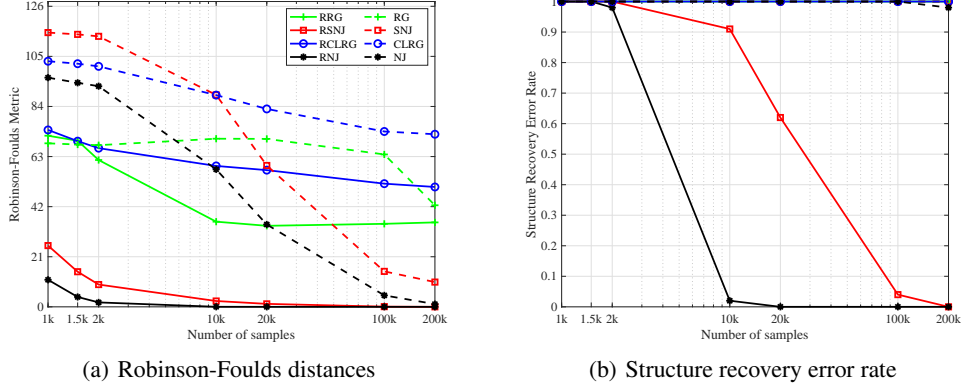


Figure 27: Performances of robustified and original learning algorithms with HMM outliers

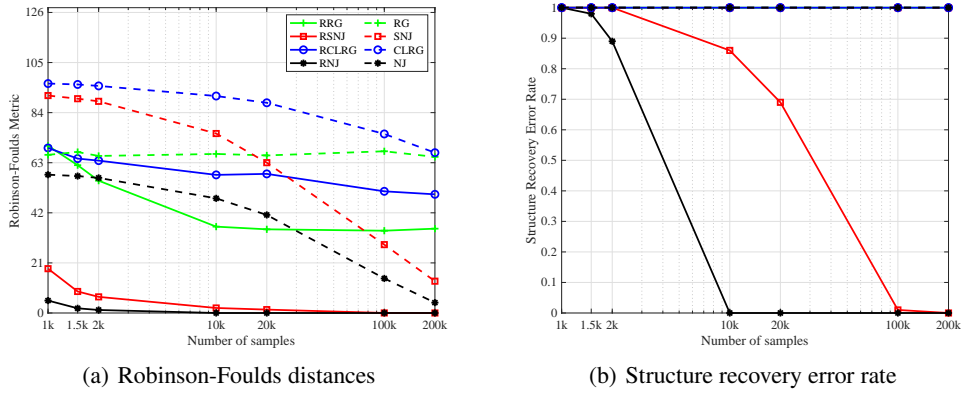


Figure 28: Performances of robustified and original learning algorithms with double binary outliers

These figures reinforce that the robustification procedure is highly effective in combating the corruptions. Furthermore, we observe that RNJ performs the best among all these algorithms for the double binary tree. However, the simulation results in Jaffe et al. [6] shows that SNJ performs better than NJ. This does not contradict our observations here. The reason lies on the choice of the parameters of the model ρ_{\min} and ρ_{\max} . In the simulations of [6], the parameter δ (defined in therein) is set to 0.9, but in our simulation, the equivalent parameter $e^{-2\rho_{\max}/\text{Diam}(\mathbb{T})}$ is 0.1. The exponential dependence on ρ_{\max} of RSNJ listed in Table 1 explains the difference between simulation results in [6] and our simulation results.

M Proofs of results in Section 4

To derive the impossibility results, we will apply Fano's inequality on two special families of graphical models, each contained in $\mathcal{T}(|\mathcal{V}_{\text{obs}}|, \rho_{\max}, l_{\max})$. Each graphical model in the families is parameterized by a quartet $(\mathbf{A}, \Sigma_r, \Sigma_n, \alpha)$. This quartet defines the Gaussian graphical model as follows. We choose a node in the tree as the root node x_r , and define the parent node and set of children nodes (in the rooted tree) of any node x_i as $\text{pa}(i)$ and $\mathcal{C}(x_i)$ respectively. The depth of a node x_i (with respect to the root node x_r) is $d_{\mathbb{T}}(x_i, x_r)$. We specify the model in which

$$\mathbf{x}_i = \mathbf{A}\mathbf{x}_{\text{pa}(i)} + \mathbf{n}_i \quad \text{for all } x_i \in \mathcal{V} \quad (\text{M.1})$$

where $\mathbf{A} \in \mathbb{R}^{l_{\max} \times l_{\max}}$ is non-singular, $\mathbf{n}_i \sim \mathcal{N}(\mathbf{0}, \alpha^{d_{\mathbb{T}}(x_i, x_r)-1} \Sigma_n)$ and \mathbf{n}_i 's are mutually independent. Since the root node has no parent, it is natural to set $\mathbf{x}_{\text{pa}(r)} = \mathbf{0}$ and $\mathbf{n}_r \sim \mathcal{N}(\mathbf{0}, \Sigma_r)$. It is easy

to verify that the model specified by (M.1) and this initial condition is an undirected GGM. Then the covariance matrix of the random vector \mathbf{x}_i is $\alpha^{\text{d}_T(x_i, x_r)} \Sigma_r$.

Proposition 14. *If \mathbf{n}_i 's for the variables at depth l are distributed as $\mathcal{N}(0, \alpha^{l-1} \Sigma_n)$, and*

$$\mathbf{A} \Sigma_r \mathbf{A}^\top + \Sigma_n = \alpha \Sigma_r \quad (\text{M.2})$$

where $\alpha > 0$ is a constant, then the covariance matrix of the variable at depth l is $\alpha^l \Sigma_r$.

We term (M.2) as the $(\mathbf{A}, \Sigma_r, \Sigma_n)$ -homogenous condition, which guarantees that covariance matrices of the random vectors in the tree are same up to a scale factor.

Proof of Proposition 14. The statement in Proposition 14 is equivalent to

$$\mathbf{A}^l \Sigma_r (\mathbf{A}^l)^\top + \sum_{i=1}^l \alpha^{i-1} \mathbf{A}^{l-i} \Sigma_n (\mathbf{A}^{l-i})^\top = \alpha^l \Sigma_r. \quad (\text{M.3})$$

We prove (M.3) by induction.

When $l = 1$, the homogenous condition guarantees that $\mathbf{A} \Sigma_r \mathbf{A}^\top + \Sigma_n = \alpha \Sigma_r$.

If (M.3) holds for $l = 1, \dots, n$, then for $l = n + 1$

$$\begin{aligned} & \mathbf{A}^{n+1} \Sigma_r (\mathbf{A}^{n+1})^\top + \sum_{i=1}^{n+1} \alpha^{i-1} \mathbf{A}^{n+1-i} \Sigma_n (\mathbf{A}^{n+1-i})^\top \\ &= \mathbf{A} (\mathbf{A}^n \Sigma_r (\mathbf{A}^n)^\top + \sum_{i=1}^{n+1} \alpha^{i-1} \mathbf{A}^{n-i} \Sigma_n (\mathbf{A}^{n-i})^\top) \mathbf{A}^\top \end{aligned} \quad (\text{M.4})$$

$$= \mathbf{A} (\alpha^n \Sigma_r + \alpha^n \mathbf{A}^{-1} \Sigma_n \mathbf{A}^{-\top}) \mathbf{A}^\top \quad (\text{M.5})$$

$$= \alpha^n (\mathbf{A} \Sigma_r \mathbf{A}^\top + \Sigma_n) \quad (\text{M.6})$$

$$= \alpha^{n+1} \Sigma_r \quad (\text{M.7})$$

as desired. \square

Proposition 15. *The undirected graphical model specified by (M.1) and the initial condition $\mathbf{x}_{\text{pa}(r)} = \mathbf{0}$, $\mathbf{n}_r \sim \mathcal{N}(\mathbf{0}, \Sigma_r)$ is GGM.*

Proof of Proposition 15. To prove that the specified model is a GGM, we need to prove that the joint distribution of all variables is Gaussian and that the conditional independence relationship induced by the edges is achieved.

According to (M.1) and the initial condition, it is easy to see that any linear combination of variables is the linear combination of independent Gaussian variables, which is Gaussian. Thus, the joint distribution of all variables is indeed Gaussian.

To show that the conditional independence is guaranteed, we show that

$$A \perp\!\!\!\perp B \mid S \text{ for any } S \text{ separates } A \text{ and } B. \quad (\text{M.8})$$

where S , A and B are all sets of nodes, and S separates A and B means that any path connected nodes in A and B goes through a node in S .

Without loss of generality, we consider the case where S , A and B consist of a single node for conciseness of the proof. The case where these sets consist of multiple nodes can be easily proved by generalizing the proof we show here.

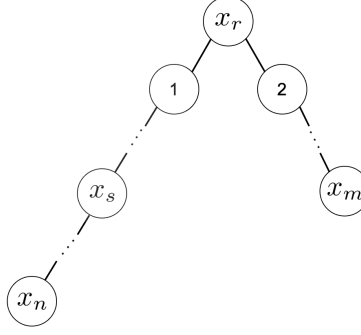


Figure 29: Illustration of the relationship among x_n , x_m and x_s .

We first consider the case where x_n and x_m belong to different branches, as shown in Fig. 29, and the depths of x_n and x_m are n and m , respectively. The separator node x_s can be anywhere along the path connecting x_n and x_m . Without loss of generality, we assume it sits in the same branch as x_n , and its depth is s , where $s < n$. Then we have

$$\mathbb{E}[\mathbf{x}_n \mathbf{x}_n^\top] = \mathbf{A}^n \boldsymbol{\Sigma}_r (\mathbf{A}^n)^\top + \sum_{i=1}^n \mathbf{A}^{n-i} \boldsymbol{\Sigma}_i (\mathbf{A}^{n-i})^\top \quad (\text{M.9})$$

$$\mathbb{E}[\mathbf{x}_m \mathbf{x}_m^\top] = \mathbf{A}^m \boldsymbol{\Sigma}_r (\mathbf{A}^m)^\top + \sum_{i=1}^m \mathbf{A}^{m-i} \boldsymbol{\Sigma}'_i (\mathbf{A}^{m-i})^\top \quad (\text{M.10})$$

$$\mathbb{E}[\mathbf{x}_t \mathbf{x}_n^\top] = \mathbf{A}^t \boldsymbol{\Sigma}_r (\mathbf{A}^n)^\top + \sum_{i=1}^t \mathbf{A}^{t-i} \boldsymbol{\Sigma}_i (\mathbf{A}^{n-i})^\top, \quad (\text{M.11})$$

where $\boldsymbol{\Sigma}_i$ and $\boldsymbol{\Sigma}'_i$ are the covariance matrices of the independent noises in each branch.

Then we calculate the distribution of conditional distribution

$$\begin{bmatrix} \mathbf{x}_n \\ \mathbf{x}_m \end{bmatrix} \mid \mathbf{x}_t \sim \mathcal{N}(\tilde{\boldsymbol{\mu}}, \tilde{\boldsymbol{\Sigma}}), \quad (\text{M.12})$$

where

$$\tilde{\boldsymbol{\Sigma}} = \begin{bmatrix} \tilde{\boldsymbol{\Sigma}}_{11} & \tilde{\boldsymbol{\Sigma}}_{12} \\ \tilde{\boldsymbol{\Sigma}}_{21} & \tilde{\boldsymbol{\Sigma}}_{22} \end{bmatrix}. \quad (\text{M.13})$$

We have

$$\begin{aligned} \tilde{\boldsymbol{\Sigma}}_{12} &= \mathbf{A}^n \boldsymbol{\Sigma}_r (\mathbf{A}^m)^\top - \left(\mathbf{A}^n \boldsymbol{\Sigma}_r (\mathbf{A}^t)^\top + \sum_{i=1}^t \mathbf{A}^{n-i} \boldsymbol{\Sigma}_i \mathbf{A}^{(t-i)\top} \right) \\ &\quad \times \left(\mathbf{A}^t \boldsymbol{\Sigma}_r (\mathbf{A}^t)^\top + \sum_{i=1}^t \mathbf{A}^{t-i} \boldsymbol{\Sigma}_i \mathbf{A}^{(t-i)\top} \right)^{-1} \mathbf{A}^t \boldsymbol{\Sigma}_r (\mathbf{A}^m)^\top = \mathbf{0}. \end{aligned} \quad (\text{M.14})$$

Thus, the conditional independence of x_n and x_m given x_s is proved.

When x_n and x_m are on the same branch, a similar calculation can be performed to prove the conditional independence property. \square

Proposition 16. For a tree graph $\mathbb{T} = (\mathcal{V}, \mathcal{E})$ where $\mathcal{V} = \{x_1, x_2, \dots, x_p\}$ and any symmetric matrix $\mathbf{A} \in \mathbb{R}^{d \times d}$ whose absolute values of all the eigenvalues are less than 1, the determinant of the matrix $\bar{\mathbf{D}}(\mathbb{T}, \mathbf{A})$, which is defined below, is $[\det(\mathbf{I} - \mathbf{A}^2)]^{p-1}$

$$\bar{\mathbf{D}}(\mathbb{T}, \mathbf{A}) = \begin{bmatrix} \mathbf{A}^{\text{d}_{\mathbb{T}}(x_1, x_1)} & \mathbf{A}^{\text{d}_{\mathbb{T}}(x_1, x_2)} & \dots & \mathbf{A}^{\text{d}_{\mathbb{T}}(x_1, x_p)} \\ \mathbf{A}^{\text{d}_{\mathbb{T}}(x_2, x_1)} & \mathbf{A}^{\text{d}_{\mathbb{T}}(x_2, x_2)} & \dots & \mathbf{A}^{\text{d}_{\mathbb{T}}(x_2, x_p)} \\ \vdots & \vdots & \ddots & \vdots \\ \mathbf{A}^{\text{d}_{\mathbb{T}}(x_p, x_1)} & \mathbf{A}^{\text{d}_{\mathbb{T}}(x_p, x_2)} & \dots & \mathbf{A}^{\text{d}_{\mathbb{T}}(x_p, x_p)} \end{bmatrix}, \quad (\text{M.15})$$

Proof of Proposition 16. Since the underlying structure is a tree, we can always find a leaf and its neighbor. Without loss of generality, we assume x_p is a leaf and x_{p-1} is x_p 's neighbor, otherwise we can exchange the rows and columns of $\bar{\mathbf{D}}(\mathbb{T}, \mathbf{A})$ to satisfy this assumption. Then we have

$$d_{\mathbb{T}}(x_{p-1}, x_p) = 1 \quad \text{and} \quad d_{\mathbb{T}}(x_p, x_i) = d_{\mathbb{T}}(x_{p-1}, x_i) + 1 \quad \text{for all } i \in [p-2]. \quad (\text{M.16})$$

Thus, we have

$$\bar{\mathbf{D}}(\mathbb{T}, \mathbf{A}) = \begin{bmatrix} \mathbf{A}^0 & \mathbf{A}^{d_{\mathbb{T}}(x_1, x_2)} & \dots & \mathbf{A}^{d_{\mathbb{T}}(x_1, x_{p-1})} & \mathbf{A}^{d_{\mathbb{T}}(x_1, x_{p-1})+1} \\ \mathbf{A}^{d_{\mathbb{T}}(x_2, x_1)} & \mathbf{A}^0 & \dots & \mathbf{A}^{d_{\mathbb{T}}(x_2, x_{p-1})} & \mathbf{A}^{d_{\mathbb{T}}(x_2, x_{p-1})+1} \\ \vdots & \vdots & \ddots & \vdots & \vdots \\ \mathbf{A}^{d_{\mathbb{T}}(x_{p-1}, x_1)} & \mathbf{A}^{d_{\mathbb{T}}(x_{p-1}, x_2)} & \dots & \mathbf{A}^0 & \mathbf{A}^1 \\ \mathbf{A}^{d_{\mathbb{T}}(x_{p-1}, x_1)+1} & \mathbf{A}^{d_{\mathbb{T}}(x_{p-1}, x_2)+1} & \dots & \mathbf{A}^1 & \mathbf{A}^0 \end{bmatrix}. \quad (\text{M.17})$$

Subtracting \mathbf{A} times the penultimate row of $\bar{\mathbf{D}}(\mathbb{T}, \mathbf{A})$ from the last row of $\bar{\mathbf{D}}(\mathbb{T}, \mathbf{A})$, we have

$$\begin{bmatrix} \mathbf{A}^0 & \mathbf{A}^{d_{\mathbb{T}}(x_1, x_2)} & \dots & \mathbf{A}^{d_{\mathbb{T}}(x_1, x_{p-1})} & \mathbf{A}^{d_{\mathbb{T}}(x_1, x_{p-1})+1} \\ \mathbf{A}^{d_{\mathbb{T}}(x_2, x_1)} & \mathbf{A}^0 & \dots & \mathbf{A}^{d_{\mathbb{T}}(x_2, x_{p-1})} & \mathbf{A}^{d_{\mathbb{T}}(x_2, x_{p-1})+1} \\ \vdots & \vdots & \ddots & \vdots & \vdots \\ \mathbf{A}^{d_{\mathbb{T}}(x_{p-1}, x_1)} & \mathbf{A}^{d_{\mathbb{T}}(x_{p-1}, x_2)} & \dots & \mathbf{A}^0 & \mathbf{A}^1 \\ \mathbf{0} & \mathbf{0} & \dots & \mathbf{0} & \mathbf{A}^0 - \mathbf{A}^2 \end{bmatrix}. \quad (\text{M.18})$$

Applying the similar column transformation, we have

$$\begin{bmatrix} \mathbf{A}^0 & \mathbf{A}^{d_{\mathbb{T}}(x_1, x_2)} & \dots & \mathbf{A}^{d_{\mathbb{T}}(x_1, x_{p-1})} & \mathbf{0} \\ \mathbf{A}^{d_{\mathbb{T}}(x_2, x_1)} & \mathbf{A}^0 & \dots & \mathbf{A}^{d_{\mathbb{T}}(x_2, x_{p-1})} & \mathbf{0} \\ \vdots & \vdots & \ddots & \vdots & \vdots \\ \mathbf{A}^{d_{\mathbb{T}}(x_{p-1}, x_1)} & \mathbf{A}^{d_{\mathbb{T}}(x_{p-1}, x_2)} & \dots & \mathbf{A}^0 & \mathbf{0} \\ \mathbf{0} & \mathbf{0} & \dots & \mathbf{0} & \mathbf{A}^0 - \mathbf{A}^2 \end{bmatrix}. \quad (\text{M.19})$$

By repeating these row and column transformations, we will acquire

$$\text{diag}(\mathbf{I}, \mathbf{I} - \mathbf{A}^2, \dots, \mathbf{I} - \mathbf{A}^2), \quad (\text{M.20})$$

which has the same determinant as $\bar{\mathbf{D}}(\mathbb{T}, \mathbf{A})$. Thus, $\det(\bar{\mathbf{D}}(\mathbb{T}, \mathbf{A})) = [\det(\mathbf{I} - \mathbf{A}^2)]^{p-1}$. \square

The proof of Theorem 5 follows from the following non-asymptotic result.

Theorem 10. Consider the class of graphs $\mathcal{T}(|\mathcal{V}_{\text{obs}}|, \rho_{\max}, l_{\max})$, where $|\mathcal{V}_{\text{obs}}| \geq 3$. If the number of i.i.d. samples n is upper bounded as follows,

$$n < \max \left\{ \frac{2(1-\delta)(\log 3^{1/3} \lceil \log_3(|\mathcal{V}_{\text{obs}}|) \rceil - 1) - \frac{2}{|\mathcal{V}_{\text{obs}}|}}{-l_{\max} \log(1 - e^{-\frac{\rho_{\max}}{\lceil \log_3(|\mathcal{V}_{\text{obs}}|) \rceil l_{\max}}})}, \frac{(1-\delta)/5 - \frac{2}{|\mathcal{V}_{\text{obs}}|}}{-l_{\max} \log(1 - e^{-\frac{2\rho_{\max}}{3l_{\max}}})} \right\} \quad (\text{M.21})$$

then for any graph decoder $\phi : \mathbb{R}^{n|\mathcal{V}_{\text{obs}}|l_{\max}} \rightarrow \mathcal{T}(|\mathcal{V}_{\text{obs}}|, \rho_{\max}, l_{\max})$

$$\max_{\theta(\mathbb{T}) \in \mathcal{T}(|\mathcal{V}_{\text{obs}}|, \rho_{\max}, l_{\max})} \mathbb{P}_{\theta(\mathbb{T})}(\phi(\mathbf{X}_1^n) \neq \mathbb{T}) \geq \delta. \quad (\text{M.22})$$

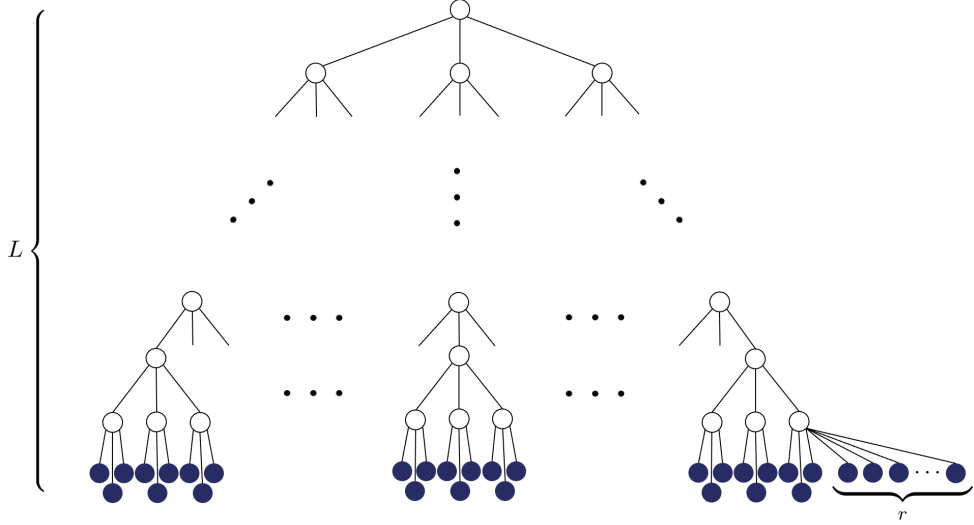
Proof of Theorem 5. To prove Theorem 5, we simply implement the Taylor expansion $\log(1+x) = \sum_{k=1}^{\infty} (-1)^{k+1} \frac{x^k}{k}$ on (M.21) in Theorem 10 taking $\rho_{\max} \rightarrow \infty$ and $|\mathcal{V}_{\text{obs}}| \rightarrow \infty$. \square

It remains to prove Theorem 10.

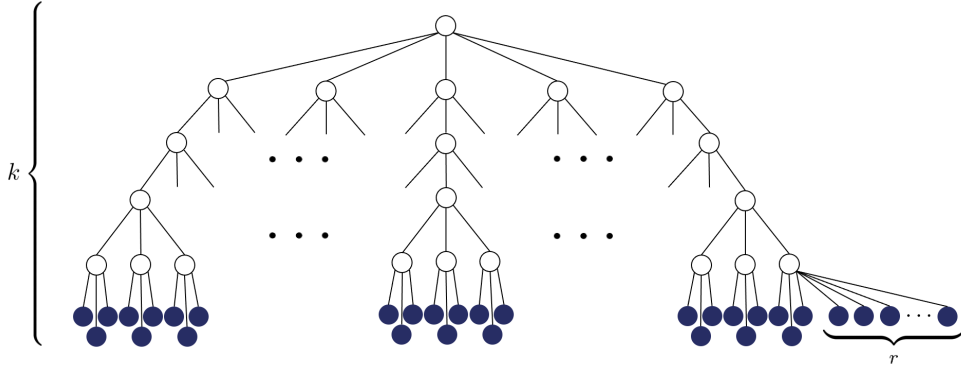
Proof of Theorem 10. To prove this non-asymptotic converse bound, we consider M models in $\mathcal{T}(|\mathcal{V}_{\text{obs}}|, \rho_{\max}, l_{\max})$, whose parameters are enumerated as $\{\theta^{(1)}, \theta^{(2)}, \dots, \theta^{(M)}\}$. We choose a model $K = k$ uniformly in $\{1, \dots, M\}$ and generate n i.i.d. samples \mathbf{X}_1^n from $\mathbb{P}_{\theta^{(k)}}$. A latent tree learning algorithm is a decoder $\phi : \mathbb{R}^{n|\mathcal{V}_{\text{obs}}|l_{\max}} \rightarrow \{1, \dots, M\}$.

Two families are built to derive the converse bound. We separately describe the families of M graphical models we consider here.

Graphical model family A We specify the structure of trees as full- m trees, except the top layer, as shown in Fig. 30. All the observed nodes are leaves. The parameters of each tree are set to satisfy the conditions in Proposition 14. Additionally, we set $\alpha = 1$ in the homogeneous condition (M.2) and set \mathbf{A} to be a symmetric matrix that commutes with Σ_r . We set $m = 3$ and $L = \lfloor \log_3(|\mathcal{V}_{\text{obs}}|) \rfloor$, then the number of residual nodes is $r = |\mathcal{V}_{\text{obs}}| - 3^L$. All these residual nodes are connected to one of parents of the observed nodes.



(a) The full 3-tree. All the observed nodes are leaves, and residual nodes are connected to one of parents of the observed nodes.



(b) The full tree with depth k , where all the internal nodes have three children except the root node.

Figure 30: The family A of graphical models considered in the impossibility result.

To derive the converse result, we use the Fano's method. Namely, Fano's method says that if the sample size

$$n < \frac{(1 - \delta) \log M}{I(\mathbf{X}_1; K)}, \quad (\text{M.23})$$

then for any decoder

$$\max_{k=1, \dots, M} \mathbb{P}_{\theta^{(k)}} [\phi(\mathbf{X}_1^n) \neq k] \geq \delta - \frac{1}{\log M}. \quad (\text{M.24})$$

We first evaluate the cardinality of this family of graphical models. We first count the number of graphical models with depth $1 \leq k \leq L$ in Fig. 30. For a specific order of labels (e.g., $1, 2, \dots, m^L$), exchanging the labels in a family does not change the topology of the tree. For instance, exchanging

the position of node 1 and node m , we obtain an identical tree. By changing the orders in the last layer, it is obvious that there are $(m!)^{m^{L-1}}$ different orders representing the same structure. For the penultimate layer, there are $(m!)^{m^{L-2}}$ different orders represent an identical structure. Thus, for a specific graphical model with depth k , there are

$$(m^{L-k+1})! \prod_{i=L-1}^{L-k+1} (m!)^{m^i} = (m^{L-k+1})! (m!)^{\frac{m^L - m^{L-k+1}}{m-1}} \quad (\text{M.25})$$

graphical models with the same distribution.

Then the number of different structures of graphical models with depth k can be calculated as

$$\frac{(m^L)!}{(m^{L-k+1})! (m!)^{\frac{m^L - m^{L-k+1}}{m-1}}}. \quad (\text{M.26})$$

The total number of different graphical models in the family we consider is

$$M = \sum_{k=1}^L \frac{(m^L)!}{(m^{L-k+1})! (m!)^{\frac{m^L - m^{L-k+1}}{m-1}}}. \quad (\text{M.27})$$

Using Stirling's formula, we have the following simplification of M :

$$M \geq \sum_{k=1}^L \frac{\sqrt{2\pi} (m^L)^{m^L+1/2} e^{-m^L}}{e(m^{L-k+1})^{m^{L-k+1}+1/2} e^{-m^{L-k+1}}} \frac{1}{(e^{-(m-1)} m^{m+1/2})^{(m^L - m^{L-k+1})/(m-1)}} \quad (\text{M.28})$$

$$= \sum_{k=1}^L \frac{\sqrt{2\pi}}{e} m^{L m^L - (L-k+1) m^{L-k+1} + (k-1)/2 - (m+1/2)(m^L - m^{L-k+1})/(m-1)} \quad (\text{M.29})$$

$$= \frac{\sqrt{2\pi}}{e} m^{(L-(m+1/2)/(m-1))m^L} \sum_{k=1}^L m^{-(L-k+1-(m+1/2)/(m-1))m^{L-k+1} + (k-1)/2} \quad (\text{M.30})$$

$$> \frac{\sqrt{2\pi}}{e} m^{(L-(m+1/2)/(m-1))m^L} m^{3m/(2m-2) + (L-1)/2} \quad (\text{M.31})$$

and

$$\log M > \log \left(\frac{\sqrt{2\pi}}{e} \right) + m^L \left(L - \frac{m + \frac{1}{2}}{m-1} \right) \log m + \left(\frac{3m}{2m-2} + \frac{L-1}{2} \right) \log m \quad (\text{M.32})$$

Thus,

$$\frac{\log M}{|\mathcal{V}_{\text{obs}}|} > \frac{1}{|\mathcal{V}_{\text{obs}}|} \log \left(\frac{\sqrt{2\pi}}{e} \right) + \frac{m^L}{|\mathcal{V}_{\text{obs}}|} \left(L - \frac{m + \frac{1}{2}}{m-1} \right) \log m + \frac{1}{|\mathcal{V}_{\text{obs}}|} \left(\frac{3m}{2m-2} + \frac{L-1}{2} \right) \log m \quad (\text{M.33})$$

$$> \frac{\log m}{m} \left(L - \frac{m + \frac{1}{2}}{m-1} \right) + \frac{1}{|\mathcal{V}_{\text{obs}}|} \log \left(\frac{\sqrt{2\pi}}{e} \right) \quad (\text{M.34})$$

$$\stackrel{(a)}{>} \frac{\log 3}{3} L - 1, \quad (\text{M.35})$$

where inequality (a) is derived by substituting $m = 3$.

Next we calculate an upper bound of $I(\mathbf{X}_1; K)$. Since $\mathbb{P}_{\mathbb{T}_k} = \mathcal{N}(0, \boldsymbol{\Sigma}_{\text{obs}}(\mathbb{T}_k))$, where $\boldsymbol{\Sigma}_{\text{obs}}$ is the covariance matrix of observed variables, we have [26]

$$I(\mathbf{X}_1; K) \leq \mathbb{E}_{\mathbb{T}_k} [D(\mathbb{P}_{\mathbb{T}_k} \| \mathbb{Q})], \quad (\text{M.36})$$

for any distribution \mathbb{Q} . By choosing $\mathbb{Q} = \mathcal{N}(0, \mathbf{I}_{l_{\max}|\mathcal{V}_{\text{obs}}| \times l_{\max}|\mathcal{V}_{\text{obs}}|})$, we have

$$D(\mathbb{P}_{\mathbb{T}_k} \| \mathbb{Q}) = \frac{1}{2} \left\{ \log \left(\det(\boldsymbol{\Theta}_{\text{obs}}(\mathbb{T}_k)) \right) + \text{trace}(\boldsymbol{\Sigma}_{\text{obs}}(\mathbb{T}_k)) - l_{\max}|\mathcal{V}_{\text{obs}}| \right\} \quad (\text{M.37})$$

$$= \frac{1}{2} \left\{ -\log \left(\det(\boldsymbol{\Sigma}_{\text{obs}}(\mathbb{T}_k)) \right) + \text{trace}(\boldsymbol{\Sigma}_{\text{obs}}(\mathbb{T}_k)) - l_{\max}|\mathcal{V}_{\text{obs}}| \right\} \quad (\text{M.38})$$

Since we consider models that satisfy the conditions in Proposition 14, the covariance matrix of any two variables is

$$\mathbb{E}[\mathbf{x}_i \mathbf{x}_j^\top] = \Sigma_r \mathbf{A}^{\text{d}_T(x_i, x_j)}. \quad (\text{M.39})$$

The covariance matrix $\Sigma(\mathbb{T}_k)$ for all the observed variables and latent variables $\mathcal{V}_{\text{obs}} \cup \mathcal{V}_{\text{hid}}$ is

$$\begin{bmatrix} \Sigma_r \mathbf{A}^{\text{d}_T(x_1, x_1)} & \dots & \Sigma_r \mathbf{A}^{\text{d}_T(x_1, x_{|\mathcal{V}_{\text{obs}}|})} & \Sigma_r \mathbf{A}^{\text{d}_T(x_1, y_1)} & \dots & \Sigma_r \mathbf{A}^{\text{d}_T(x_1, y_{|\mathcal{V}_{\text{hid}}|})} \\ \vdots & \ddots & \vdots & \vdots & \ddots & \vdots \\ \Sigma_r \mathbf{A}^{\text{d}_T(x_{|\mathcal{V}_{\text{obs}}|}, x_1)} & \dots & \Sigma_r \mathbf{A}^{\text{d}_T(x_{|\mathcal{V}_{\text{obs}}|}, x_{|\mathcal{V}_{\text{obs}}|})} & \Sigma_r \mathbf{A}^{\text{d}_T(x_{|\mathcal{V}_{\text{obs}}|}, y_1)} & \dots & \Sigma_r \mathbf{A}^{\text{d}_T(x_{|\mathcal{V}_{\text{obs}}|}, y_{|\mathcal{V}_{\text{hid}}|})} \\ \Sigma_r \mathbf{A}^{\text{d}_T(y_1, x_1)} & \dots & \Sigma_r \mathbf{A}^{\text{d}_T(y_1, x_{|\mathcal{V}_{\text{obs}}|})} & \Sigma_r \mathbf{A}^{\text{d}_T(y_1, y_1)} & \dots & \Sigma_r \mathbf{A}^{\text{d}_T(y_1, y_{|\mathcal{V}_{\text{hid}}|})} \\ \vdots & \ddots & \vdots & \vdots & \ddots & \vdots \\ \Sigma_r \mathbf{A}^{\text{d}_T(y_{|\mathcal{V}_{\text{hid}}|}, x_1)} & \dots & \Sigma_r \mathbf{A}^{\text{d}_T(y_{|\mathcal{V}_{\text{hid}}|}, x_{|\mathcal{V}_{\text{obs}}|})} & \Sigma_r \mathbf{A}^{\text{d}_T(y_{|\mathcal{V}_{\text{hid}}|}, y_1)} & \dots & \Sigma_r \mathbf{A}^{\text{d}_T(y_{|\mathcal{V}_{\text{hid}}|}, y_{|\mathcal{V}_{\text{hid}}|})} \end{bmatrix}$$

$$= \left(\mathbf{I}_{|\mathcal{V}| \times |\mathcal{V}|} \otimes \Sigma_r \right) \begin{bmatrix} \mathbf{V} & \mathbf{B} \\ \mathbf{B}^\top & \mathbf{H} \end{bmatrix} \quad (\text{M.40})$$

$$= \left(\mathbf{I}_{|\mathcal{V}| \times |\mathcal{V}|} \otimes \Sigma_r \right) \bar{\mathbf{D}}(\mathbb{T}_k, \mathbf{A}) \quad (\text{M.41})$$

where $\mathbf{A} \otimes \mathbf{B}$ is the Kronecker product of matrices \mathbf{A} and \mathbf{B} . Letting $\Sigma_r = \mathbf{I}$, it is obvious that $\bar{\mathbf{D}}(\mathbb{T}, \mathbf{A})$ is a positive definite matrix. Furthermore, $\mathbf{H} - \mathbf{B}^\top \mathbf{V}^{-1} \mathbf{B}$ is positive semi-definite matrix, since it is the inverse of the principal minor of $\bar{\mathbf{D}}^{-1}$. Thus we have

$$\det(\bar{\mathbf{D}}(\mathbb{T}_k, \mathbf{A})) = \det(\mathbf{V}) \det(\mathbf{H} - \mathbf{B}^\top \mathbf{V}^{-1} \mathbf{B}) \quad (\text{M.42})$$

$$\stackrel{(a)}{\leq} \det(\mathbf{V}) \det(\mathbf{H}) \stackrel{(b)}{=} \det(\mathbf{V}) [\det(\mathbf{I} - \mathbf{A}^2)]^{|\mathcal{V}_{\text{hid}}| - 1}, \quad (\text{M.43})$$

where inequality (a) is derived from Minkowski determinant theorem [27], and (b) comes from the fact that all the latent variables themselves form a tree. Also, we have that

$$\det(\bar{\mathbf{D}}(\mathbb{T}_k, \mathbf{A})) = [\det(\mathbf{I} - \mathbf{A}^2)]^{|\mathcal{V}_{\text{hid}}| + |\mathcal{V}_{\text{obs}}| - 1}. \quad (\text{M.44})$$

Thus, we have

$$\det(\mathbf{V}) \geq [\det(\mathbf{I} - \mathbf{A}^2)]^{|\mathcal{V}_{\text{obs}}|}, \quad (\text{M.45})$$

which implies that

$$\log(\det(\Sigma_{\text{obs}}(\mathbb{T}_k))) \geq \log([\det(\Sigma_r)]^{|\mathcal{V}_{\text{obs}}|} [\det(\mathbf{I} - \mathbf{A}^2)]^{|\mathcal{V}_{\text{obs}}|}) \quad (\text{M.46})$$

$$= |\mathcal{V}_{\text{obs}}| \log(\det(\Sigma_r) \det(\mathbf{I} - \mathbf{A}^2)). \quad (\text{M.47})$$

The mutual information can thus be upper bounded as

$$I(\mathbf{X}_1; K) \leq \frac{1}{2} |\mathcal{V}_{\text{obs}}| (-\log(\det(\mathbf{I} - \mathbf{A}^2)) + \text{trace}(\Sigma_r) - \log(\det(\Sigma_r)) - l_{\max}) \quad (\text{M.48})$$

Combining inequalities (M.28) and (M.48), we can deduce that the any decoder will construct the wrong tree with probability at least δ if

$$n < \frac{2(1 - \delta)(\log 3^{1/3} L - 1)}{-\log(\det(\mathbf{I} - \mathbf{A}^2)) + \text{trace}(\Sigma_r) - \log(\det(\Sigma_r)) - l_{\max}} \quad (\text{M.49})$$

By choosing $\Sigma_r = \mathbf{I}$ and letting the eigenvalues of \mathbf{A} are all the same, we have

$$\rho_{\max} = -\frac{2L}{2} \log(\det(\mathbf{A}^2)) = -2l_{\max} L \log(\lambda(\mathbf{A})) \quad (\text{M.50})$$

and

$$\text{trace}(\Sigma_r) - \log(\det(\Sigma_r)) - l_{\max} = 0. \quad (\text{M.51})$$

Furthermore, we have

$$\log(\det(\mathbf{I} - \mathbf{A}^2)) = l_{\max} \log(1 - \lambda(\mathbf{A})^2) = l_{\max} \log(1 - e^{-\frac{\rho_{\max}}{L l_{\max}}}). \quad (\text{M.52})$$

By choosing $\delta' = \delta + \frac{1}{\log(M)}$, we have that the condition

$$n < \frac{2(1 - \delta')(\log 3^{1/3} L - 1) - \frac{2}{|\mathcal{V}_{\text{obs}}|}}{-l_{\max} \log(1 - e^{-\frac{\rho_{\max}}{L l_{\max}}})} \quad (\text{M.53})$$

guarantees that

$$\max_{\theta(\mathbb{T}) \in \mathcal{T}(|\mathcal{V}_{\text{obs}}|, \rho_{\max}, l_{\max})} \mathbb{P}_{\theta(\mathbb{T})}(\phi(\mathbf{X}_1^n) \neq \mathbb{T}) \geq \delta' \quad (\text{M.54})$$

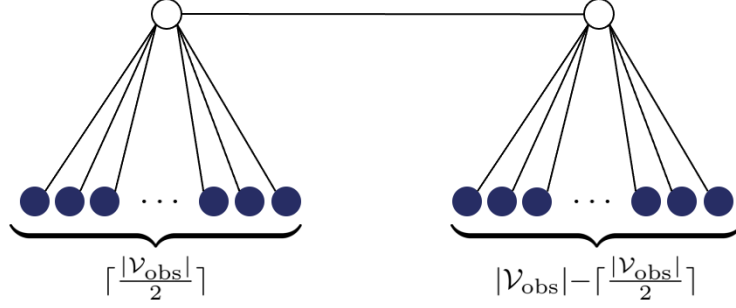


Figure 31: The family B of graphical models considered in the impossibility result.

Graphical model family B We consider the family of graphical models with double-star substructures, as shown in Fig. 31. Then the number of graphical models M in this family is lower bounded as

$$\begin{aligned} M &> \frac{1}{2} \binom{|\mathcal{V}_{\text{obs}}|}{\lceil |\mathcal{V}_{\text{obs}}|/2 \rceil} > \frac{\sqrt{2\pi} |\mathcal{V}_{\text{obs}}|^{|\mathcal{V}_{\text{obs}}|+1/2} e^{-|\mathcal{V}_{\text{obs}}|}}{2(en^{n+1/2}e^{-n})(e(|\mathcal{V}_{\text{obs}}| - n)^{|\mathcal{V}_{\text{obs}}|-n+1/2}e^{-(|\mathcal{V}_{\text{obs}}|-n)})} \\ &= \frac{\sqrt{2\pi}}{2e^2} \frac{|\mathcal{V}_{\text{obs}}|^{|\mathcal{V}_{\text{obs}}|+1/2}}{n^{n+1/2}(|\mathcal{V}_{\text{obs}}| - n)^{|\mathcal{V}_{\text{obs}}|-n+1/2}} \end{aligned} \quad (\text{M.55})$$

when $n = \lceil |\mathcal{V}_{\text{obs}}|/2 \rceil$. Since $n \geq |\mathcal{V}_{\text{obs}}| - n$, we further have

$$M > \frac{\sqrt{2\pi}}{2e^2} \frac{|\mathcal{V}_{\text{obs}}|^{|\mathcal{V}_{\text{obs}}|+1/2}}{n^{|\mathcal{V}_{\text{obs}}|+1}} = \sqrt{\frac{\pi}{2e^4|\mathcal{V}_{\text{obs}}|}} \left(\frac{|\mathcal{V}_{\text{obs}}|}{n}\right)^{|\mathcal{V}_{\text{obs}}|+1} \quad (\text{M.56})$$

and

$$\frac{\log(M)}{|\mathcal{V}_{\text{obs}}|} > \frac{|\mathcal{V}_{\text{obs}}| + 1}{|\mathcal{V}_{\text{obs}}|} \log\left(\frac{|\mathcal{V}_{\text{obs}}|}{\lceil |\mathcal{V}_{\text{obs}}|/2 \rceil}\right) + \frac{1}{|\mathcal{V}_{\text{obs}}|} \log\left(\sqrt{\frac{\pi}{2e^4|\mathcal{V}_{\text{obs}}|}}\right) \quad (\text{M.57})$$

$$> \frac{|\mathcal{V}_{\text{obs}}| + 1}{|\mathcal{V}_{\text{obs}}|} \log 2 + \frac{1}{|\mathcal{V}_{\text{obs}}|} \log\left(\sqrt{\frac{\pi}{2e^4|\mathcal{V}_{\text{obs}}|}}\right) > \frac{1}{10} \quad (\text{M.58})$$

By choosing $\Sigma_r = \mathbf{I}$ and letting all the eigenvalues of \mathbf{A} to be the same, we have

$$\rho_{\max} = -\frac{3}{2} \log(\det(\mathbf{A}^2)) = -3l_{\max} \log(\lambda(\mathbf{A})) \quad (\text{M.59})$$

and

$$\text{trace}(\Sigma_r) - \log(\det(\Sigma_r)) - l_{\max} = 0. \quad (\text{M.60})$$

Furthermore, we have

$$\log(\det(\mathbf{I} - \mathbf{A}^2)) = l_{\max} \log(1 - \lambda(\mathbf{A})^2) = l_{\max} \log(1 - e^{-\frac{2\rho_{\max}}{3l_{\max}}}). \quad (\text{M.61})$$

By choosing $\delta' = \delta + \frac{1}{\log(M)}$, we have that the condition

$$n < \frac{(1 - \delta')/5 - \frac{2}{|\mathcal{V}_{\text{obs}}|}}{-l_{\max} \log(1 - e^{-\frac{2\rho_{\max}}{3l_{\max}}})} \quad (\text{M.62})$$

guarantees that

$$\max_{\theta(\mathbb{T}) \in \mathcal{T}(|\mathcal{V}_{\text{obs}}|, \rho_{\max}, l_{\max})} \mathbb{P}_{\theta(\mathbb{T})}(\phi(\mathbf{X}_1^n) \neq \mathbb{T}) \geq \delta' \quad (\text{M.63})$$

as desired. \square